Optimal Selection and Placement of Phasor Measurement Units and Their Application for Power System Protection

Submitted in partial fulfilment of the requirements
For the award of the degree of

DOCTOR OF PHILOSOPHY

By
N Venkataphanendrababu
(Roll No. 701407)

Supervisor
Dr. P Suresh Babu

Co-Supervisor
Prof. D V S S Siva Sarma

DEPARTMENT OF ELECTRICAL ENGINEERING
NATIONAL INSTITUTE OF TECHNOLOGY
WARANGAL – 506004, TELANGANA STATE, INDIA
MAY-2019

APPROVAL SHEET

This Thesis entitled "**Optimal Selection and Placement of the Phasor Measurement Units and Their Application for Power System Protection**" by **N Venkataphanendrababu** is approved for the degree of Doctor of Philosophy

Examiners

_____

_____

_____

Supervisor
Dr. P Suresh Babu
Assistant Professor
EED, NIT Warangal

Co-Supervisor
Prof. D V S S Siva Sarma
Professor
EED, NIT Warangal

Chairman
Prof. S Srinivasa Rao
Professor & Head,
EED, NIT Warangal

Date: _____

**DEPARTMENT OF ELECTRICAL ENGINEERING
NATIONAL INSTITUTE OF TECHNOLOGY
WARANGAL – 506 004**

DEPARTMENT OF ELECTRICAL ENGINEERING
NATIONAL INSTITUTE OF TECHNOLOGY WARANGAL

CERTIFICATE

This is to certify that the thesis entitled **"Optimal Selection and Placement of the Phasor Measurement Units and Their Application for Power System Protection"**, which is being submitted by **Mr. N Venkataphanendrababu** (Roll No. 701407), is a bonafide work submitted to National Institute of Technology, Warangal in partial fulfilment of the requirement for the award of the degree of **Doctor of Philosophy** in Department of Electrical Engineering. To the best of our knowledge, the work incorporated in this thesis has not been submitted elsewhere for the award of any degree.

Dr. P Suresh Babu
(Supervisor)
Assistant Professor
Department of Electrical Engineering
National Institute of Technology
Warangal – 506004

Dr. DVSS Siva Sarma
(Co-Supervisor)
Professor
Department of Electrical Engineering
National Institute of Technology
Warangal – 506004

Date:

Place: Warangal

DECLARATION

This is to certify that the work presented in the thesis entitled "**Optimal Selection and Placement of Phasor Measurement Units and Their Application for Power System Protection**" is a bonafide work done by me under the supervision of **Dr. P Suresh Babu** and **Prof. D V S S Siva Sarma,** Department of Electrical Engineering, National Institute of Technology, Warangal, India and was not submitted elsewhere for the award of any degree.

I declare that this written submission represents my ideas in my own words and where others ideas or words have been included. I have adequately cited and referenced the original sources. I also declare that I have adhered to all principles of academic honesty and integrity and have not misrepresented or fabricated or falsified any idea/date/fact/source in my submission. I understand that any violation of the above will be a cause for disciplinary action by the Institute and can also evoke penal action from the sources which have thus not been properly cited or from whom proper permission has not been taken when needed.

<div align="right">

N Venkataphanendrababu

(Roll No: 701407)

</div>

Date:

Place: Warangal

ACKNOWLEDGEMENTS

ℋ
List of Figures

List of Tables

List of symbols

Ω	Angular Frequency
Δ	Generator Phase Angle
p, q	Bus indices
N	Set of buses
n	Number of buses
s_p	Bus observability function
c_{pq}	Binary connectivity variable
l	Line index
L	Set of lines
x_q	Binary decision variable for PMU at bus q
m_{pq}	Binary measurement variable at p with PMU at q
m_q^{max}	Measurement limitation of bus q
x_r	Real valued solution
x_b	Binary valued solution
p_a	Probability with which the host bird can discover cuckoo's eggs
A	Step size
σ	Flipping operator
Γ	Random number
n_r	Number of buses in rth region (or island)
R	Number of regions
A_p	Network connectivity of pth region
x_p	Binary variable vector of pth region
A	Network connectivity matrix
G_i	Generator existence index at bus i
L_i	Load existence index at bus i
M_i	PMU existence index at bus i
R	Regional matrix
R_k	Regional matrix at kth iteration
$R_k{}'$	R_k after corrections
x_j	Binary decision variable for the PDC at j^{th} bus

S_p PMU observability function

c_{ij} Bus observability matrix for PMU at i^{th} bus with j as its connected bus

L_{jk} Critical line between j and k

Abbreviations

PMU	Phasor Measurement Unit
OPP	Optimal PMU Placement
WAMS	Wide-Area Measurement System
SCADA	Supervisory Control And Data Acquisition
GPS	Global Positioning System
AC	Alternating Current
PLL	Phase Locked Loop
PPS	Pulse Per Second
PDC	Phasor Data Concentrator
RMS	Root Mean Square
DFT	Discrete Fourier Transform
DC	Direct Current
LOF	Loss-Of-Field
ZIB	Zero Injection Bus
ILP	Integer Linear Programming
IQP	Integer Quadratic Programming
DFS	Depth First Search
MST	Minimum Spanning Tree
GA	Genetic Algorithm
PSO	Particle Swarm Optimization
IEEE	Institute of Electrical and Electronics Engineers
CS	Cuckoo Search
BCS	Binary Cuckoo Search
SLRG	State Level Regional Grid
RIG	Region of Indian Grid
AP	Andhra Pradesh
TN	Tamil Nadu
KL	Kerala
KA	Karnataka
SRIG	Southern Region of Indian Grid

WRIG	Western Region of Indian Grid
ERIG	Eastern Region of Indian Grid
NERIG	North-Eastern Region of Indian Grid
NRIG	North Region of Indian Grid
HV	High Voltage
UHV	Ultra High Voltage
EHV	Extra High Voltage
NEW	North-East-West
UIG	United Indian Grid
FACTS	Flexible AC Transmission System
HVDC	High Voltage DC
Hz	Hertz
SOI	System Observability Index

ABSTRACT

The Wide Area Monitoring, Protection and Control (WAMPAC) of power systems are becoming essential tools for the system engineers in preventing blackouts. Whenever the power system operates in stressed mode and if suppose an event happens on a system element (particularly critical element), it may initiate cascading of events. At this condition, if the system engineers are unable to protect the rest of system and, control the abnormalities the system loses the power supply completely. This particular situation where the system loses generation-load balance is said to be Blackout condition. Interestingly, the WAMPAC schemes can enable the engineers to take remedial actions to avoid Blackouts by providing the synchronous data. This synchronized data will be provided by the device called Phasor Measurement Unit (PMU). So, the PMUs should be deployed in such a way that they could observe the system completely and economically. And, the process of installing of PMUs is subjected to different constraints.

Initially, an Optimal PMU Placement scheme (OPP) is suggested to obtain the minimum number of PMUs for system complete observability. It considers the observability constraints under both normal and abnormal conditions. This OPP problem also considers zero-injection buses for placing PMUs. This algorithm applies a Binary Cuckoo Search (BCS) technique to solve the OPP problem. The suggested method is tested on few standard IEEE test systems and has been practiced for different State Level Regional power Grids (SLRGs) of the Indian power grid and United Indian Grid (UIG). The obtained results are also compared with the methods that have been already applied for standard IEEE test systems and SLRGs, and were proved to be the best and effective. Also, to maximize the observability redundancy, the second contribution introduces Optimal Placement of Phasor Measurement Units for maximizing the observability. It uses a performance index called System Observability Index (SOI) with the help of n_p which represents the number of the buses observed for more than one time. The proposed method is tested on few of the IEEE test systems and then applied to Southern Region of Indian power Grid(SRIG).

The significant feature of Wide-Area Measurement System (WAMS) is to recover the data during communication failure. So, the third contribution presents a novel scheme of partitioning a PMU installed power network into a number of WAMS regions to make power system restoration process simpler. This algorithm also proposes the optimal placement of

Phasor Data Concentrators (PDCs) in each region to archive the data received from PMUs. This partition considers the restoration constraints like transformer equivalent bus, generation-load balance and the observability of region for the partitioning of a power system. The proposed scheme is demonstrated with an IEEE-30 bus system, and then applied to IEEE-39, IEEE-118 bus systems and Indian Grid (IG-75) system.

In practical substations, buses exist at different voltage levels. The bus which is being observed inside the substation should not translate to buses at other voltage levels becoming observed inside the same substation unless the tap ratios are known. And, all the methods developed were based on the thumb rule that the PMU installed bus could observe all the buses connected to it including itself even though the practical tap ratios are not known. So, the authors have assumed that the buses with different voltages can be decoupled. Unfortunately, it will increase both search space and bus number. From this, it is clear that the authors have only concentrated on reducing the number of PMUs rather than reducing substation number. To answer this, the fourth contribution has proposed the concept of optimal coverage of substation by assuming that one PMU could observe the whole substation provided the tap ratios are known. Thereafter, it introduces the identification of critical elements considering the Blackout concept. Finally, it proposes a new OPP problem considering the critical elements and the optimal substation coverage. The proposed method has been tested on some standard test systems and then applied to a practical Indian regional grid.

The fifth contribution proposes improved line protection against single phase-ground fault using synchronized phasor data. This algorithm prevents the relay from mal-operation caused by high fault resistance. The fault detection action will be taken according to a particular phase difference relation between fault point voltage and set point voltage. This method is tested on a practical single machine single line system.

This research has successfully proposes an accurate and robust wide-area measurement system, and maximizes the observability. Then it suggests a restoration strategy for a PMU-installed power system with minimum restoration time. Later, it identifies an optimal PMU set that could observe the critical elements in power system to avoid power system Blackouts. Finally, it suggest a simple and accurate fault identification technique which is immune to fault resistance,

Contents

Chapter-1:

INTRODUCTION

1.1. Wide Area Measurement System

A wide-area measurement system can be referred as a monitoring system that collects parametric data from the grid with more coarseness and in synchronized real time, and then utilize that information for safe operation, improved learning and grid reliability as shown in Figure 1.1. This advanced measurement technology provides a great informational means and operational structure that help in analyzing and monitoring the complex behavior exhibited by big power systems. The measurements taken from various parts of the system will not be fully integrated unless they were measured at an exactly same instant. The most important requirement of WAMS is that the measurements must be synchronized. These measurements are precisely time synchronized against the Satellite-based Global Positioning System (GPS). Then these measurements are combined to give an integrated and high-resolution view of power system operating conditions. The primary and also first data source for this particular system is the Phasor Measurement Unit (PMU) that produces extreme quality measurements of bus angles as well as frequencies in addition to more traditional quantities [1]. In their existing form, WAMS might be used as a stand-alone structure which supplements the grid's conventional Supervisory Control And Data Acquisition (SCADA) strategy. Like a complementary strategy, WAMS is mainly developed to improve the operator's real-time monitoring in the format of situational awareness together with the information utilized between systems to guarantee a secured as well as reliable electrical grid function. This wide-area data especially visualizes the dynamic state of the complete system.

A significant contribution involving WAMS technologies was proven during the failure of Western Electricity Coordinating Council (WECC), the Western power system on August 10, 1996. During this particular blackout, WECC system had been separated into four asynchronous islands alongside a heavy loss of load. The outcomes of this specific separation when compared with the dynamic data being supplied by WAMS have inspired too many strategic approaches like remedial action schemes (RAS) by the power utilities. The information reinforced that the power grid functioning in WECC is considerably depends upon the current strategy models. And, these models were proven to be insufficient in predicting system responses. The most prominent advantage with WAMS is the data constituting the precursors of the impending electrical grid failure. This data could have permitted the operators to take cautionary actions thereby minimizing the impact of

disturbance [2]. The cascading failure of 1996 was one of the most significant driving factors for additional WAMS improvement as well as enhancement.
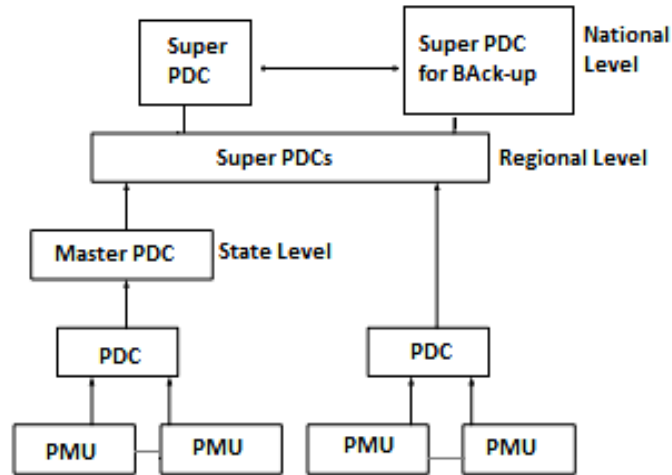
Figure 1.1: WAM structure

1.1.1. Phasor Measurement Unit

The Phasor Measurement Unit (PMU) measures the power system parameters like voltage, current, frequency etc. It is capable of measuring the synchronized phasors of voltage and current. This synchronism can be achieved by time sampling of the voltage and current waveforms using a common synchronizing signal from the Global Positioning Satellite (GPS). This makes the PMU the best and most important measuring devices in the foregoing power system monitoring, protection and control. Phasor Measuring Unit (PMU) uses GPS transmission for synchronizing the sampling clocks in-order to estimate phasors with a common reference. The first PMU was developed at Virginia Tech laboratory. PMUs provide instantaneous state of the entire power system. The GPS provides pulses at an accuracy of 1µs which corresponds to 0.018^{0} for a 50Hz system. The GPS signal with 1PPS uses a PLL to create the sampling pulses [3]. Figure 1.2 shows the functional representation of Phasor Measurement Unit.
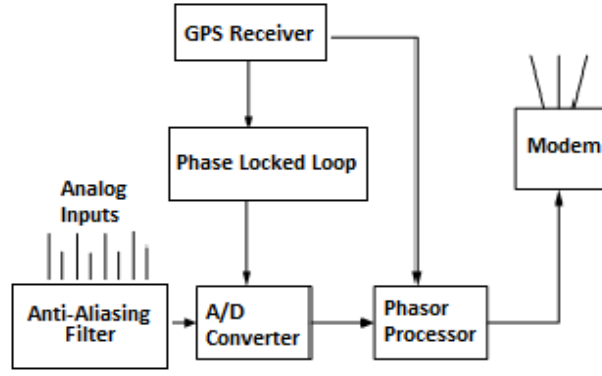
Figure 1.2: The Functional block diagram of PMU

1.1.2. Phasor Measurement Technique

A pure sinusoidal waveform can be represented by an unique complex number which is known as a phasor. Let us consider a sinusoidal signal as,

$$X(t) = X_m Cos(\omega t + \phi) \tag{1.1}$$

The phasor representation of this signal can be written as

$$X(t) = \frac{X_m}{\sqrt{2}} e^{j\phi} = \frac{X_m}{\sqrt{2}} (Cos\phi + jSin\phi) \tag{1.2}$$

The sinusoidal signal and its phasor representation are shown in Fig. 1.3. Most commonly, the phasor representation of an input signal is determined by applying the Discrete Fourier Transform (DFT) to the input signal.

1.1.3. Discrete Fourier Transform

Since the phasor calculation requires sampled data, an Anti-aliasing filter must be applied to the signal before the data samples are taken. An anti-aliasing filter limits the bandwidth of the pass band to less than or equal to ($\leq$) half of the data sampling frequency. This criterion is to satisfy the Nyquist criterion. And after, the phasor estimator calculates the phasor representation of the input signal.

If X_k (k=1, 2, 3…N-1) represents N samples of the periodic signal considered for one period, then the phasor representation is given by,

$$X = \frac{\sqrt{2}}{N} \sum_{k=0}^{N-1} X_k e^{-j2\pi k/N} \tag{1.3}$$

4
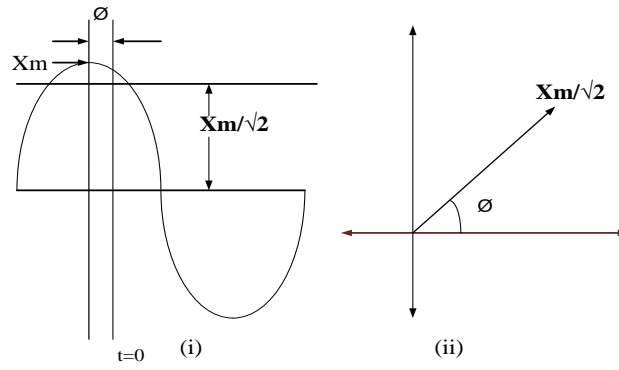
Figure 1.3: Phasor representation of a sinusoidal signal.

It is to be noted that for a real input signals the DFT results in complex conjugate components which will appear at '±ω'. The DFT eliminates harmonics from the input signal. PMUs use different types of updating formulas for phasor calculation as it is a continuous process. They may be non-recursive and recursive for the estimation of phasors during nominal frequency condition. Even though the non-recursive calculations are stable numerically, they are not suggested because of computational complexity. This problem can be overcome by a recursive formula keeping the same multipliers for common samples in two windows.

1.2. Applications of Wide-Area Data in Power System Protection

1.2.1. WAMS Based Fault Location

In general, the location of fault can be determined either based on phasor measurements or travelling wave concept. But, indeed it would be possible to estimate the location of fault from either of the ends if wide area measurements are used [4]. According to [5, 6], the fault can be determined based on fault detection index. This index is comprised of two complex phasors and the angle difference between them. The pictorial representation of a wide-area based fault detection and location method is shown in Figure 1.4. From Figure 1.4, based on the data collected by the relay from its local PMU, the relay sends a command signal to its circuit breaker. The communication channel enables the data transfer between the adjacent relaying units. Even though the series compensation improves transient stability and power transfer capability, it causes an uncertainty by means of the variations in series compensation voltage during a fault. So, the protection has become a most challenging job and an important topic of investigation for the relay vendors and protection experts.
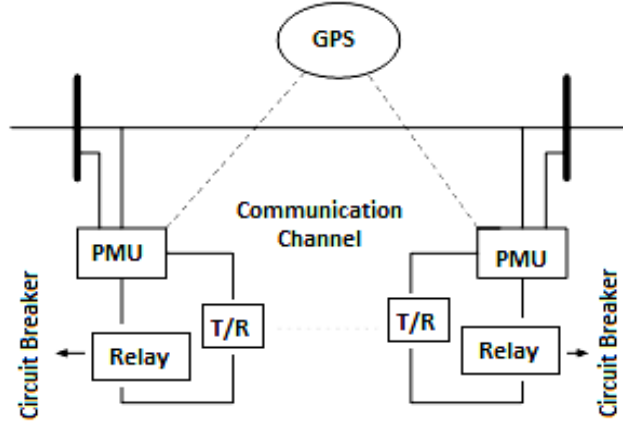
Figure 1.4: Wide area protection structure

Answering these issues, authors [7, 8] have initially studied the series compensation impact online protection strategies. A protection scheme with fixed and controllable series capacitors in combination with Metal Oxide Varistor (MOV) is suggested in [9]. Later, a WAM system based fault location algorithm is suggested in [10]. It calculates the voltage drop across the series compensation device by considering the device model. This algorithm needs the synchronous measurement data measured exclusively from the both ends of line to calculate the location of a fault in a line. The Wide-area measurements will also help in determining and identifying the faulty section by comparing the magnitudes of sequence voltages and the phase angles of sequence currents at each node [11].

1.2.2. Supervisory Control of Back-Up Zone Protection

In general, the back-up zone usually removes some of the system elements more than that of required by the operation of the primary zone of protection. It is particularly true in the case of zone-3 backup protection for the lines going away from substations with considerable in-feed. This is very dangerous during wide-area disturbances as it could lead to cascading failures as we seen recently during India blackouts [12]. Due to this, the back-up protection such as zone-3 was scrutinized and was removed in many situations. But this problem cannot be left unanswered as the back-up zone-3 protection is still required in certain scenarios. The only solution for this problem is to supervise zone-3 by monitoring the relays in its vicinity [13]. It means, if zone-3 sees impedance characteristics inside its protection zone then it should not be operated unless it is seen by the zone-1 relay. Moreover, the shortcoming in

using distance relays is that their settings have to be reset for every change in the network structure [14].

As shown in Figure 1.5, the back-up relay reach for long transmission lines would be set significantly large. Whenever the loading of line increases, the apparent impedance seen by this relay approaches, and may enter the tripping zone of relay under very heavy loads and lead to tripping. This condition where the impedance characteristic observed by distance relay enters the relay protective zone due to the power shift in transmission line is referred as load encroachment.
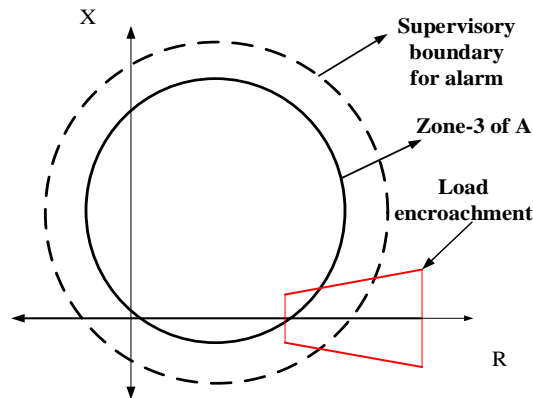
Figure 1.5: Load Encroachment effect on zone-3 Characteristics

The WAMS data can give us an additional perspective to determine whether there is a need to take preventive action necessarily or not. This can be done by allowing the relays to differentiate a trip condition from a block condition using multiple views of the system. The adjacent PMUs provide excellent information for supervising the over-reach of distance relays. For the system in Figure 1.6(a), using the information from the buses B and C, relay A can identify a violation of load-ability limit with respect to a system fault and decides whether Zone-3 pickup is appropriate. From Figure 1.6(b), if zone-3 of relay A picks-up, the PMUs at relays B and C would be asked to find whether the apparent impedance seen by them represents a fault or not. If the impedance trajectory is not due to a fault, then obviously the pick-up of zone-3 at relay A is due to something other than a fault, and it must be stopped immediately from tripping.

1.2.3. Adaptive Out-of-step Relaying

An out-of-step relay calculates the rotor angle difference between two equivalent systems and utilizes it along with breaker status to determine swing stability.
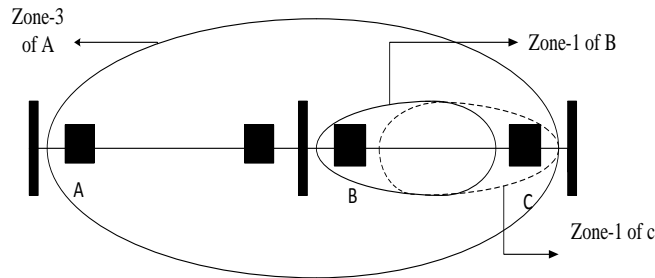
Figure1.6(a): SampleTestSystem
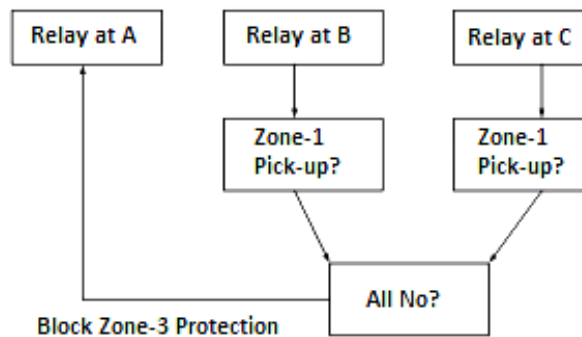
Figure 1.6(b): Supervision of zone-3 protection

Once the out-of-step condition is detected, the selective tripping order will be issued. The selective tripping must ensure a reasonable load-generation match within each island. When a transient occurs, most of the line relays see apparent impedance in their R-X plane. As depicted in Fig. 1.7, during power swing, the distance relay at bus A may see two types of impedance trajectories (Z-Z or Y-Y).
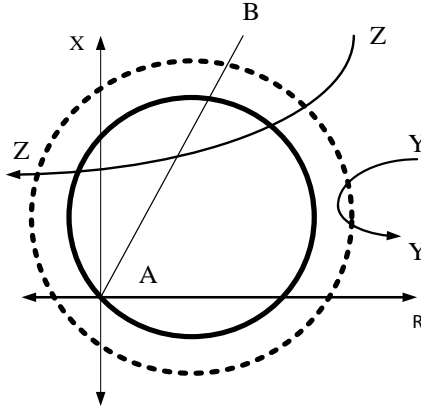
Figure 1.7: Impedance trajectory during transients.

The trajectory Y-Y corresponds to stable swing while the trajectory Z-Z corresponds to unstable swing. In any case, it is clear in that the impedance trajectory might enter any one of the trip zones of the relay. And, the traditional out-of-step relays have been known to mal-operate as the prevailing system conditions have not been foreseen during their design. But, the PMU based adaptive out-of-step relay recognizes the changes in the power system and adapt the settings accordingly.

During the outage of an important transmission line, the adaptive out-of-step relay installed between two systems predicts the power angle characteristics of the post-clearing system and calculates the successive relative angle measurements to estimate the phase shift in mechanical power (P_m) during the loss of generation [15]. Along with the above applications, PMU technology can also be applied in system validation and accurate postmortem analysis.

1.2.4. Coherent Group Detection

A coherent group is a specific group of generators in which all the generators, after an occurrence of disturbance, swing together. On the occurrence of disturbance the rotor angle difference between any two generators will be drifted. This makes the group of generator swing away from the rest of the system [16]. On the clearance of disturbance, this group will swing back to synchronism with the remaining part of the system. While analyzing transient stability, this group of generators can be referred to a single equivalent generator which removes high frequency and inter-generator modes from.

After the occurrence of fault, if coherent units have same velocity and acceleration, their phase angle differences will become constant and it is given by

$$\delta_x(t) - \delta_y(t) = \delta_{xy}(0) = const\,ant \qquad (1.4)$$

$$\frac{d}{dt}\delta_x = \frac{d}{dt}\delta_y$$

$$\frac{d^2}{dt^2}\delta_x = \frac{d^2}{dt^2}\delta_y \qquad (1.5)$$

The wide-area information obtained from the PMUs located nearby generators or group of generators is used to calculate the frequency and the rate of change of frequency. Then, from the equations (1.4), (1.5) and the calculated data from synchronized measurements, it could be straightforward to identify the group of generators referred as a coherent group.

1.2.5. Intelligent islanding

Once the coherent groups were found, the next step is to either adapt out-of-step relay if the rate of change of frequency is stable or separate the coherent group from the rest of the system intelligently if the rate of change of frequency is unstable. Intelligent islanding is the process of separating an unstable swinging group from the stable system intelligently. Here, intelligence means nullifying the generation-load mismatch in each new area by the proper shedding of loads prior to separation process [17]. This intelligence will come either by estimating the phasor difference between two areas or by observing the differential frequency in the same two areas, as shown in Fig. 1.8 [18].

This estimation of phasor difference or differential frequency in two islands could be effective if there is a dedicated PMU on each node of the inter-tie line connecting two areas.
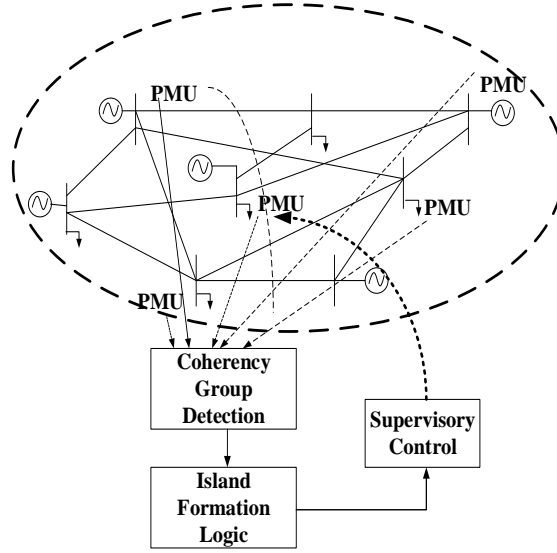
Figure 1.8: Intelligent islanding based on coherency group detection

1.2.6. Adaptive Loss-Of-Field Relaying

When the field of an alternator is lost the synchronous machine draws reactive power from an infinite bus connected to it. This excess reactive power drawn by the machine may damages rotor. This, in turn, reduces the voltage at the terminals of the synchronous generator, and causes Loss-Of-Field (LOF). Again, this condition immediately causes severe voltage collapse in the rest of the system connecting to it. Hence, the LOF condition should be identified as fast as possible. During LOF, the final impedance locus falls into the fourth quadrant of R-X diagram, as shown in Fig. 1.9. So, any relay exhibiting its operating characteristics in fourth quadrant is appropriate for this application.

The LOF relay settings include the Thevenin reactance (X_t) of the power system at generator terminals and the synchronous reactance (X_d) of machine. As any configuration change in the system near to an alternator terminals changes X_t, the relay should be able to adapt to these variations and to estimate the new setting for a unit or group of units. From Figure 1.9, the deep inner circle represents LOF characteristics of a traditional relay. When the network configuration changes, a new LOF setting corresponding to the new network configuration will be measured from the wide-area knowledge, and then the relay will adapt itself to the new condition [19]. The middle circle is the adaptive characteristic of the relay obtained from the wide-area data available at the terminal of the generator.

11
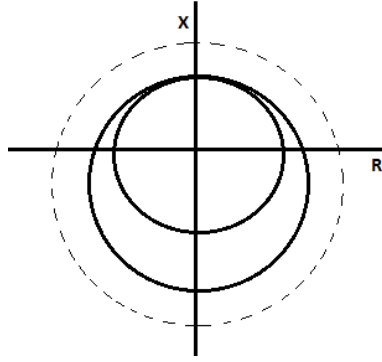
Figure 1.9: Adaptive LOF relay

The outer circle in Figure 1.9 serves the supervision of relaying during the opening of a field, shorting of field and voltage regulator failure. This characteristic was drawn by estimating the impedance locus at generator terminals for different contingencies.

1.2.7. Adaptive system restoration

As the blackouts are unavoidable, it is mandatory that the strategies for restoring power should be at reduced cost and with less delay. So, more importance is given to the immediate power restoration in-order to minimize the inconvenience to users. The pre-calculated restoration approaches available from the planning studies are inappropriate because the present system condition might be completely different from the one considered during planning studies [20, 21]. The real-time wide-area data provides a powerful alternative for formulating a restoration policy which takes the prevailing state of the power system into account [22]. Even though many computerized restoration methods are available to apply, it is enticing to use an accommodative restoration strategy in which the computer program recommends a restoration plan for any islands that have been formed and blacked-out and can be reconnected once they have been energized.

The real-time data provided by PMUs has helped much in restoring the power system after European blackout in 2003 by providing the review of phase angle information that was not known during the restoration of initial line outage [23]. During the recent disturbance in Europe on November 4, 2006 [24], PMU has revealed the readings of re-closing attempts between two areas including the final successful re-closing between those two areas and eventually with the third area. In the absence of real-time data, many unsuccessful attempts were made to restore the system successfully because successful restoration could only be attained after the phase angles of two separated areas became agreeable.

1.2.8. Adaptive dependability and security

In general, relays have two states of failure. They are, the relay should not operate when it should, and the relay will operate when it may not be required. These two situations can be described as "security and dependability". Whenever the relay fails to trip during a fault, the system may be driven into instability. So, irrespective of the optimal clearing, it is necessary to clear the fault within the primary clearing time without fail. But, every non-optimal operation of relay costs an acceptable inconvenience. This is the significance of high dependability in power system protection under normal conditions [24].

When the power system is in stressed state, the consequence of a mal-trip is far more catastrophic. This could result in cascading failures and lead to a complete system blackout. An adaptive security-dependability problem can be answered by considering three protection systems and by a voting logic from all of them. The scheme of improving security-dependability balance is presented in Fig. 1.10. Here, the wide-area data will play a vital role in giving the trip signal to breaker just by taking the decision from the remaining two of the three relays. Even though this increased security reduces dependability; this avoids cascading failures and improves reliability under stressed condition. One of the most familiar examples of improving security-dependability balance is the adaptation of zone-3 protection. The attractive feature of this adaptive voting is that it generates tripping logic without modifying actual relays.
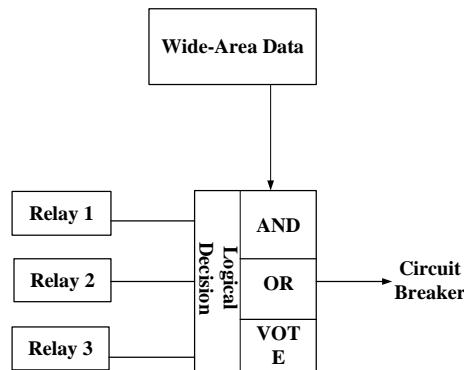
Figure 1.10: WAM based Adaptive Dependability and Security

Along with the above applications, wide-area measurements could also help in the following applications [25]:

- Generation-load mismatch detection

- Identification of generator trip locations
- Many more applications in the sense of power system monitoring and controlling.

1.3. Introduction to Optimal PMU Placement

The PMU located on one bus not only measures its own voltage phasor but also the current phasors in all lines connected to it. Hence, using Kirchhoff's Laws the PMUs located at one bus observe its own and all the buses which are connected to it. The goal of optimal PMU placement (OPP) problem is to identify the minimal set of PMUs along with their placement to observe the system completely.

1.3.1. Concept of Observability
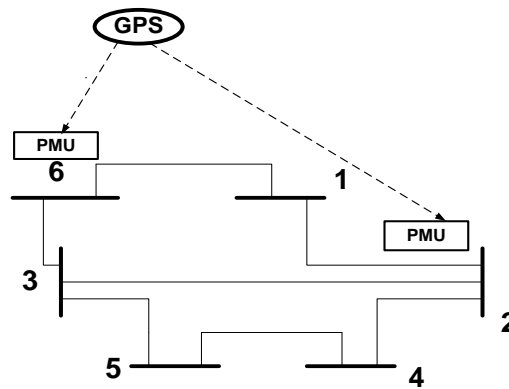
Figure 1.11: IEEE-6 bus test system

Figure 1.11 shows an IEEE-6 bus system installed with the PMUs located at buses 6 and 2. The bus whose measurements are taken directly by a PMU mounted over it is called a 'directly observable bus'. And, the bus whose measurements are taken by a PMU installed on a bus connected to it is called an 'indirectly observable bus'. From the Figure 1.11, the buses 6 and 2 represent direct observable buses whereas the buses 1, 3 and 4 represent indirectly observable buses. If the bus is neither a direct bus nor an indirect bus, the bus can be called as unobservable bus. Here, bus 5 represents unobservable bus. For an electric network to be completely observable, it is indispensable that all of its nodes should be observable either directly or indirectly.

1.3.2. The significance of ZIB in OPP problem

Generally, zero-injection buses (ZIBs) are switching-stations. As their behavior is significant during abnormal conditions, they cannot be ignored from wide-area monitoring.

And, they should be considered as normal buses while forming OPP problem. Even though this consideration increases the search space and reduces the solution speed, under abnormal conditions, the idea of locating PMUs considering zero-injection buses makes the monitoring of the system more reliable. As the planning studies are judged by their accuracy rather than their speed of operation, the present problem has mainly concentrated on accuracy in placing PMUs than the speed of operation.

The cost of PMUs varies according to the number of channels available for measurement. PMUs with limited number for channel can make limited number of channels observable. So, the selection of channels will influence the number of PMUs.

1.4. Literature Review

1.4.1. Observability based PMU placement

An integer linear programming (ILP) based optimal PMU placement for system observability was introduced in [26]. An ILP based method for electrical networks with and without conventional measurements was implemented in [27]. Later this method was extended in [28] to ZIB effect. The algorithm [29] extends to incorporate conventional measurements to identify the optimal PMU locations. This scheme also gives the PMU locations under any desired level of redundancy. An ILP based multi-stage PMU placement is suggested in [30]. It models zero-injection constraints as linear. In [31], a nonlinear integer programming problem is transformed into an equivalent integer linear programming (ILP) for the joint placement of PMU and conventional measurement units.

Paper [32] suggests another IQP approach that uses the network connectivity matrix to determine optimal PMU locations. Authors [33-35] have solved the OPP problem for system complete observability using DFS algorithm. The PMU placement strategies using this approach are presented in [35, 36].

In [37], pioneering research on PMU placement is proposed using simulated annealing (SA). A rule-based OPP considering unobservable buses is presented in [38]. Later, authors [39] have suggested a graph-theoretic approach using SA to solve the pragmatic communication-constrained PMU placement problem. Sensitivity constrained OPP method to ensure the dynamic data of power system by observing the system completely is suggested in [40].

The PMU placement for system complete observability using GA is proposed in [41]. In [42], an immunity genetic algorithm (IGA) is applied to identify the PMU locations for system complete observability. A binary PSO based optimal PMU placement considering line/PMU outage is proposed in [44]. But, it hasn't considered zero-injection buses and channel limits. In the presence of conventional measurements, authors have suggested another PMU placement strategy using binary PSO in [45]. It considers zero-injection effect.

In [46], a Tabu Search (TS) which is a gradient-descent optimization method is applied to solve the OPP for complete observability. On integrating the Differential evolution (DE) with the Pareto non-dominated sorting and differential evolution algorithm, a PMU placement technique has been proposed in [47]. Iterated local search (ILS) based PMU placement is suggested in [48] based on the assumption that a PMU installed bus could estimate the current phasors leaving that particular bus. Based on the Greedy algorithm, a secure PMU placement against data injection attacks is developed in [49]. A Multi-objective PMU Placement method Considering Observability and measurement Redundancy using ABC Algorithm is suggested in [50].

To make the wide-area monitoring system robust, the OPP problem should offer complete system observability by considering the outage of any transmission line or a loss of PMU (or loss of its communication link). Very few papers have considered these two aspects as critical, and implement efficiently. For instance, article [51] presented an OPP solution by considering some pre-specified contingencies which could drive the system into instability. But there were very few chances for these contingencies to occur even though they are critical for the system stability. A three-stage optimal PMU placement method is presented in [52] using network connectivity information. It considers single PMU outage with and without considering the zero-injection bus. The integer quadratic based PMU placement policy was suggested in [53] without including zero-injection effect. It considers both normal as well as the outage of a transmission line or PMU conditions. But, it hasn't considered channel limitations. References [54, 55] recommended the OPP methods considering contingencies for conventional measurement devices. Also, the method in [56] presented an optimal solution for OPP problem taking a single measurement/branch contingency into account. Recently papers [57] and [58] have proposed an ILP based OPP problem considering the depth of one un-observability and one redundancy respectively. Unfortunately, they failed in considering

16

line/PMU contingencies and channel limits together. Also, none of them have considered Zero-Injection buses.

1.4.2 Power System Restoration based WAMS Partition

After the blackout, the power system elements are needed to be restored. This can be achieved by a restoration strategy called Build-up strategy. As the delay in the restoration causes inconvenience to consumers, and subjects the system to many economic and political costs, the power system restoration should be fast and effective. From the power system studies proposed in [59], a Build-up strategy is recommended here. It follows mutual interconnection of islands after restoring them separately. The Build-up strategy and its importance are clearly explained in [59-62]. But the authors are failed in introducing the ideas to sectionalize a network into separate islands. Later, authors suggested a scheme [63] to sectionalize a system into separate islands, but it is said to be failed in producing more number of islands as it doesn't consider Generation-Load constraint during initial partitioning.

1.4.3 Critical elements Based PMU Placement

While placing PMUs considering the critical contingencies, it is essential to implement a policy that considers both the lines and buses based on their role in driving the system to system blackout. In [64], critical elements are identified based on their transient behaviour using fuzzy classification. But, the definition of fuzzy variables has made it more complicated. Later, paper [65] has identified critical buses based on their bus connectivity their operating voltage levels. Similarly, paper [66] presents an OPP problem taking a single contingency into account. But, nowhere, they have considered critical transmission lines/buses outage that could lead to the system blackout. So, apparently, the resultant optimal placement would never assure a secured wide-area protection system.

1.4.4 Protection of transmission line in power system

Initially, a two end phasor estimation based line protection algorithm was introduced in [67]. Later, a fault detection index based algorithm [68-70] was suggested. In [71-76], synchronized voltage and current measurements obtained from both the ends of a line were used to determine the fault. Considering arcing, fault location algorithm was proposed in [77, 78]. Later, authors found that the decaying D.C. component present in transient current is

having a significant effect in estimating the fault [79, 80]. So, authors propose an algorithm for removing decaying D.C component to detect faults in the transmission system accurately in [81]. After, a mimic filter is designed to eliminate the D.C. offset [82]. A method based on the recursive relation between even and odd samples was proposed in [83] to develop a modified DFT algorithm to identify faults. Later, an iterative current filtering technique is suggested in [84]. Even though all these methods were accurate enough, they were compromised with time because of their complexity. Moreover, they haven't suggested any idea to improve the immunity of protection algorithm to the resistance involved faults.

Later, [85, 86] outline a fault detection method for resistance faults by compensating resistance calculated from the power at relaying point. Next, high-resistance faults are identified by differentiating the active power flow [84]. Recently, by calculating the real power drawn by the fault resistance the in-line fault has been found [88]. Authors [89, 90] have improved the immunity of protection by adjusting the relay setting values. But, all the above methods haven't used the voltage phasor data for their analysis even though they have succeeded in detecting the ground faults involving fault resistance. Very recently, a line protection method is proposed by comparing the voltage phasors [91]. But significantly, this method has not considered synchronized data for its estimation.

1.5   Motivation and Contributions

Just before the Blackout in India in July 2012, the system was weakened by several scheduled outages of transmission lines connecting two significant areas of the NEW Grid i.e. Western region (WR) with Northern region (NR) boundary. That time Bina-Gwalior-Agra (a single) line was the only main 400kv AC inter-tie line connecting these two boundaries. As many of the NR utilities drew excessive power from the grid, there was an overloading on this inter-tie link, which eventually got tripped by zone-3 of distance relay. This was happened just because of the load encroachment seen by zone-3 distance relay. But, however, no fault was observed there. Since the inter-regional tie was weakened already, the tripping of 400 kV inter-tie line has stimulated the NR system to completely isolate from the WR. This has initiated the condition of blackout [92]. If we observe the sequence of events:

1. Inter-regional transmission corridors connecting Western region (WR) with Northern region (NR) were weakened by several scheduled outages of transmission lines.

2. Overloading on Bina-Gwalior-Agra inter-tie link.

3. Mal-tripping of inter-tie line by zone-3 relay.

The recommendations made by the committee are [93]:

1. To deploy adequate number of PMUs to improve the visibility and real-time monitoring of power systems.

2. To formulate a faster restoration algorithm.

3. To monitor the critical elements closely.

This case is just one of many examples where mal-operation of protection schemes, whether by design flaw, or poor maintenance, or simple mistakes, have played a significant role in large events on the grid. As the society depends so heavily on the critical energy infrastructure, large events on the grid reflect directly on its economies. Thus, the idea of using wide-Area data measurement strategy would be more effective as this data increases the reliability and security of the electric grid by making the WAMPAC philosophy accurate.

Moreover, in power systems, line-to-ground fault is the most frequent fault. Particularly, if a line-to-ground fault occurs with fault resistance, it may mal-operate the relays protecting that particular zone. Sometimes, this causes unnecessary tripping of healthy lines, and it may lead to cascading failure. So, there is a need of extensive research in the area of power system protection.

In this research, after suggesting the optimal PMU placement strategy considering normal and abnormal constraints, it formulates a methodology to maximize the observability redundancy. Then it presents the design and partition of WAMS considering stable restoration policy. And then, it formulates critical element based PMU placement considering optimal substation coverage. At last, an improved line protection scheme against single phase-ground fault using synchronized phasor data is proposed.

1.6. Organization of the Thesis

The thesis work is organized into six chapters and presented as follows:

The **first Chapter** introduces to Wide-Area Measurement System and Phasor Measurement Unit. Later, it gives a brief insight into the principle of measuring phasor quantities using phasor measurement units. Then, it provides the applications of phasor measuring units exclusively for improving power system protection.

In the **second Chapter,** PMUs have been placed in the power system considering ZIB buses for placement. This placement has considered three types of constraints such as normal operating conditions, line/PMU failure conditions, and channel limits. This optimization is carried out using Binary Cuckoo Search (BCS) algorithm. After validating the algorithm with standard IEEE test systems, it is applied for different Regional Indian Grids (RIGs).

In the **third Chapter**, to maximize the observability redundancy, we introduced a performance index called System Observability Index (SOI) with the help of n_p which represents the number of buses which would be observed for more than one time. The proposed method is tested on few of the IEEE test systems and then applied to Southern Region of Indian power Grid(SRIG) of Indian Power Grid.

In the **fourth Chapter**, a restoration based sectionalizing method for a PMU installed network is proposed. It considers power generation-load balance constraints during initial system partitioning. It also considers observability constraints at the final stage of the sectionalizing process. These two constraints have increased the stability and observability of feasible islands. In the end, it also suggests an optimal location strategy for Phasor Data Concentrators (PDCs) to provide phase angle data across the lines between any two islands.

In the **fifth Chapter**, the optimal coverage of substation has been done by assuming that one PMU could observe the whole substation provided the tap ratios are known, and then introduces critical elements identification in the Blackout point of view. Finally, it proposes a new OPP problem considering the critical elements whose outage lead to system blackout, and the optimal substation coverage.

In the **sixth Chapter,** an improved line protection scheme against single phase-ground fault using synchronized phasor data is proposed. This algorithm prevents the relay mal-operation caused by high fault resistance. This algorithm calculates the phase difference between relay point voltage and fault point voltage based on the relation between negative sequence of relay point current and fault point current. After, the calculated phase difference between relay point voltage and fault point voltage will be compared with set-point voltage phase referred from the relay point voltage phase. The fault detection action will be taken according to a certain phase difference relation between fault point voltage and set point voltage.

The **seventh Chapter** concludes the research. It also presents the future scope of this research work.

Chapter-2:

OPTIMAL PMU PLACEMENT FOR POWER SYSTEMS UNDER BOTH NORMAL AND LINE/PMU FAILURE CONDITIONS USING BINARY CUCKOO SEARCH (BCS)

2.1. Statement of the OPP problem

The PMU located at a bus measures not only its voltage phasor but also the current phasors in all the lines connected to it. As the line parameters are already available, the PMUs located at one bus observe all the buses which are connected to it using Kirchhoff's Law. The goal of OPP problem is to calculate the minimal set of PMUs and their locations to observe the system completely. The problem can be formulated as follows:

Minimize

$$\sum_{q \in N} x_q \tag{2.1}$$

Subjected to

$$s_p(x) \geq 1 , \quad \forall p \in N \tag{2.2}$$

Where

$$s_p(x) = \sum_{q \in N} c_{pq} x_q , \quad \forall p \in N \tag{2.3}$$

Here, x_q represents binary decision variable for PMU at bus q; p and q are the bus indices; N represents the set of network buses. Equation (2.1) represents the objective function for PMU installation. From equation (2.2), s_p represents bus observability function at bus p. The binary connectivity parameter c_{pq} can be defined as,

$$c_{pq} = \begin{cases} 1, \text{if } p = q \\ 1, \text{if buses } p, q \text{ are connected} \\ 0, \text{otherwise} \end{cases} \tag{2.4}$$

For the bus to be observable, it must be connected to at least one PMU-installed bus. So, for the bus and all its incident buses to be observable the value of observability function s_p should be equal to or greater than 1.

2.1.1. Considering Abnormal Condition

In this section, we will consider the contingencies like line outage and/or measurement failure to formulate a line/PMU failure constraint.

2.1.1.1. Line outage/PMU failure Constraint

The set of Observability functions for PMU failure case will also have the connectivity parameters for line outage case. So, the set of observability constraints for line outage case is a subset of the observability constraints for PMU failure case. The idea of

adding these two sets of constraints logically will provides the observability on the either of the two cases. In this proposed method, to consider line outage/ loss of PMU, the constraint equation (2.2) can be rewritten as,

$$s_p \geq 2, \quad \forall p \in N, \quad \forall l \in L \tag{2.5}$$

2.1.1.2. Channel limitations

The data measured from PMUs will be communicated to the data concentrators located at regional and national level dispatch centres. This needs the PMUs featuring multi-channel communication. But, the proposed OPP problem considers the channel limits. This consideration is taken into account by replacing $\sum c_{pq} x_q$ with $\sum c_{pq} m_{pq} xq$ in (2.3). So, the observability function becomes,

$$s_p = \sum_{q \in N} c_{pq} m_{pq} x_q, \forall p \in N \tag{2.6}$$

Where, m_{pq} is calculated such that,

$$\sum_{q \in N} c_{pq} m_{pq} \leq m_q^{\max} \tag{2.7}$$

Here, the variable m_{pq} represents the measurement at bus p with the PMU located at q bus. And, m_q^{max} represents the maximum number of channel measurements at bus q. In this work, m_q^{max} is taken to be 3.

The present OPP problem is binary optimization problem whose solution is a set of zeros (0s) and ones (1s). Here, binary one represents presence of PMU and binary zero represents absence of PMU. Since the proposed algorithm is needed to be solved using a binary coded optimization tool, we have come up with a meta-heuristic algorithm called Binary Cuckoo Search (BCS) which has the capability of handling binary optimization problems.

2.2. Proposed Binary Cuckoo Search (BCS)

The peculiar behavior of the cuckoo bird is that it lays eggs in a bird's nest to let that bird hatch eggs. Then it follows different strategies to minimize the chances of destroying eggs by the host bird. This strategy and behavior have led to the introduction of a new naturally-inspired optimization algorithm called Cuckoo Search (CS) algorithm [94]. This Meta-heuristic algorithm was invented by Xin-SheYang and Suash Deb in the year of 2009. From the basic cuckoo search algorithm, each cuckoo uses Levy's flights to search a new nest for laying its egg. Levy flight is a model walk function to direct a cuckoo towards a new nest, which is random and characterized by some pre-defined step lengths for obeying power-law

distribution. These levy flights are very helpful in optimizing any problems of engineering and sciences. According to standard CS, every cuckoo will search for the nest on ensuring the following rules ideally.

Rule 1: Each cuckoo should lay only one egg at a time, and choose nest randomly.

Rule 2: The best nest with an egg of most and highest fitness should be passed on to the next generation.

Rule 3: The number of host nests should be fixed, and the probability (p_a) with which the host bird can discover the egg laid by the cuckoo should lie in the range of [0, 1], i.e., $p_a \in [0, 1]$.

The equations 2.8 and 2.9 together help in generating new solution using levy flights with their random steps from the levy distribution function. Moreover, the random walk process helps cuckoo in its consecutive jumping by obeying power-law step-length distribution with a heavy tail.

$$x_i^{t+1} = x_i^t + \alpha \oplus levy(\lambda) \tag{2.8}$$

$$levy \sim u = t^{-\lambda} \tag{2.9}$$

Here, x_i^t and x_i^{t+1} are the solutions at instants t and t+1. Parameter α represents the step size whose value varies according to the scale of the problem of interest. The operator $\oplus$ does the entry-wise multiplications. Even though this operator is as similar as that of PSO, the random walk in CS is more efficient than that of PSO. The search space for the standard CS is continuous, means its solution is a set of real number. Hence, it cannot be applied for the problems like binary optimization problems (example: OPP problem) whose solution should be in terms of bits. So, a new version of CS algorithm, called Binary Cuckoo Search, is introduced here, which can handle binary optimization problems.

2.2.1. Binary Cuckoo Search (BCS)

Essentially the BCS contains two functional blocks. The first block contains two cuckoo dynamic operations namely Levy flights and binary solution representation (BSR) [95]. Here, Levy flight will be used to search a new cuckoo. As the main intention of applying BCS is to handle binary optimization problems efficiently, the BCS has to transform a real-valued solution (x_r) to a binary value (x_b). This can be done with the help of sigmoid function. The sigmoid function will calculate the flipping chances of each cuckoo. Later, these flipping

chances will be used to compute the binary value of that particular cuckoo. This transformation can be done as follows:

$$\sigma(x_r) = \frac{1}{\left(1 + e^{x_r}\right)} \qquad (2.10)$$

Where $\sigma(x_r)$ represents the flipping chance of bit 'x_b'. After getting $\sigma(x_r)$, we will compare it with a randomly generated number γ, where $\gamma \in [0,1]$ for each dimension of 'r'. Then the transformation will be done as follows [94].

$$x_b = \begin{cases} 1, if \gamma < \sigma(x_r) \\ 0, otherwise \end{cases} \qquad (2.11)$$

These two operations (Levy flights and BSR) will combine the basic CS algorithm, with a sigmoid function to achieve BCS. The second functioning block consists both selection operator and objective function. Here, the selection operation is nothing but the elitism phenomenon that is applied in the genetic algorithm.

2.2.2. BCS Algorithm

step1: Read Abandon factor, P_a and the objective function represented interms of objective and constraints.

step2: Initialize the population of N host nests, where, N is the number of network buses. Nest represents the set of solutions. Each bit in a solution represents the bus number.

step3: while (t<maximum generation) or (convergence criterion), repeat the steps 4 to 12. Otherwise, stop the procedure.

step4: Obtain a cuckoo (let i) randomly using Levy flight

step5: Obtain its binary representation by BSR algorithm and calculate its fitness S_i.

step6: Select a nest from N (let j) arbitrarily

step7: Obtain its binary representation by BSR algorithm and calculate its fitness S_j.

step8: If (S_i>S_j), replace j by the new solution and go to next step9, else go directly to step9.

step9: Obtain the binary representation from the BSR algorithm for all nest and, evaluate their fatnesses.

step10: Abandon a fraction(P_a) of worse nests. Build new nests at new locations via Levy flights.

step11: Obtain the binary representation there, using BSR algorithm and, calculate their fitness.

step12: Keep the nests with the highest fitness, and arrange the solutions in descending order

of their fitness, and find the latest best.

The application of BCS to the proposed problem is explained in Appendix-C with the help of IEEE-9 bus system.
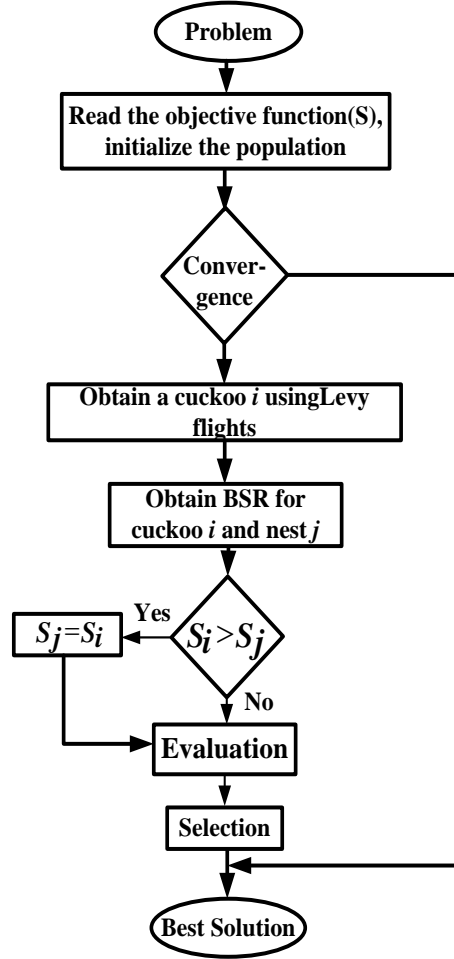
Figure 2.1: Flowchart of the proposed Binary Cuckoo Search (BCS)

2.3. Results and discussions

2.3.1. IEEE- standard test systems

The proposed BCS technique is tested, as given in Tables 2.1, 2.2, 2. 4 and 2.5, on IEEE-9, IEEE-14, IEEE-30, IEEE-57 IEEE-118, and then, applied for different state-level regional grids and SRIG. It is observed that it has improved the results for all systems, particularly for large systems. When this technique is applied for IEEE-9, IEEE-14, IEEE-30, IEEE-57and IEEE-118 systems [96], it produced best results, as shown in Tables 2.3 and 2.6, for all the cases like complete observability with and without considering channel limits, complete observability under

line/measurement outage with and without considering channel limits. Later, the proposed BCS based OPP method is applied to different State Level Regional Grids (SLRGs) of Southern Region of Indian Power Grid (SRIPG), different Region of Indian Power Grids (RIPGs) of India and the complete SRIG.

Table 2.1: PMU locations under normal operating conditions

System	Locations of PMUs	Total no. of PMUs
IEEE-9 bus	4,6,8	3
IEEE-14bus	2,6,8,9	4
IEEE-30bus	2,4,6,10,11,12,19,24,26,29	10
IEEE-57bus	1,4,9,20,24,27,29,30,32,36,38,39,41,45,46,51,54	17
IEEE-118bus	2,5,9,12,13,17,21,23,26,29,34,37,42,45,49,53,56,62,64,71, 75, 77,80,85,86,90,94,101,105,110,115,116	32

Table 2.2: PMU locations under normal operating conditions considering channel limits

System	Locations of PMUs	Total no. of PMUs
IEEE-9 bus	1,6,8	3
IEEE-14bus	2,6,8,9	4
IEEE-30bus	1,2,6,9,10,12,19,23,26,27	10
IEEE-57bus	1,6,9,15,19,22,25,27,29,32,36,38,39,41,46,50,54	17
IEEE-118bus	3,5,10,12,15,17,21,23,25,29,34,37,42,45,49,53, 56,62,64,68,71,75,77,80,85,87,90,92,96,100,105, 110,115	33

Table 2.3: Results comparison for complete observability under normal conditions

method	IEEE-9	IEEE-14	IEEE-30	IEEE-57	IEEE-118
BCS	3	4	10	17	32
IP[26]	n/a	4	10	17	32
ILP[27]	n/a	4	10	17	32
BPSO[45]	n/a	4	n/a	17	32
IP[29]	n/a	4	n/a	n/a	32

This says that, unlike other techniques, the proposed method has been tested on all IEEE test systems and has proven that it finds the optimal number of PMUs successfully.

Table 2.4: PMU locations under Line/PMU failure

System	Locations of PMUs
IEEE-9	1,2,3,4,6,8
IEEE-14	1,2,3,6,7,8,9,11,13
IEEE-30	1,2,4,6,7,8,9,10,11,12,13,15,17,18,19,21,24,25,26,29,30
IEEE-57	1,2,4,6,9,11,12,15,19,20,22,24,25,26,28,29,30,32,34,36,37, 38,39,41,44,46,47,50,51,53,54,56
IEEE-118bus	1,3,5,7,9,10,11,12,15,17,19,21,22,24,26,27,28,30,31,32,34,36, 1,3,5,7,9,10,11,12,15,17,19,21,22,24,26,27,28,30,31,32,34,36,108, 110,111,112,114,116,117,118

*.n/a: Not applied

Under line/PMU failure, since each bus should be observed by atleast two PMUs, the required number of PMUs under line/PMU failure becomes more than that under normal condition.

Table 2.5: PMU locations under Line/PMU failure considering channel limits

System	Locations of PMUs	Total no. of PMUs
IEEE-9	1,2,3,4,6,8	6
IEEE-14	2,4,5,6,7,8,9,10,13	9
IEEE-30	1,3,5,6,7,8,9,10,11,12,13,15,17,18,19,21,24,25,26,29,30	21
IEEE-57	1,3,4,6,9,11,12,15,19,20,22,24,26,28,29,30,31,32,33,35,36,38,39,41,45,46,47,50,51,53,54,56,57	33
IEEE-118bus	2,3,5,6,9,10,11,12,15,17,19,21,22,24,25,27,29,30,31,32,34,35,37,40,42,44,45,46,49,50,51,52,54,56,59,62,64,65,66,68,70,71,73,75,76,77,78,80,84,85,86,87,89,90,92,94,96,100,102,105,107,109,110,111,112,115,116,117	68

Table 2.6: Number of PMUs for complete observability under Line/PMU failure conditions

method	IEEE-9	IEEE-14	IEEE-30	IEEE-57	IEEE- 118
BCS	6	9	21	32	68

This says that, we have exclusively found the number and the locations of PMU under line/PMU failure (on ignoring zero-injection effect) required for the system complete observability. Since the channels are limited to 3 and, each bus, in almost all the test systems, could dedicatedly observe at most 3 of its adjacent buses through incidence lines, the change in PMU number is not significant from the OPP without channel limits to the OPP with channel limits.

2.3.2. Southern Region of Indian power Grid

Southern Region of Indian power Grid (SRIG) consists Kerala (KL), Karnataka (KA), Tamil Nadu (TN) and United Andhra Pradesh (AP) states [97]. The BCS presented in the previous section is applied to each State Level Regional Grid and then to southern Region of Indian Power Grid.

2.3.2.1 United Andhra Pradesh (AP)

It consists of 76 buses (of both Andhra Pradesh and Telangana states) connected through 112 lines. The proposed BCS optimization technique described above has been applied to the grid for both complete observability and observability under line outage/ PMU failure cases, and the results are given in Tables 2.7 and 2.8. These two cases are again repeated with and without considering channel limits. With the help of a single-line diagram

obtained PMU number and locations in AP grid under normal and line/PMU failure conditions are presented in Fig. 2.2 and Fig. 2.3. The location of PMUs for the above two cases and, with and without considering the measurement channel limits are given in Table 2.9 and Table 2.10. The selected buses for PMU location are highlighted with a rectangular red box around them.

From the Table 2.7, it is clear that United Andhra Pradesh SLRG can be monitored, under normal operating conditions, completely just by placing 21 PMUs. From Table 2.8, if we place 51 PMUs, then the AP SLRG measurement system will become more robust, which can monitor the grid even under line-outage or PMU outage. Tables 2.9 and 2.10 reveal that AP SRLG needs 21 and 52 PMUs for complete observability under normal and line/PMU outage conditions on considering limiting measurement channels. It is just because many buses in AP SLRG have more than three channels.

Table 2.7: Number of PMUs and their locations for AP SLRG under normal operating conditions

Method	No.of PMUs	Locations of PMUs
ILP,[57]	28	107,110,112,115,121,122,127,128,132,134,135,136,145,147,150,157,159,163 ,165,169,170,171,179,180,182,183,184,185
BCS	21	107,112,110,115,117,118,121,122,127,128,132,145,147,152,154,136, 157,159,163,165,181

Table 2.8: Number of PMUs and their locations for AP SLRG under Line/PMU failure conditions

Method	No.of PMUs	Locations of PMUs
ILP [57]	-	-
BCS	51	106,107,108,110,111,112,115,116,117,118,119,120,121,122,123,124,127,12 8,129,132,133,136,138,141,143,145,146,147,148,150,152,154,157,158,159, 160,162,163,164,165,166,167,169,170,171,174,175,176,179,180,181

Table 2.9: Number of PMUs and their locations for AP SLRG under normal operating conditions, considering channel limits

Method	No.of PMUs	Locations of PMUs
ILP, Ref[57]	-	-
BCS	21	107,110,112,115,120,122,127,128,132,136,138,145,146 ,152,154,157,159,162,165,169,170

Table 2.10: Number of PMUs and their locations for AP SLRG under Line/PMU failure conditions considering channel limitations

Method	No.of PMUs	Locations of PMUs
ILP, [57]	-	-
BCS	52	106,107,108,110,111,112,113,115,116,117,118,119,120,121,122,123,124,1 27,128,129,132,133,136,137,141,143,145,146,147,148,150,152,154,157,15 8,159,160,161,162,163,164,165,166,167,169,170,174,175,177,179,180,181
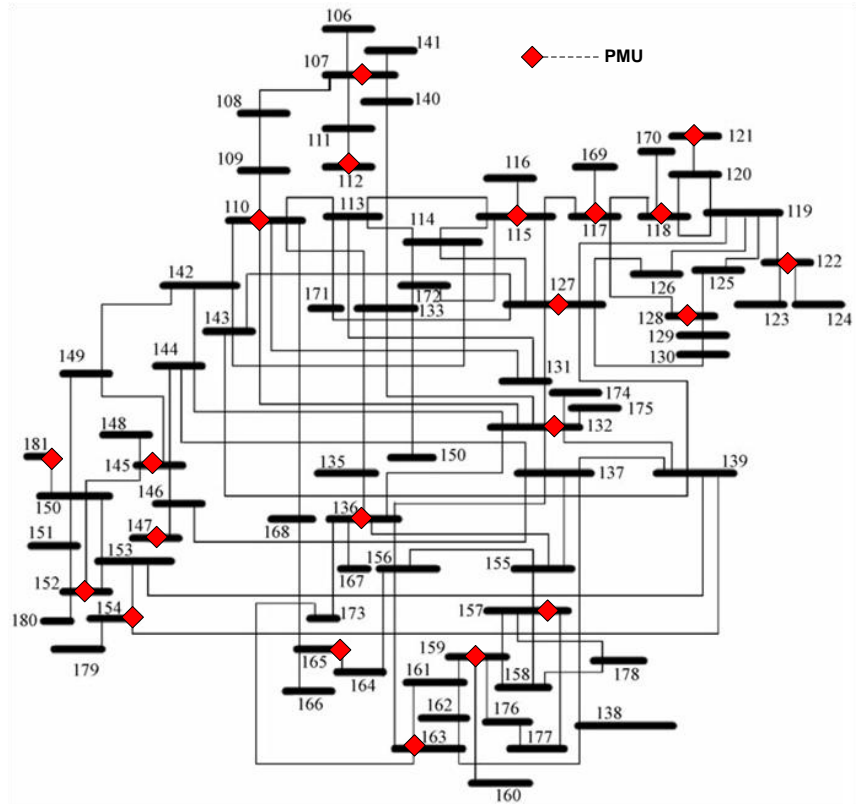
Figure 2.2: Location of PMUs for AP SLRG for complete observability under normal conditions
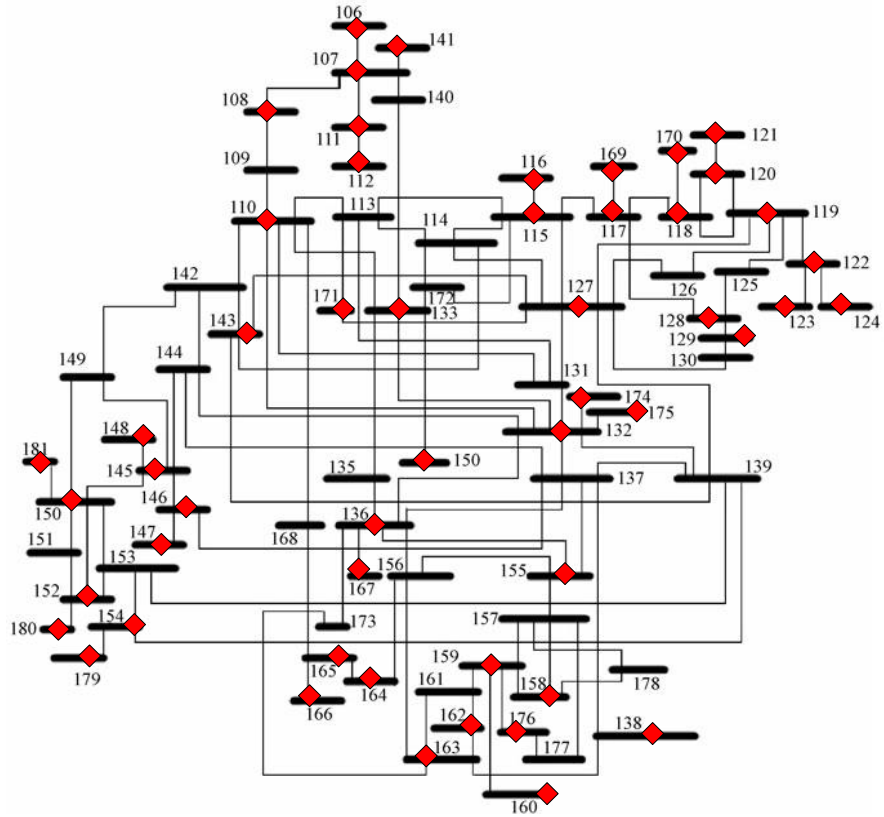
Figure 2.3: Location of PMUs for AP SLRG for complete observability under line/PMU failure conditions

30

2.3.2.2 Tamil Nadu (TN)

This is the biggest state level regional grid (SLRG) in SRIPG with 83 buses connected through 126 branches. On applying the proposed optimization technique to this grid, it is cleared that TN SLRG requires 20 and 48 PMUs for both complete observability and observability under line outage/ PMU failure cases, as shown in Tables 2.11 and 2.12. Obtained PMU locations in TN grid with and without considering line/PMU failure are presented with the help of single-line diagram in Fig. 2.4 and Fig. 2.5. And, interestingly the same TN SLRG needs again 20 and 48 PMUs with the locations given in Table 2.13 and Table 2.14 for complete observability on considering channel limits for both the normal and line/PMU outage cases. The reason for this is that every bus has at-most 4 channels on average.

Table 2.11: Number of PMUs and their locations for TN SLRG under normal operating conditions

Method	No.of PMUs	Locations of PMUs
ILP,[57]	20	6,7,9,12,19,22,27,30,33,35,47,48,50,54,58,60,63,67,73,75
BCS	20	5,7,10,12,19,22,27,30,33,35,40,44,48,54,58,60,63,67,73,75

Table 2.12: Number of PMUs and their locations for TN SLRG under Line/PMU failure conditions

Method	No.of PMUs	Locations of PMUs
ILP,[57]	-	-
BCS	48	1,4,6,7,9,10,12,13,14,16,19,22,23,25,27,28,30,31,32,33,35,36,37,42,43,44,47,48,50,54,56,57,58,59,60,61,63,64,65,67,71,72,73,74,75,76,79,83

Table 2.13: Number of PMUs and their locations for TN SLRG under normal operating conditions considering channel limits

Method	No.of PMUs	Locations of PMUs
ILP, [57]	-	-
BCS	22	5,7,8,10,12,19,22,27,28,30,33,42,48,49,54,58,60,63,67,73,75,81

Table 2.14: Number of PMUs and their locations for TN SLRG under Line/PMU failure conditions considering channel limitations

Method	No.of PMUs	Locations of PMUs
ILP, [57]	-	-
BCS	49	1,4,6,7,9,10,12,13,14,16,18,19,20,23,24,27,28,30,31,32,33,34,36,37,38,40,41,44,47,48,50,52,54,56,58,60,62,63,64,65,67,69,71,73,75,76,78,79,83
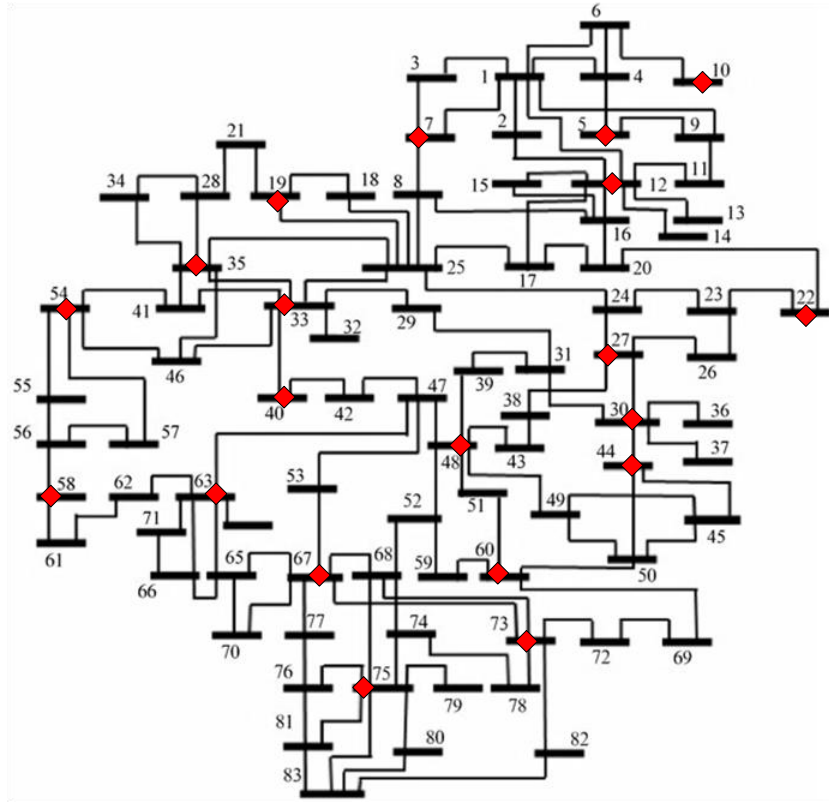
Figure 2.4: Location of PMUs for TN SLRG for complete observability under normal conditions
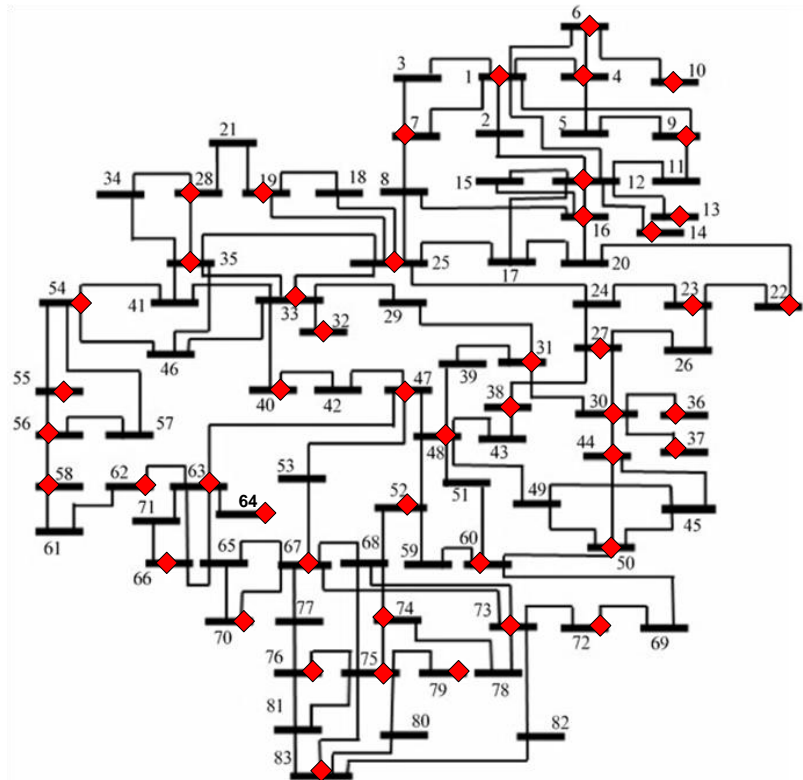
Figure 2.5: Location of PMUs for TN SLRG for complete observability under line/PMU failure conditions

2.3.2.3 Kerala (KL)

The Kerala SLRG for the above two conditions are identified, as shown in Fig. 2.6 and 2.7, tabulated in Tables 2.15 and 2.16 respectively. From the tables it is proven that it needs 7 and 15 PMUs for normal and line/PMU failure conditions respectively. Later, on considering channel limitations for the two conditions mentioned above, it is confirmed that the grid needs 7and 15 PMUs, as given in Tables 2.17 and 2.18, with changed locations from the above two cases. The method proposed in [57] is failed in observing bus number 105. But the proposed BCS has successfully found a solution with 7 PMUs which could even observe bus number 105.

Table 2.15: Number of PMUs and their locations for KL SLRG under normal operating conditions

Method	No.of PMUs	Locations of PMUs
ILP, Ref [57]	-	-
BCS	7	88,89,93,95,99,103,105

Table 2.16: Number of PMUs and their locations for KL SLRG under Line/PMU failure conditions

Method	No.of PMUs	Locations of PMUs
ILP, [57]	-	-
BCS	15	84,85,86,87,89,92,93,95,97,98,99,101,102,104,105

Table 2.17: Number of PMUs and their locations for KL SLRG under normal operating conditions considering channel limits

Method	No.of PMUs	Locations of PMUs
ILP, [57]	-	-
BCS	7	88,89,92,95,99,102,105

Table 2.18: Number of PMUs and their locations for KL SLRG under Line/PMU failure conditions considering channel limitations

Method	No.of PMUs	Locations of PMUs
ILP, [57]	-	-
BCS	15	84,85,86,87,89,92,93,95,96,98,99,100,101,104,105
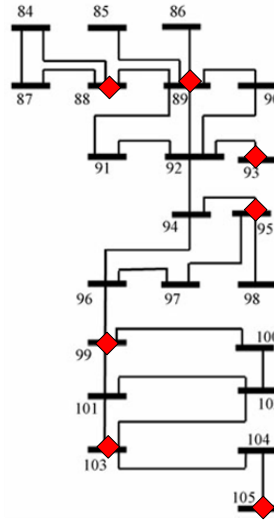
Figure 2.6: Location of PMUs for KL SLRG for complete observability under normal conditions
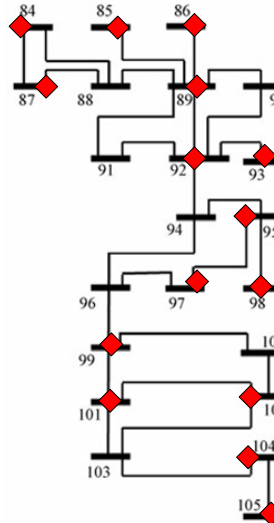
Figure 2.7: Location of PMUs for KL SLRG for complete observability under line/PMU failure conditions

The observability of the network for the PMU locations obtained can also be verified using the formulae given in the Appendix-D.

2.3.2.4. Karnataka (KA)

The Karnataka SLRG consists of 25 buses of UHV, EHV, and HV. It has 44 interconnections among these 25 buses. The optimal locations of PMUs in this SLRG for both system complete observability and observability under any line/PMU failure are obtained using the proposed BCS technique. The obtained results are shown in Fig. 2.8 and Fig. 2.9, and are given in Tables 2.19 and 2.20 respectively. The PMU locations in a grid are represented by means of red boxes over that particular bus. The paper [57] proposed with ILP based OPP has again failed in locating PMUs for KA SLRG.

But from the BCS results, it is clear that KA SLRG needs 10 PMUs for system complete observability under normal condition and 19 PMUs for complete observability under line/PMU failure condition. The results of OPP for both system observability under normal condition and observability under line/PMU outage condition while considering measurement channel limits are given in Table 2.21 and Table 2.22.

Table 2.19: Number of PMUs and their locations for KA SLRG under normal operating conditions

Method	No.of PMUs	Locations of PMUs
ILP, [57]	-	-
Proposed	10	185,188,192,194,196,201,203,205,207,208

Table 2.20: Number of PMUs and their locations for KA SLRG under Line/PMU failure conditions

Method	No.of PMUs	Locations of PMUs
ILP, [57]	-	-
BCS	19	183,185,188,189,191,192,194,196,197,198,199,201,202,203,204,205,206,207,208

Table 2.21: Number of PMUs and their locations for KA SLRG under normal operating conditions, considering channel limits

Method	No.of PMUs	Locations of PMUs
ILP, Ref57]	-	-
BCS	10	184,189,191,194,196,202,203,205,207,208

Table 2.22: Number of PMUs and their locations for KA SLRG under Line/PMU failure conditions considering channel limitations

Method	No.of PMUs	Locations of PMUs
ILP, Ref[57]	-	-
BCS	19	183,184,188,190,191,192,194,196,197,198,199,201,202,203,204,205,206,207,208
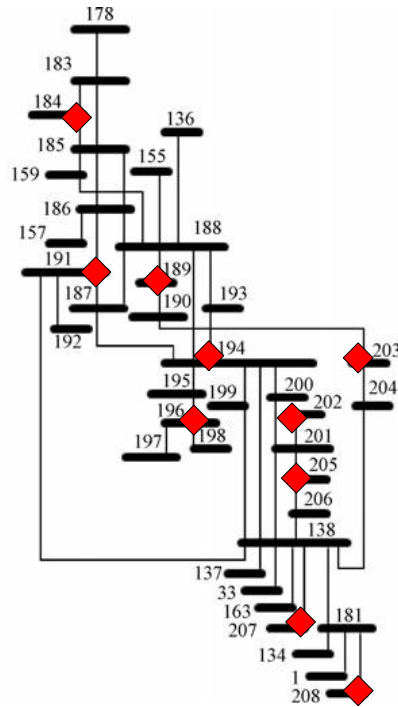
Figure 2.8: Location of PMUs for KA SLRG for complete observability under normal conditions
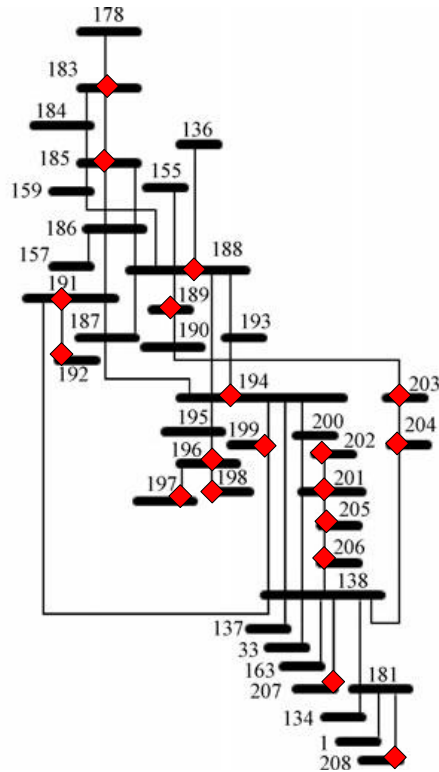
Figure 2.9: Location of PMUs for KA SLRG for complete observability under line/PMU failure conditions

2.3.3. Indian Power Grid

Indian power grid, before December 2013, was divided into five regions namely northern region of Indian power Grid (NRIG), North-Eastern Region of Indian power Grid (NERIG), Southern Region of Indian power Grid (SRIG), Western Region of Indian power Grid (WRIG), and Eastern Region of Indian power Grid (ERIG) [96]. This **chapter** studies the PMU placement for the above five Regional Indian power Grids.

2.3.3.1. Southern Region of Indian Grid (SRIG)

The Southern Region of Indian power Grid (SRIG) has 208 buses including HV, EHV and UHV buses. This section optimally locates PMUs for complete SRIG by applying the proposed BCS algorithm to the grid formed by interconnecting all four (AP, TN, KA, and KL) SLRGs. The results for both, the complete system observability under normal and line/PMU failure, conditions are given in Table 2.23 and Table 2.24. The locations of the obtained PMUs are shown in the Fig. 2.10 and Fig. 2.11. From the results, it is clear that SRIG needs 56 and 132 PMUs for complete system observability under normal and line/PMUs outage conditions respectively. The results of OPP for both system observability under normal condition and observability under line/PMU outage condition while considering measurement channel limits are given in Table 2.25 and Table 2.26.

Table 2.23: Number of PMUs and their locations for SRIG under normal operating conditions

Method	No.of PMUs	Locations of PMUs
ILP, [57]	58	1,9,10,12,22,25,27,28,30,33,47,48,50,54,58,60,63,65,73,75,76,88,89,93, 95,99,104,107,110,112,115,121,122,127,128,132,135,138,145,147,152,1 54,157,159,163,165,167,169,170,171,181,182,185,188,192,196,201,203
BCS	56	5,6,7,12,19,20,23,30,33,35,38,47,48,50,54,58,60,63,65,73,75,84,89,93,95 ,96,102,105,107,110,112,115,117,118,121,122,127,128,132,136,138,145, 147,152,154,157,159,163,165,181,183,188,190,191,196,201

Table 2.24: Number of PMUs and their locations for SRIG under normal operating conditions considering channel limits

Method	No.of PMUs	Locations of PMUs
ILP, [57]	-	-
BCS	57	5,7,8,10,12,19,22,27,28,30,33,42,48,49,54,58,60,63,67,7 3,75,76,88,89,92,95,99,102,105,107,110,111,115,117,11 8,121,122,127,128,132,136,138,145,147,152,154,157,15 9,161,165,181,184,188,190,191,196,201

Table 2.25: Number of PMUs and their locations for SRIG under Line/PMU failure conditions

Method	No.of PMUs	Locations of PMUs
ILP, [57]	-	-
BCS	132	1,3,4,6,9,10,12,13,14,16,19,22,23,25,26,27,28,30,31,32,33,35,36,37,42,43, 45,47,48,49,54,56,57,58,59,60,62,63,64,66,67,69,70,71,73,75,76,78,79,83, 85,86,87,88,89,92,93,95,96,98,99,100,103,104,106,107,108,110,111,112,1 13,115,116,117,118,119,120,121,122,123,124,127,128,130,132,133,134,1 36,138,141,142,145,146,147,148,150,152,154,157,158,159,160,161,163,1 64,165,166,167,169,170,174,175,177,179,180,181,184,185,188,190,191,1 92,194,196,197,198,201,202,203,205,207,208

Table 2.26: Number of PMUs and their locations for SRIG under Line/PMU failure conditions considering channel limitations

Method	No.of PMUs	Locations of PMUs
ILP,[57]	-	-
BCS	134	1,5,6,7,9,10,12,13,14,16,19,22,23,25,27,28,30,31,32,33,35,36,37,40, 41,42,43,44,45,48,52,53,54,56,58,60,61,63,64,66,67,69,73,75,76,78, 79,83,84,85,86,88,89,92,93,95,96,98,99,100,102,104,105,106,107,108, 110,111,112,113,115,116,117,118,119,120,121,122,123,124,127,128, 130,132,133,134,136,137,138,141,142,145,146,147,148,150,152,154, 156,157,158,159,160,161,163,165,166,167,169,170,171,174,175,176, 179,180,181,183,184,187,188,190,191,192,194,196,197,198,201,202, 203,205,207,208

2.3.3.2. Western Region of Indian power Grid (WRIG)

WRIG consisting of four states (Chhattisgarh, Maharashtra, Madhya Pradesh and Gujarat) with 77 buses of UHV, EHV, and HV connected through 145 lines. The number and the locations of PMUs required for observing the WRIG completely, under normal and line/PMU failure conditions, with and without considering the channel limits are given in the Table 2.277 and Table 2.28. The PMUs are also located graphically as shown in Fig. 2.12 and Fig. 2.13. From these results, it is known that WRIG requires 19 and 44 PMUs to observe the system under normal and line/PMU outage cases in both of which channel limits were ignored. Similarly, the system requires 20 and 45 PMUs for observing the system under normal and line/PMU outage cases, where channel limits were considered. It is to be noted that the PMU locations are numbered as per the numbers given for buses.
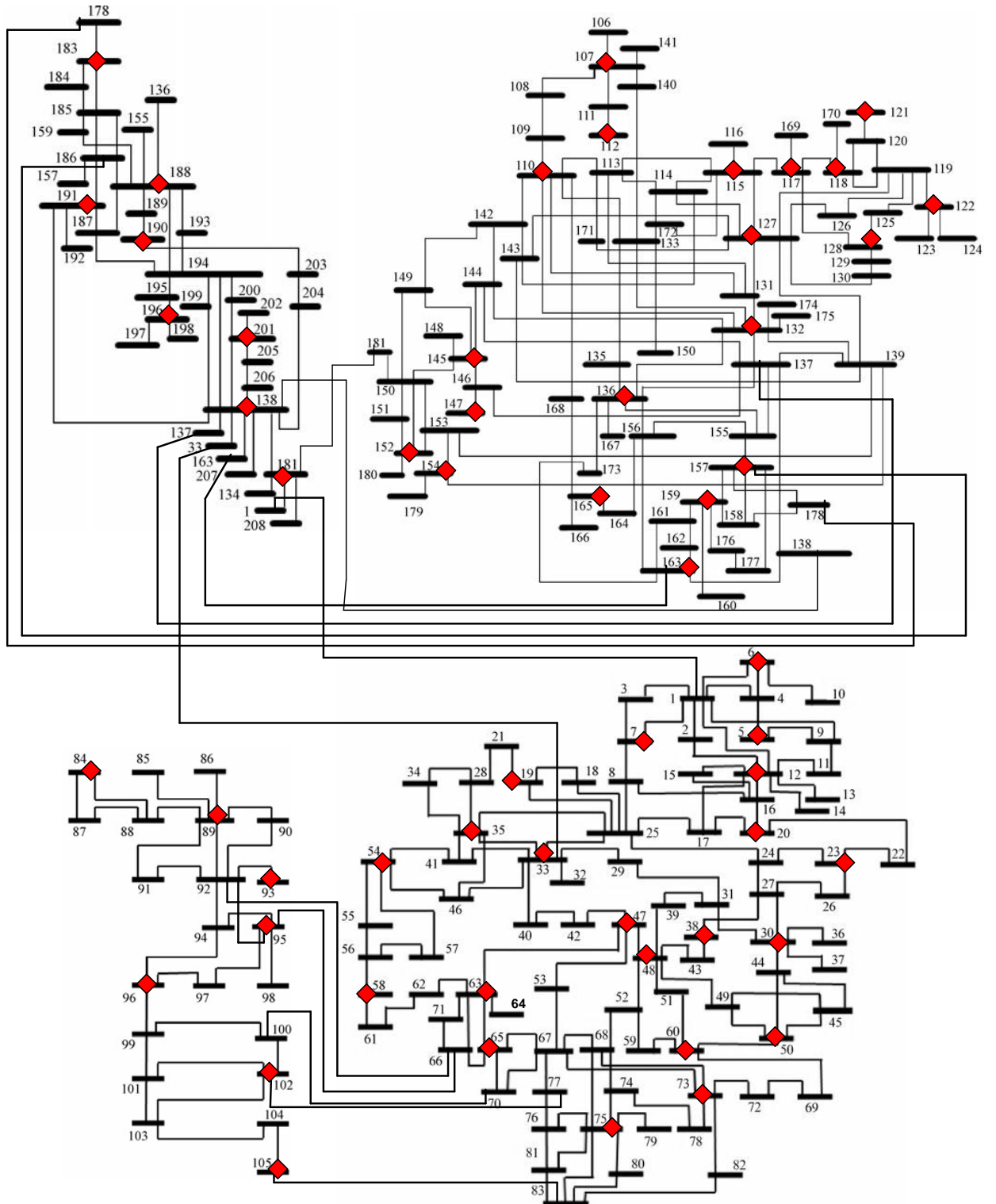
Figure 2.10: PMU locations in SRIG for complete Observability under normal operating conditions
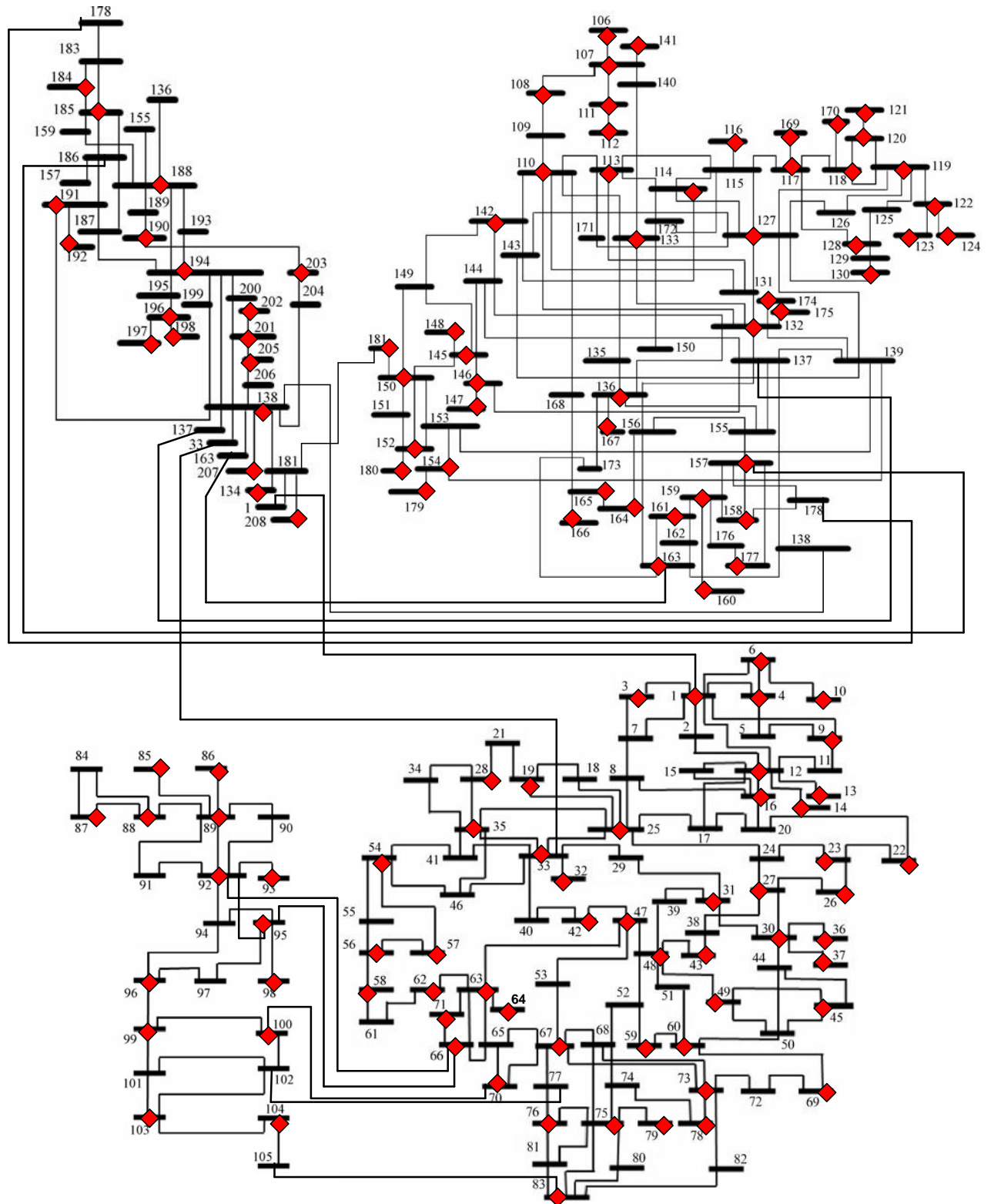
Figure 2.11: PMU locations in SRIG for complete Observability under line outage/ PMU failure condition

Table 2.27: PMU locations for WRIG under normal and line/PMU outage conditions, without considering channel limitations

System	under normal operating conditions	under line/PMU outage conditions
WRIG	418,421,425,429,433,439,440,443,448,456,460,464,466,471,474,480,485,488,491. No. of PMUs:19	418,420,421,423,425,426,427,431,432,433,438,439,440,442,443,446,448,449,453,454,455,457,460,461,464,466,467,468,469,470,471,472,473,474,475,477,478,480,485,486,488,489,491,493. No. of PMUs:44

Table 2.28: PMU locations for WRIG under normal and line/PMU outage conditions considering channel limitations

System	under normal operating conditions	under line/PMU outage conditions
WRIG	418,421,425,429,432,435,443,445,448,454,456,460,464,466,471,474,480,486,489,491. No. of PMUs:20	418,420,421,424,425,426,427,429,432,433,436,437,439,440,441,443,445,448,449,451,454,456,457,460,461,464,466,467,468,469,470,471,472,473,474,475,477,479,480,485,486,488,489,490,492. No. of PMUs:45
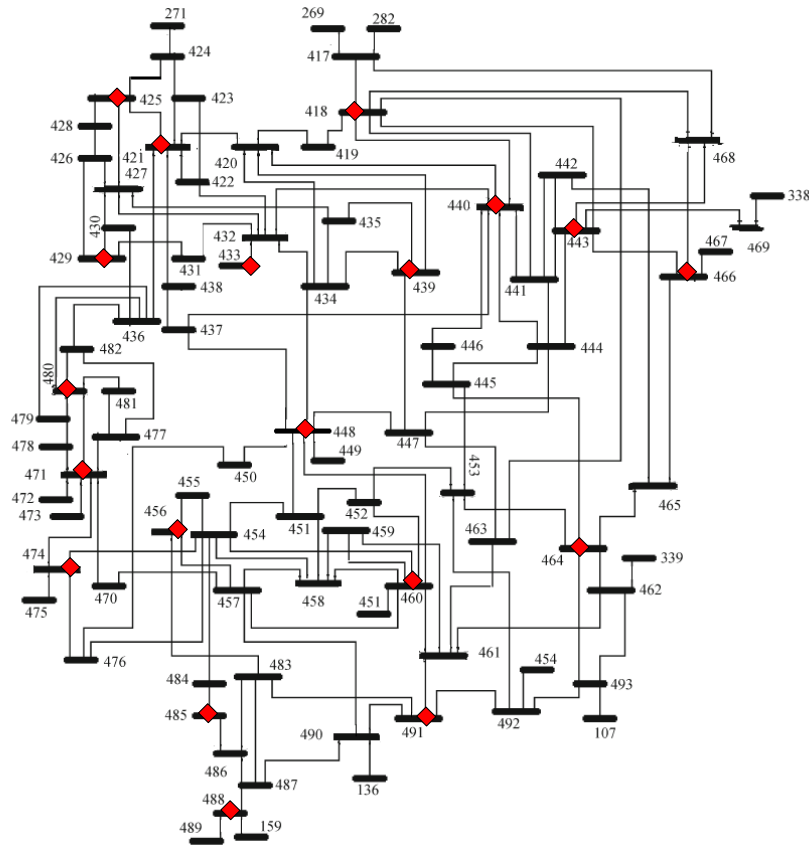
Figure 2.12: PMU locations in WRIG for complete Observability under normal operating conditions

41
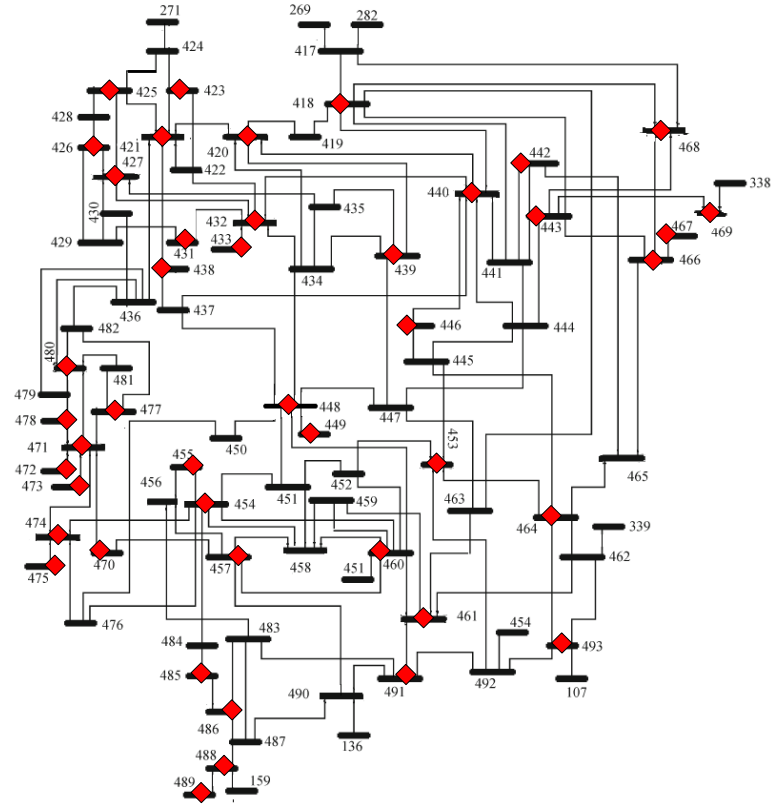
Figure 2.13: PMU locations in WRIG for complete Observability under line / PMU failure condition

2.3.3.3. Eastern Region of Indian power Grid (ERIG)

Eastern Region of Indian power grid (ERIG) has five states. It is the only RIG to be having connectivity with all the remaining IRGs. It has 90 buses including UHV, EHV, and HV transmission lines. The ERIG requires 24 and 57 PMUs to observe the system completely, under normal and line/PMU outage cases where the channel limits were ignored. Similarly, it requires 25 and 58 PMUs for observing the system under normal and line/PMU outage cases, where channel limits were considered. The locations of PMUs required for observing the WRIG completely, under normal and line/PMU failure conditions, with and without considering the channel limits are given in the Table 2.29 and Table 2.30 and, are represented graphically in Fig. 2.14 and Fig. 2.15.

Table 2.29: PMU locations for ERIG under normal and line/PMU outage conditions, without considering channel limitations.

System	under normal operating conditions	under line/PMU outage conditions
ERIG	314,317,320,321,326,329,332,336,341,343,345,351,352,354,360,367,374,375,377,385,388,391,396,402. No. of PMUs:24	314,315,316,317,319,320,321,322,324,326,327,329,331,332,334,337,338,339,340,341,343,345,346,348,351,352,353,354,356,360,361,362,364,367,369,370,373,374,375,376,377,378,380,381,384,385,388,389,391,392,395,396,397,398,399,401,402. No. of PMUs:57

Table 2.30: PMU locations for ERIG under normal and line/PMU outage conditions, considering channel limitations

System	under normal operating conditions	under line/PMU outage conditions
ERIG	314,317,320,321,326,329,331,336,339,341,345,348,351,352,354,360,368,374,375,378,384,388,391,396,402. No. of PMUs:25	314,315,316,317,319,320,321,323,324,326,327,329,330,332,334,336,338,339,340,341,345,347,348,351,352,353,354,357,360,361,362,363,365,366,367,369,370,373,374,375,376,377,378,379,382,384,385,388,389,391,392,393,396,397,398,399,401,402. No. of PMUs:58
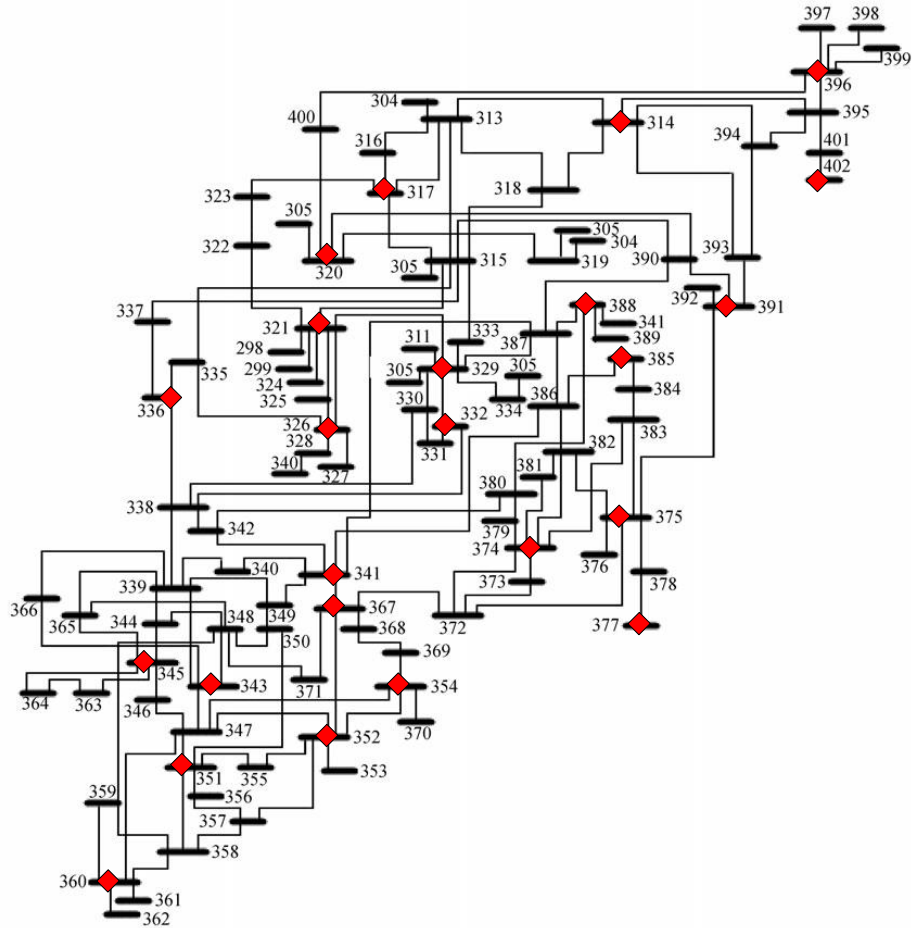
Figure 2.14: PMU locations in ERIG for complete Observability under normal operating conditions
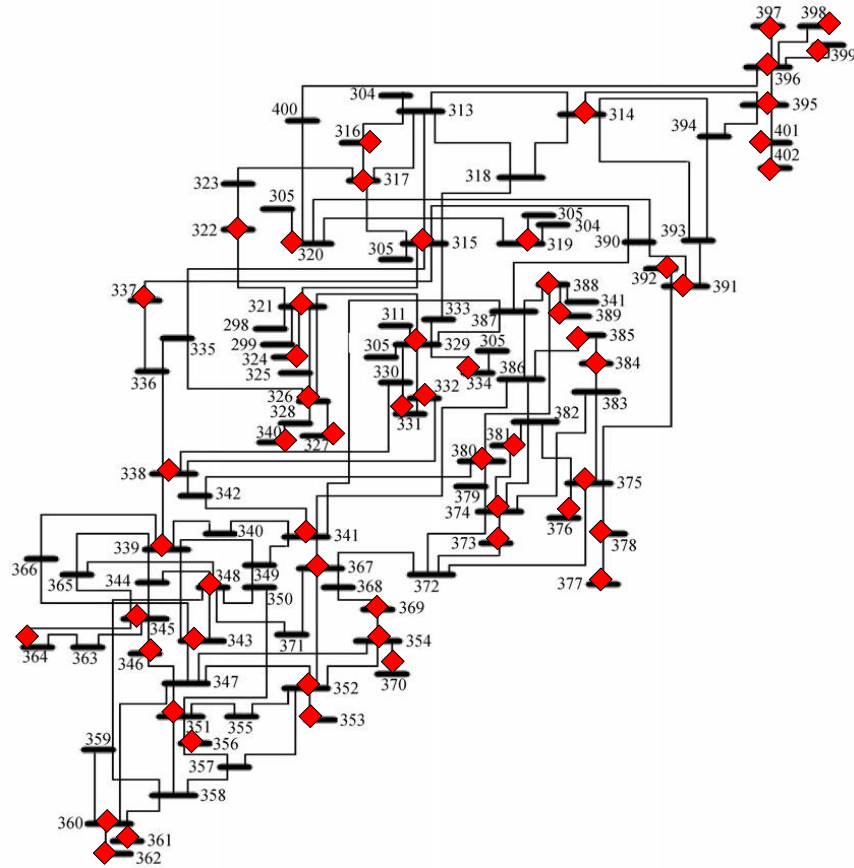
Figure 2.15: PMU locations in ERIG for complete Observability under line / PMU failure condition

2.3.3.4. Northern Region of Indian power Grid (NRIG)

NRIG is the biggest RIG that covers almost 30% of India's geographical area, among all five regions. It has seven states and two union territories. It consists of 104 buses including UHV, EHV, and HV buses. From the results obtained, as shown in Table 2.31 and Table 2.32, it is proven that NRIG requires 27 and 65 PMUs to observe the system completely, under normal and line/PMU outage cases where the channel limits were ignored. Similarly, it requires 28 and 68 PMUs for observing the system under normal and line/PMU outage cases, where channel limits were considered. The locations of PMUs are mentioned Fig. 2.16 and Fig. 2.17.

Table 2.31: PMU locations for NRIG under normal and line/PMU outage conditions, without considering channel limitations

System	under normal operating conditions	under line/PMU outage conditions
NRIG	209,212,216,218,224,228,231,233,236,243,248,250,252,259,262,265,269,271,277,281,286,296,302,303,306,308,310. No. of PMUs:27	209,210,211,212,213,216,217,218,219,220,221,222,224,225,226,228,229,231,233,234,236,238,241,243,244,245,247,248,250,252,253,259,260,261,263,265,266,267,269,271,272,275,277,278,279,280,281,282,284,285,286,287,290,293,296,297,299,301,302,303,306,308,309,310,312. No. of PMUs:65

Table 2.32: PMU locations for NRIG under normal and line/PMU outage conditions, considering channel limitations

System	under normal operating conditions	under line/PMU outage conditions
NRIG	209,212,216,221,224,228,231,232,236,242,248,250,252,259,261,265,269,271,277,280,286,296,302,303,304,306,309. No. of PMUs:27	209,210,211,212,214,216,217,218,219,220,221,222,224,225,226,228,229,231,233,234,236,238,241,243,244,245,248,249,250,252,253,259,260,262,263,265,266,267,269,271,272,275,277,278,279,280,281,282,284,285,286,287,289,293,295,296,297,300,301,302,303,305,308,309,312. No. of PMUs:65
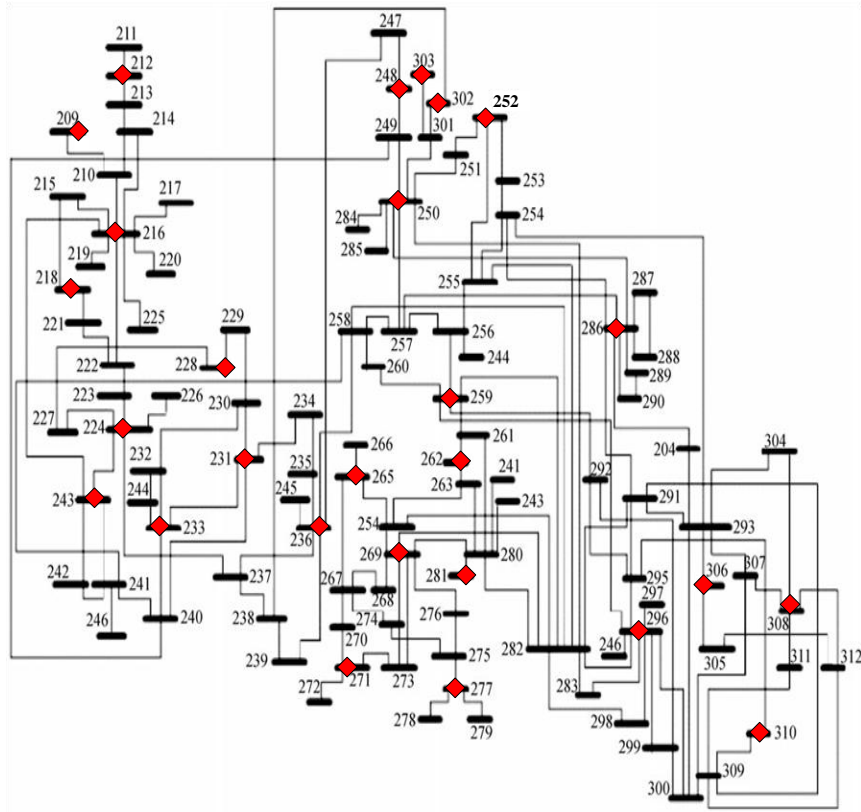
Figure 2.16: PMU locations in NRIG for complete Observability under normal operating conditions
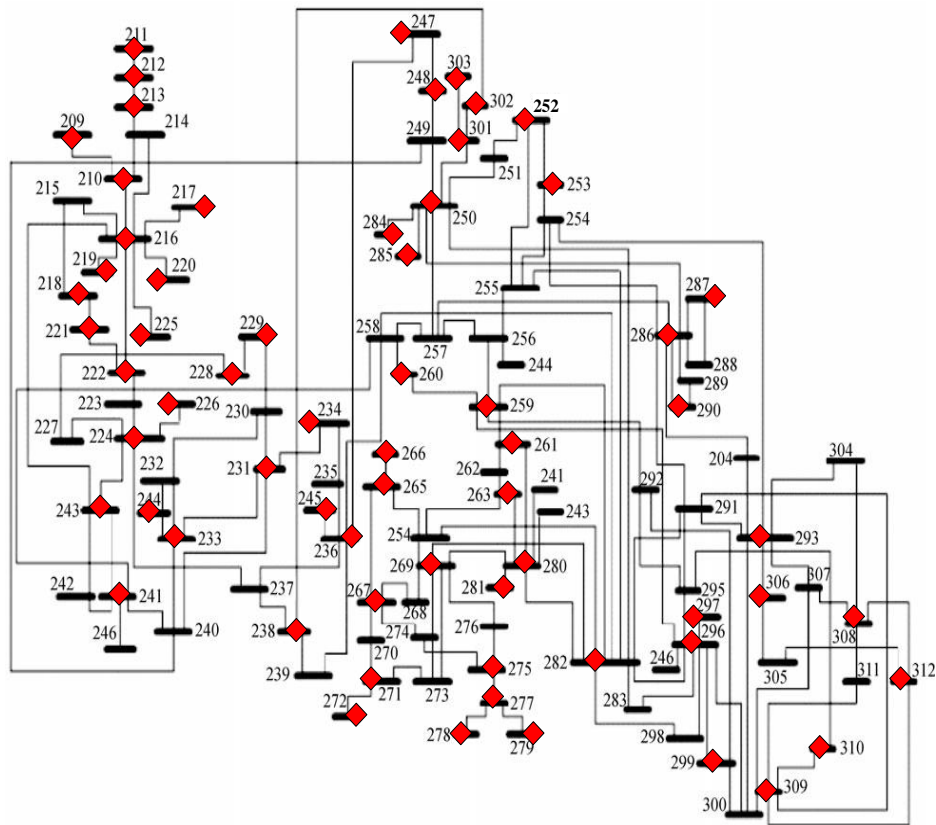
Figure 2.17: PMU locations in NRIG for complete Observability under line / PMU failure condition

2.3.3.5. North-eastern Regional Indian power Grid (NERIG)

North-eastern Regional Indian power Grid (NERIG) has seven states consisting 14 buses of UHV, EHV, and HV type. As shown in Tables 2.33, and 2.34, Figures 2.18, and 2.19, it is clear that NERIG needs 5 and 12 PMUs for complete system observability under normal and line/PMUs outage conditions respectively irrespective channel limitations.

Table 2.33: PMU locations for NERIG under normal and line/PMU outage conditions

System	under normal operating conditions	under line/PMU outage conditions
NERIG	404,406,407,411,413. No. of PMUs:5	403,404,405,406,407,409,410,412,413,414,415,416. No. of PMUs:12

Table 2.34: PMU locations for NERIG under normal and line/PMU outage conditions considering channel limitations

System	under normal operating conditions	under line/PMU outage conditions
NERIG	404,405,409,411,413. No. of PMUs:5	403,404,405,406,407,409,410,411,413,414,415,416. No. of PMUs:12
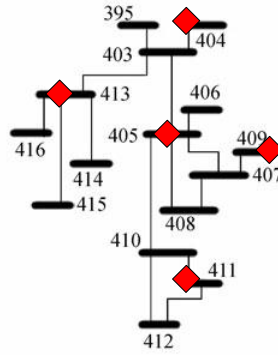
Figure 2.18: PMU locations in NERIG for complete Observability under normal operating conditions
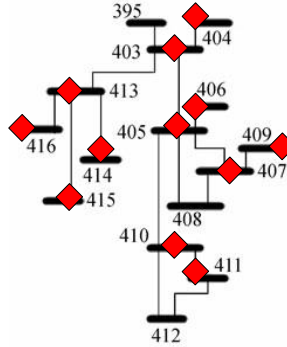
Figure 2.19: PMU locations in NERIG for complete Observability under line / PMU failure condition

3.5.3.6. United Indian Grid (UIG)

After successful synchronization of SRIG to NEW (Northern-Eastern-Western) grid, on December 31st, 2013, India became the nation with one grid and one frequency. So the wide-area measurement system must be reliable and robust. This section presents an optimal PMU location which can observe the whole Indian Grid even under abnormal conditions like line/PMU outage case, which has considered the new synchronous line connected between SRIG and the NEW grid of India. This section also gives the detailed locations of PMUs for Indian Grid under both normal and abnormal conditions on considering channel limitations also. The results are tabulated in Tables 2.35 and 2.36.

Table 2.35: PMU locations for UIG under normal and line/PMU outage conditions

System	under normal operating conditions	under line/PMU outage conditions
UIG	5,6,7,12,19,22,27,30,33,35,47,48, 50,55,56,58,60,63,70,73,75,76,8 4,89,93,95,96,103,105,107,110,1 11,115,117,118,121,122,126,127 ,128,132,136,138,145,146,152,1 57,159,163,165,168,169,179,181 ,185,188,190,191,196,201,204,2 05,209,212,216,221,224,226,229 ,231,236,239,242,243,244,247,2 50,252,259,262,265,269,271,277 ,281,286,296,301,304,305,309,3 11,315,317,320,321,326,332,338 ,339,345,351,352,354,359,360,3 67,374,375,378,381,385,388,391 ,395,396,401,403,405,409,411,4 13,420,421,428,431,433,435,441 ,445,447,448,456,460,466,471,4 74,480,484,486,488,492. No. of PMUs:142	1,5,6,7,9,10,12,13,14,15,19,20,22,23,25,27,28,30, 31,32,33,35,36,37,38,42,44,45,47,48,54,56,57,58, 59,60,61,63,64,67,69,70,71,73,74,75,77,79,81,83, 85,86,87,88,89,92,93,95,96,98,99,101,104,105,10 6,107,109,110,111,112,115,116,117,118,119,120, 122,123,124,125,127,129,130,132,133,134,136,13 8,141,142,145,146,147,148,151,152,154,157,158, 159,160,161,163,164,165,166,167,169,170,171,17 4,175,177,179,180,181,184,185,188,190,191,192, 194,196,197,198,201,202,203,205,207,208,209,21 0,211,212,213,216,217,218,219,220,221,223,224, 225,226,228,229,230,231,232,235,236,238,241,24 3,244,245,248,249,250,252,254,255,259,260,261, 262,265,266,267,269,271,272,275,277,278,279,28 0,281,282,284,285,286,287,290,292,293,295,296, 297,301,302,303,304,305,309,312,314,317,318,32 0,321,322,324,326,327,328,329,330,332,333,336, 337,338,339,345,346,350,351,352,353,354,356,35 8,360,361,362,364,366,367,368,370,371,373,374, 375,376,377,378,380,381,384,385,387,388,389,39 1,392,393,396,397,398,399,401,402,403,404,405, 406,407,409,410,412,413,414,415,416,419,420,42 1,423,425,426,429,432,433,434,436,438,439,441, 443,445,446,448,449,450,452,454,456,457,460,46 1,463,465,466,467,471,472,473,474,475,477,478, 480,483,484,486,488,489,493. No. of PMUs:313

2.4. Economies of OPP problem

This section gives the net cost savings by the proposed optimal PMU placement problem. For better illustration, consider AP state level regional grid that requires 21 and 48 PMUs for observing 76 buses completely under normal and line/PMU outage cases. If a PMU costs 1unit, then the cost incurred for AP SLRG is 76 units without considering optimal PMU placement. On considering optimal PMU placement under both conditions, AP SLRG needs to expend only 21 and 48 units of cost which saves 72.37% and 31.58%. Similarly, by considering OPP, TN SLRG saves 75.90% and 42.17%, KL SLRG saves 68.18% and 31.82% and KA SLRG saves 60% respectively for system complete

Table 2.36: PMU locations for UIG under normal and line/PMU outage conditions considering channel limitations

System	under normal operating conditions	under line/PMU outage conditions
UIG	3,5,6,12,20,23,25,27,28,30, 33,41,45,47,48,56,60,62,64 ,67,71,73,75,76,88,89,93,9 5,99,100,104,107,110,111, 115,117,120,122,127,128,1 32,136,138,145,147,152,15 4,159,163,165,170,177,178 ,181,184,187,190,191,194, 196,201,210,212,216,221,2 24,229,231,236,239,242,24 4,248,250,254,255,260,262 ,265,267,269,272,277,280, 286,295,296,301,305,308,3 12,315,317,321,327,332,33 8,340,341,343,344,345,351 ,352,360,369,370,371,373, 376,377,379,381,384,389,3 92,393,396,401,404,405,40 7,410,413,418,421,424,428 ,430,432,435,441,445,448, 453,454,457,461,462,466,4 71,475,480,483,484,488. No. of PMUs:146	1,5,6,7,9,10,12,13,14,16,18,20,21,22,24,25,26,27,28,30,31, 32,33,35,36,37,40,43,44,47,48,50,51,52,54,55,56,59,61,62, 63,64,66,67,69,70,72,74,75,77,78,79,81,82,83,84,85,86,88, 89,92,93,95,96,98,99,103,104,106,107,108,110,111,112,11 5,116,117,118,119,120,122,123,124,127,128,129,132,133, 134,136,138,141,142,145,146,147,148,150,152,154,157,15 9,160,161,162,164,165,166,167,169,170,171,173,174,175, 177,178,179,180,181,183,185,189,190,191,192,193,194,19 5,196,197,198,201,202,204,206,207,208,209,210,211,212, 214,216,217,218,219,220,221,222,224,225,226,227,229,23 0,233,234,235,236,237,238,241,243,244,245,248,249,250, 252,253,258,259,261,263,265,266,267,269,271,272,276,27 7,278,279,280,281,282,284,285,286,287,290,293,295,296, 297,300,301,303,304,305,308,309,313,315,316,320,321,32 2,323,324,326,327,331,332,333,334,337,338,339,340,341, 343,345,347,348,351,352,353,354,357,360,361,362,363,36 7,368,370,372,374,375,376,377,378,379,382,384,385,388, 389,391,392,393,394,396,397,398,399,401,402,403,404,40 5,406,407,409,410,411,413,414,415,416,418,419,421,422, 425,427,428,429,431,432,433,434,436,438,442,445,446,44 7,448,449,452,453,454,456,458,461,465,466,467,469,470, 471,472,473,474,475,478,480,481,483,484,486,488,489,49 1,493. No. of PMUs:319
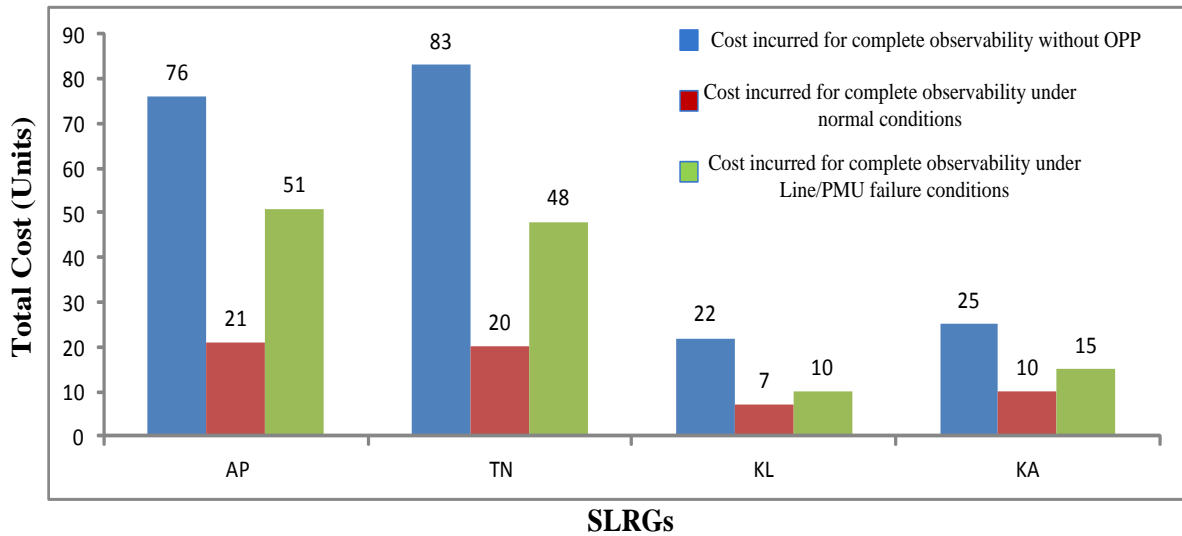
Figure 2.20: Comparison between number of buses and the number of PMUs required for State level power grids under both normal and line/PMU outage conditions
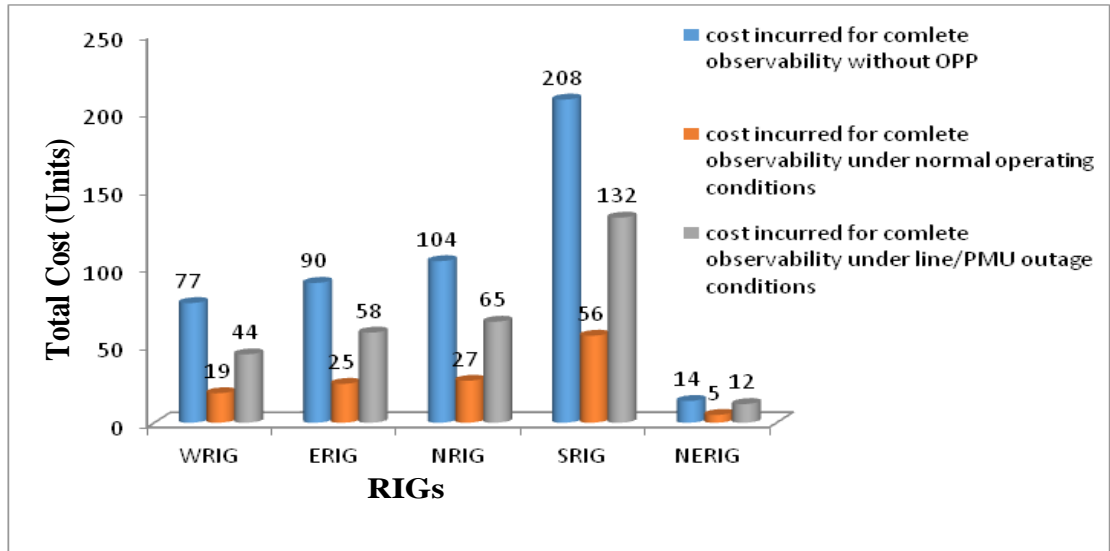
Figure 2.21: Comparison between number of buses and the number of PMUs required under both normal and line/PMU outage conditions, for all RIGs

observability under normal and line/PMU outage conditions. The costs incurred for different SLRGs to place PMUs under normal and line/PMU failure conditions are shown in Fig. 2.20 graphically. Similarly, on considering optimal PMU placement under both conditions, WRIG needs to expend only 19 and 44 units of cost which saves 75.32% and 42.85%. Similarly, by considering OPP, ERIG saves 72.22% and 35.56%, NRIG saves 74.04% and 37.5%, SRIG saves 73.07% and 24%, and, NERIG saves 64.29% and 14.29% respectively for system complete observability under normal and line/PMU outage conditions. The costs incurred for different IRGs and UIG for PMU placement under normal and line/PMU failure conditions are shown in Fig. 2.21 graphically.

2.5. Summary

The power system is highly prone to faults which may cause line outages or measurement system failures. This thesis has considered even these conditions also for finding PMU placements. The proposed BCS method has solved the OPP problem for system complete observability under both normal and abnormal conditions in power system accurately. The proposed method has been tested on few IEEE standard test systems and then applied for four the state level regional grids (SLRG) of Southern Region of Indian power Grid (SRIG) and five Regional Indian power Grids of United Indian power Grid (UIG). From the results and discussions, it is verified that the proposed method has successfully optimized the OPP problem and, also has benefited economically.

Chapter 3:

OPTIMAL PLACEMENT OF PHASOR MEASUREMENT UNITS FOR MAXİMİZİNG OBSERVABİLİTY

3.1. Introduction

The objective of the proposed OPP problem using Binary Bat Algorithm (BBA) is to find the least number of PMUs for system complete observability by considering all possible (line/PMU) contingencies with only one contingency (either one line outage or one PMU failure) at a time, and channel limits. Also, to maximize the observability redundancy, we introduced a performance index called System Observability Index (SOI) with the help of n_p which represents the number of buses which would be observed for more than one time.

3.2. System Observability Index (SOI)

It is a parameter that tells the level of system observability. It can be defined as the ratio of the number of buses observed for at least once to the total number buses in the system. It is given by,

$$SOI = 1 + \frac{No.of\ buses\ observed\ for\ more\ than\ one\ time\ (n_p)}{N} \tag{3.1}$$

This value is typically greater than or equal to ($\geq$) unity. If *SOI* is unity, then the system is said to be completely observable with all the buses having zero measurement redundancy. Otherwise, if *SOI* is greater than unity, then the system is completely observable with the percent of measurement redundancy equal to an amount by which *SOI* exceeds unity. Higher the SOI higher will be the system redundancy level. So, the PMU set that corresponds to high *SOI* can be considered as the best solution to OPP problem. The above formula will hold good for normal operating conditions. But, under line/PMU outage conditions, the No. of buses observed for more than twice will be considered instead of No. of buses observed for more than one time (n_p).

3.3. OPP formulation for maximizing observability

To achieve maximum redundancy, the objective function can be defined as follows,
Maximize,

$$u^T C_{pq} x_q \tag{3.2}$$

Subjected to,

$$\sum_{q=1}^{N} x_q = n_0 \tag{3.3}$$

$$C_{pq} x_q \geq u \tag{3.4}$$

Where, u is a vector of length N and is given by $u=[1,1...1]^T$ for observability under normal operating conditions, and is $u=[2,2...2]^T$ for observability under line/PMU outage conditions. And n_0 is the optimal number of PMUs obtained from the main optimal PMU placement problem for system observability.

This optimal solution will be considered whenever there exist multiple solutions in actual OPP problem. From this solution, n_p will be calculated and, then *SOI* can be calculated as,

$$SOI = \frac{1}{N}(O) \tag{3.5}$$

Where, O is system observability index and is given by,

$$O = n_p + N \tag{3.6}$$

The function (**3.5**) will be optimized until it produces optimal n_p that could produce maximum *SOI*. Maximum *SOI* provides measurement redundancy even when there would be some abnormalities like line/PMU failure. Once the main optimal PMU placement problem has been solved, the *SOI* function will be maximized subjecting it to main OPP constraints and additional constraint that the number of PMUs should be restricted to n_0.

3.3.1. Calculation of n_p

The observability of buses can be computed effectively using the equation given below.

$$[O]_{N \times 1} = C_{pq} x_q \tag{3.7}$$

Where C_{pq} represents the system connectivity matrix and x_q is the column matrix which gives PMU locations. For the system to be observable completely, none of the element of the matrix O should be zero. And then,

$$[N_P]_{N \times 1} = [O]_{N \times 1} - u_{N \times 1} \tag{3.8}$$

Where the number of non-zero elements of *[N_p]* gives the number of buses observed more than one time (n_p).

3.4. Proposed Binary Bat Algorithm

3.4.1. Bat Algorithm

Bat algorithm is a heuristic algorithm, which is proposed recently [98]. It was inspired by the bats with their echolocation behavior for finding the optimal point. In this algorithm,

artificial bats are considered as particles (or agents). When the bats chase prey, they will try to reduce the loudness and increase the rate of ultrasonic sound emitted. These two characteristics were adopted in designing the Bat Algorithm (BA) [98]. In BA, each bat is provided with a position vector, velocity vector and a frequency vector. Each of these parameters is updated after each-iteration using the following equations.

$$v_i(t+1) = v_i(t) + (x_i(t) - g_{best})f_i \qquad (3.9)$$

$$x_i(t+1) = x_i(t) + x_i(t+1) \qquad (3.10)$$

$$f_i = f_{min} + (f_{max} - f_{min})\beta \qquad (3.11)$$

Where f_i is the frequency of the ith bat, which is updated in each-iteration. As per the literature, we have set $f_{min}=0$ and $f_{max}=2$. g_{best} is the best solution attained so far, and β is the random number of a uniform distribution.

If we observe all the above equations, it could be inferred that artificial bats will have a diverse tendency to the best solution even though they are with different frequencies. The random walk of each bat to perform the exploitation is as follows.

$$x_{new} = x_{old} + \gamma L^t \qquad (3.12)$$

Here γ represents random number, and it is a random value between 0 and 1. L represents the loudness of the sound emitted from a bat. Since $L\epsilon(0,1)$, its value is initially asuumed as 0.25. And, the emission rate (r) is initialized as 0.1.

The advantages of this method over earlier optimization techniques are it improves local minima avoidance and convergence speed. These advantages are just because of the parameters such as pulse emission rate (r) and loudness (L), which are the controlled parameters used to balance the optimization with the intensive local search. They are given by,

$$L_i(t+1) = \varepsilon L_i(t) \qquad (3.13)$$

$$r_i(t+1) = r_i(0)[1 - \exp(-\alpha t)] \qquad (3.14)$$

Where ϵ and α are the constants. Typically, ε should be in between (0, 1) and α should be greater than zero. Here, in the simulation, we have considered the range for α and ε in between 0.9 to 0.98.The L and r will be updated until the new solutions are converging towards the best solution.

3.4.2. Binary Bat Algorithm (BBA)

In BA, the bats are moving around the continuous search space. But, the present OPP problem is binary optimization problem whose solution is a set of zeros (0s) and ones (1s). Here, binary one represents the presence of PMU and binary zero represents absence of PMU. But, the search space for the standard BA is continuous, means its solution is a set of real number. Hence, it cannot be applied for the problems like binary optimization problems (example, OPP problem) whose solution should be in terms of bits. So, a new version of BA algorithm, called Binary Bat Algorithm (BBA), is introduced here, which can handle binary optimization problems.

The population represents the bits equal to the number of buses in a particular system. If any of the bits is 1, then it means there would be a PMU at that bus, otherwise no PMU. In Binary Bat Algorithm (BBA), the agents will move in a discrete search space.This movement can only be done by flipping the various numbers of bits [99]. So, while designing BBA, as it uses only two bits (0's and 1's), the standard position and velocity updating processes have to be modified. It is just because it is difficult to add a real-valued velocity to a position vector in a binary search space. Here, this problem has been answered by changing the position of the bat with respect to the probability of its velocity [100, 101]. This procedure needs a transfer function for mapping velocity with its probability to update the position. Also, the chosen transfer function has to obey the rules listed below.

➢ The transfer function range must be within the limits [0, 1].
➢ The transfer function should be enough sensitive so that it could provide all the probabilities of changing the position for all the ranges of absolute values of velocities.
➢ The return values of transfer function should vary proportionally for every change in the velocity.

The transfer function thus obtained from the above guidelines will make sure that it can map accurately the search space in continuous domain to that of in discrete domain [99]. The transfer function that we considered here is a V-shaped transfer function and is as give below [102].

$$s\left(v_i^k(t)\right) = \left| \frac{2}{\pi} \arctan\left(\frac{\pi}{2} v_i^k(t) \right) \right|$$

(3.15)

$$x_i^k(t+1) = \begin{cases} x_i^k(t)^{-1}, \text{ rand} < s\left(v_i^k(t+1)\right) \\ x_i^k(t), \text{ rand} \geq s\left(v_i^k(t+1)\right) \end{cases} \qquad (3.16)$$

Where x_i^k and v_i^k indicate position and velocity of ith particle respectively at iteration t in k^{th} dimension. Here equation (3.15) is used as a transfer function for mapping velocities to the probabilities of flipping their positions. Equation (3.16) is employed to update the position of the bat. The algorithm of this Binary Bat technique is given below.

Algorithm:

step1: Read the objective function and constraints. Initialize bat population, pulse emission rate (r) and loudness (l).

step2: Define the pulse frequency (f_i).

step3: while (t < max. number of iterations), go to step4, else go to stop.

step4: Modify the frequency and update the velocity.

step5: Calculate the transfer function using equation (1) and update the positions using equation (2).

step6: If (rand $>r_i$), go to step7, else go to step8.

step7: Select g_{best} from the best solution set randomly, and change some of the dimensions of position vector with some of the dimensions of the g_{best}. End if.

step8: Create a new solution by flying arbitrarily.

step9: If (rand < l and $f(x_i) < f(g_{best})$) go to step 10, else go to step11.

step10: Adopt the new solutions. Increase r_i and L_i. End if.

step11: Obtain the g_{best} by ranking the bats.

step12: Stop.

3.5. Results and Discussions

The number and the locations of PMUs to maximize observability obtained by applying the proposed BBA technique to standard IEEE test systems under normal and line/PMU outage conditions are given in Tables 3.1, 3.2, 3.3 and 3.4.

Table 3.1: Complete Observability under normal conditions

system	Location of PMUs	No. of PMUs
IEEE-14	2,6,7,9	4
IEEE-30	1, 2, 6, 9, 10, 12, 15, 19, 25, 27	10
IEEE-57	1,4,9,15,20,2,4,26,29,3,1,32,36,3,8,39,41,4,7,50,54	17
IEEE-118	1,5,9,12,15,17,20,23,25,29,34,37,42,45,49,52,56,62,63,68,71, 75,77,80,85,87,90,94,101,105,110,114	32

Table 3.2: Complete observability under normal operating conditions considering channel limits.

System	Locations of PMUs	No. of PMUs
IEEE-14	2,6,7,9	4
IEEE-30	2,4,6,9,1,0,12,18,2,4,25,27	10
IEEE-57	1,6,9,15,19,21,24,28,31,34,37,38,41,47,50,53,56	17
IEEE-118	1,5,10,12,15,17,20,23,25,29,34,37,40,45,49,53,56,62,64,68,71, 75,77,80,85,87,90,92,96,100,105,110,115	33

Table 3.3: Complete observability under Line/PMU failure

System	Locations of PMUs	No. of PMUs
IEEE-14	1,2,4,,6,7,8,,9,11,13	9
IEEE-30	1,2,3,6,7,8,9,10,11,12,13,15,17,19,20,22,24,25,26,27,29	21
IEEE-57	1,3,4,6,9,11,12,15,19,20,22,24,25,27,28,29,31,32,34,36,37,38 ,41,45,46,47,50,51,53,54,56,57	32
IEEE-118	1,2,5,6,9,10,11,12,15,17,19,21,22,25,27,28,30,31,32,34,36,37 ,40,42,43,45,46,49,51,52,54,56,57,59,61,62,64,66,68,70,71,7 2,73,75,77,78,80,84,85,86,87,89,91,92,94,96,100,101,105,10 7,108,110,111,112,114,116,117,118	68

Table 3.4: complete observability under Line/PMU failure considering channel limits.

System	Locations of PMUs	No. of PMUs
IEEE-14	2,4,5,,6,7,8,,9,10,13	9
IEEE-30	1,2,3,,5,6,8,,9,10,11,1,2,13,15,1,6,18,19,2,2,24,25,2,6,29,30	21
IEEE-57	1,3,,4,6,9,11,12,15,19,20,22,24,25,27,28,29,30,32,34,36,37,3 8,39,41,44,46,47,50,51,53,54,56	32
IEEE-118	1,2,5,7,9,10,11,12,15,17,19,21,22,24,26,27,29,30,31,32,34,35 ,37,40,41,44,45,46,49,50,51,52,54,56,59,62,63,65,66,68,70,7 1,73,75,76,77,78,80,83,85,86,87,89,91,92,94,96,100,101,105, 107,108,110,111,112,115,116,117	68

3.5.1. Southern Regional Indian power Grid (SRIG)

Southern Regional Indian power Grid (SRIG) is the only IRG that was connected asynchronously to the remaining parts of the Indian power grid till December 31, 2012, after which it was synchronized to the rest of Indian power grid to form a single Indian grid. The locations of PMUs are given in Tables 3.5 and 3.6.

Table 3.5: PMU locations of SRIG

System	PMU locations under normal operating conditions	PMU locations under line/PMU outage conditions
SRIG	5,7,8,10,12,19,22,27,28,30,33,42,48,49,54,58,60,63,67,73,75,76,88,89,92,95,99,102,105,107,110,111,115,117,118,121,122,127,128,132,136,138,145,147,152,154,157,159,161,165,181,184,188,190,191,196,201.	1,3,4,6,9,10,12,13,14,16,19,22,23,25,26,27,28,30,31,32,33,35,36,37,42,43,45,47,48,49,54,56,57,58,59,60,62,63,64,66,67,69,70,71,73,75,76,78,79,83,85,86,87,88,89,92,93,95,96,98,99,100,103,104,106,107,108,110,111,112,113,115,116,117,118,119,120,121,122,123,124,127,128,130,132,133,134,136,138,141,142,145,146,147,148,150,152,154,157,158,159,160,161,163,164,165,166,167,169,170,174,175,177,179,180,181,184,185,188,190,191,192,194,196,197,198,201,202,203,205,207,208.

Table 3.6: PMU locations of SRIG considering channel limitations

System	PMU locations under normal operating conditions	PMU locations under line/PMU outage conditions
SRIG	5,7,8,10,12,19,22,27,28,30,33,42,48,49,54,58,60,63,67,73,75,76,88,89,92,95,99,102,105,107,110,111,115,117,118,121,122,127,128,132,136,138,145,147,152,154,157,159,161,165,181,184,188,190,191,196,201.	1,5,6,7,9,10,12,13,14,16,19,22,23,25,27,28,30,31,32,33,35,36,37,40,41,42,43,44,45,48,52,53,54,56,58,60,61,63,64,66,67,69,73,75,76,78,79,83,84,85,86,88,89,92,93,95,96,98,99,100,102,104,105,106,107,108,110,111,112,113,115,116,117,118,119,120,121,122,123,124,127,128,130,132,133,134,136,137,138,141,142,145,146,147,148,150,152,154,156,157,158,159,160,161,163,165,166,167,169,170,171,174,175,176,179,180,181,183,184,187,188,190,191,192,194,196,197,198,201,202,203,205,207,208

3.5.2. System Observability Index Results

Table 3.7: System observability indices

System	Under normal conditions		Under line/PMU outage conditions	
	No.of buses observed more than one time(n_p)	SOI	No.of buses observed more than two times(n_p)	SOI
IEEE-14	4	1.29	6	1.43
IEEE-30	14	1.47	13	1.43
IEEE-57	13	1.23	13	1.23
IEEE-118	36	1.31	46	1.39
SRIG	59	1.29	66	1.32

Table 3.8: System observability indices considering channel limits

System	Under normal conditions		Under line/PMU outage conditions	
	No.of buses observed more than one time(n_p)	SOI	No.of buses observed more than two times(n_p)	SOI
IEEE-14	4	1.29	6	1.43
IEEE-30	12	1.4	13	1.43
IEEE-57	15	1.26	12	1.21
IEEE-118	44	1.37	46	1.39
SRIG	59	1.29	66	1.32

For the same number of PMUs obtained from the observability based optimal PMU placement presented in first contribution, this method maximizes the total observability of the network. From the Tables 3.7 and 3.8, it is clear that, on average the proposed algorithm provides 32 and 36 percentages of measurement redundancy under normal and Line/PMU outage conditions respectively. The proposed method yields the best solution for OPP problem that could maximize the observability.

3.6. Conclusion

The faults that would occur in the power system could cause line/PMU outage. The proposed algorithm has considered even these conditions also for finding PMU placements. The proposed BBA method has solved the OPP problem under both normal and abnormal conditions in power system accurately. The proposed method has been tested on few IEEE standard test systems, and then applied for Southern Region of Indian power Grid (SRIG). From the results and discussions, it is verified that the proposed method has successfully obtained the PMUs set for maximizing the measurement redundancy.

POWER SYSTEMS RESTORATION BASED WIDE-AREA MEASUREMENT SYSTEMS PARTITION

4.1. Introduction

Despite of many attempts made to improve the protection measures, the power system is still highly prone to the interruptions in power supply. Sometimes, the power supply to a complete network will be lost and causes the complete outage of network elements like generators, transformers and loads. This phenomenon called Blackout is the most dangerous outage than any other outage [103]. So, the power system elements need to be restored after blackout. Moreover, the number of islands decides the restoration time. This can be achieved by a restoration strategy called Build-up strategy. The power system restoration is an effective measure as the delay in the restoration causes damage to consumers, and subjects the system to many economic and political costs. From the power system studies proposed in [59], a Build-up strategy is recommended here. It follows mutual interconnection of islands after restoring them separately. The Build-up strategy and its importance are explained in [59-62]. But the authors are failed in introducing the ideas to sectionalize a network into separate islands. Later, authors suggested a scheme [63] to sectionalize a network into separate islands, but it has failed in producing stable islands as it doesn't consider Generation-Load constraint during initial partitioning. Generally, during restoration, a circuit breaker between two buses should not be closed with larger phase angle because it may damage the system by causing unwanted outages. Moreover, if the PMU installed power system is partitioned; it may lose observability because of the line openings between islands. The proposed technique has partitioned without disturbing the observability of every bus in every island.

This section proposes a restoration based sectionalizing method for a PMU installed network. It is a model based algorithm that can handle even large-scale networks. Unlike [63], it considers power generation-load balance constraint during initial system partitioning. It also considers observability constraint at the final stage of the sectionalizing process. These two constraints have really increased the stability and observability of feasible islands. This would probably help power companies in protecting the power systems from large catastrophes like Blackouts just by isolating the islands that are being faulted. In the end, it also suggests an optimal location strategy for Phasor Data Concentrators (PDCs) to provide phase angle data across the lines between any two islands.

4.2. Optimal PMU Placement

This section will optimize the number of PMUs required for observing the system completely. In this work, it is assumed that the PMU placement has been done before partitioning the network. The Optimal PMU Placement is done using the Binary Cuckoo Search (BCS) technique proposed in the section 2.2. The PMU locations obtained are tabulated in Table 4.1.

Table 4.1: PMU Locations for different test systems

Test system	Locations of PMUs
IEEE-30	2, 3, 6, 9, 10, 12, 15, 19, 25, 27.
IEEE-39	2,6,9,10,12,14, 17, 20, 22, 23, 26, 29, 33
IEEE-118	2,5,9,12,15,17,21,34,29,25,27,32,45,37,42,49,56,64,62,53,68,70,71,76,77,80,94,101,105,85,90,86,110
IG-75	4,13, 6,17,18,20,24,25,29,30,31,32,33,34,35,40,41,43,44,49,51,54,69,70,73

4.3. Constraints for WAMS Power System Restoration

After sectionalizing the network, each island should be observable independently. For this, the process of network partition should be undergone three constraints like transformer equivalent bus, generation-load balance and observability of each island. The constraints will be explained as follows.

4.3.1. Generation-Load balance

This constraint ensures that there should be enough amount of active power to supply all the loads in each island. It can be represented as,

$$\sum_{i=1}^{n_r} P_{Gi} > \sum_{i=1}^{n_r} P_{Li} \text{ , } i = 1, 2, 3.....r. \tag{4.1}$$

Where r represents the number of regions, n_r represents the number of buses in each island, P_{Gi} gives maximum generation at i^{th} bus and P_{Li} gives the load at i^{th} bus. This constraint must be satisfied in each-iteration of network partitioning.

4.3.2. Joining the islands on either side of the transformer

For the individual regions to run independently, it is required that the transformer and its buses should be allocated to the same region. This can be achieved by joining the islands that are being present on either side of the transformer. This constraint will be applied only after partitioning the complete system initially.

4.3.3. Observability of islands

This constraint will be checked by,

$$A_P \times x_P \geq \begin{bmatrix} 1 \\ 1 \\ . \\ . \\ 1 \end{bmatrix}_{k \times k} \qquad (4.2)$$

Where the matrix A_p gives the system connectivity of pth region. It can be calculated from (4.3). The vector x_p of pth region is the binary variable vector, k is the number of buses in p^{th} island. This is the last constraint that will be applied only after checking the second constraint. This constraint needs to be satisfied by each island; otherwise, the island becomes unobservable.

4.4. Proposed Network Sectionalizing

Here, the partition method is illustrated as follows.

4.4.1. Initial Network partition

After considering the system, the first step is to identify the number of islands. For this, let us consider the network connectivity matrix A whose elements can be defined as,

$$A_{ij} = \begin{cases} 1, if \ i = j \ or \ buses \ i \ and \ j \ are \ connected \\ 0, otherwise \end{cases} \qquad (4.3)$$

During restoration, all the stable regions must be connected to restore the system completely. So, while partitioning the system, it should be assured that each region should have at least one generator and an allowable load connected to it. Initially, the number of regions can be selected as follows,

$$r = \min \left\{ \sum_{i=1}^{n} G_i, \sum_{i=1}^{n} L_i, \sum_{i=1}^{n} M_i \right\} \qquad (4.4)$$

Where,

$$G_i = \begin{cases} 1, if \ there \ is \ a \ generator \ at \ bus \ i \ connected \\ \quad with \ an \ affordable \ load \\ 0, otherwise \end{cases} \qquad (4.5)$$

$$L_i = \begin{cases} 1, & \text{if there is a load bus at bus } i \\ 0, & \text{otherwise} \end{cases} \tag{4.6}$$

$$M_i = \begin{cases} 1, & \text{if bus } i \text{ has PMU} \\ 0, & \text{otherwise} \end{cases} \tag{4.7}$$

After selecting the number of regions (r), a matrix R called regional matrix would be formulated. The matrix R is a $r \times n$ matrix in which each row corresponds to one region. Initially, all elements in every-row of the matrix R set to 0 except for the buses with a generator and an affordable load. Then, the next order regional matrix can be calculated using (4.8) given below.

$$R_k = R_{k-1} \times A, k > 1 \tag{4.8}$$

Where, A is system connectivity matrix, R_{k-1} is R'_{k-1} after corrections. This equation will be calculated iteratively until all the nodes (or buses) of the system were assigned. The corrections needed for higher order regional matrix will be defined as below:

1. The node once assigned, it should not be reassigned to any other region in next iteration.

2. If any entry in the regional matrix is greater than unity, it should be corrected to 1 before the matrix is being considered for next order regional matrix.

3. If a node appears in one region, then it can be assigned to that particular region provided this assignment should satisfy the first constraint of restoration. Otherwise the entry should be reset before it is being considered for next iteration.

4. If a node appears for more than one region, based on the nature of the bus it can be assigned to a region as follows:

Load bus:

- If a load bus appears in more than two regions, it should be assigned to a region which could afford the load with less generation-load margin. This idea is to increase the number of regions (islands).

- If there no single region that could supply the load alone, the regions that are incident to load bus could be combined to supply the load.

Zero-Injection Bus (ZIB):

- If a ZIB appears in more than one region, then it should be assigned to a region with less power rating. This idea also is to increase the number of regions.

Generator bus:

- If a generator bus appears in more than one region, then it is suggested to assign it to a region with less power rating. This idea is to improve the stability of an island.

4.4.2. Final network partition

For the islands to be observable, the observability constraint needs to be verified. If it is not satisfied, the buses whose entries represent '0' needs to be made observable by moving them into their adjacent islands provided the restoration constraints would not be disturbed. While making the unobservable buses observable, few situations that may arise will be handled as follows:

1. Unobservable bus is Load/Generator bus

The bus will be moved to an island via boundary line where it would be made observable provided this movement should not disturb the first and second restoration constraints. If this change causes violation of any constraint, the home island and the target islands are needed to be joined.

2. Unobservable bus is ZIB

If the unobservable bus is a ZIB, it should be moved to a region where it would be observable.

4.5. Phasor Data Concentrator Placement

The Phasor Data Concentrator archives the data from multiple PMUs installed over a wide area and aligns it for analytics /visualization. So, this must be placed in every island to provide the data for certain functions like wide-area monitoring and protection. This section presents a new methodology to place PDCs in each island optimally with respect its PMU locations. The problem of PDC placement can be defined as follows:

Minimize

$$\sum_{j=1}^{r} x_j \qquad (4.9)$$

Subjected to

$$S_p \geq 1 \qquad (4.10)$$

Where

$$S_p = \sum_{i=1}^{n_r} c_{ij} x_j \qquad (4.11)$$

$$c_{ij} = \begin{cases} 1, if\ bus\ i\ has\ PMU, or\ j\ is\ PMU\ observed\ bus \\ 0, itherwise \end{cases} \qquad (4.12)$$

Where x_j is a binary PDC placement variable, S_p is a PMU location constraint function at bus p, c_{ij} is a network path connectivity matrix. Once the network is partitioned, this method will be applied for all the islands.

4.6. Results and Discussions

4.6.1. IEEE 30-bus system

The partition method is illustrated by considering an IEEE-30 bus system shown in Fig. 4.1.
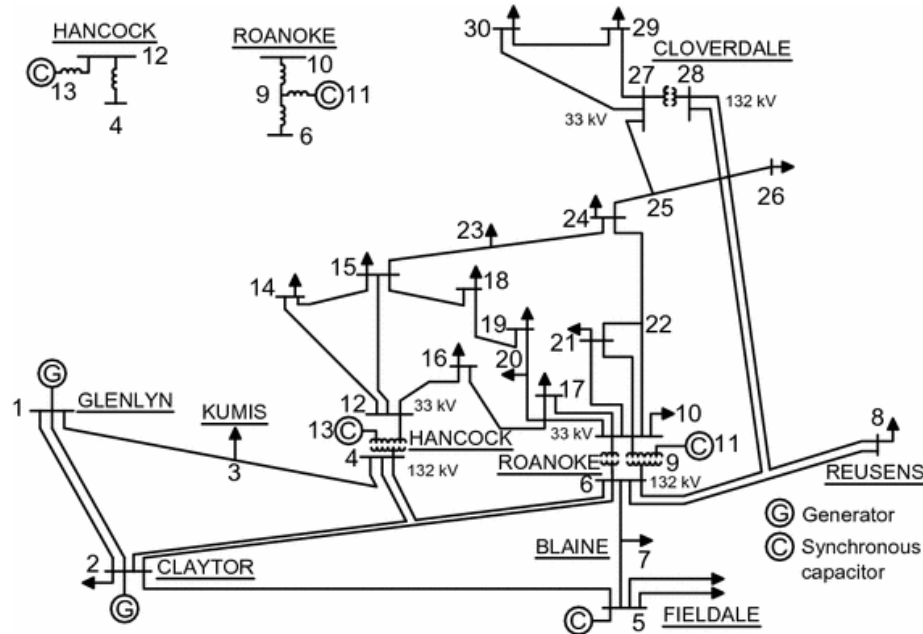
Figure 4.1: IEEE-30 bus system

The proposed methodology has been clearly explained with the help of the flowchart shown in Fig. 4.2.
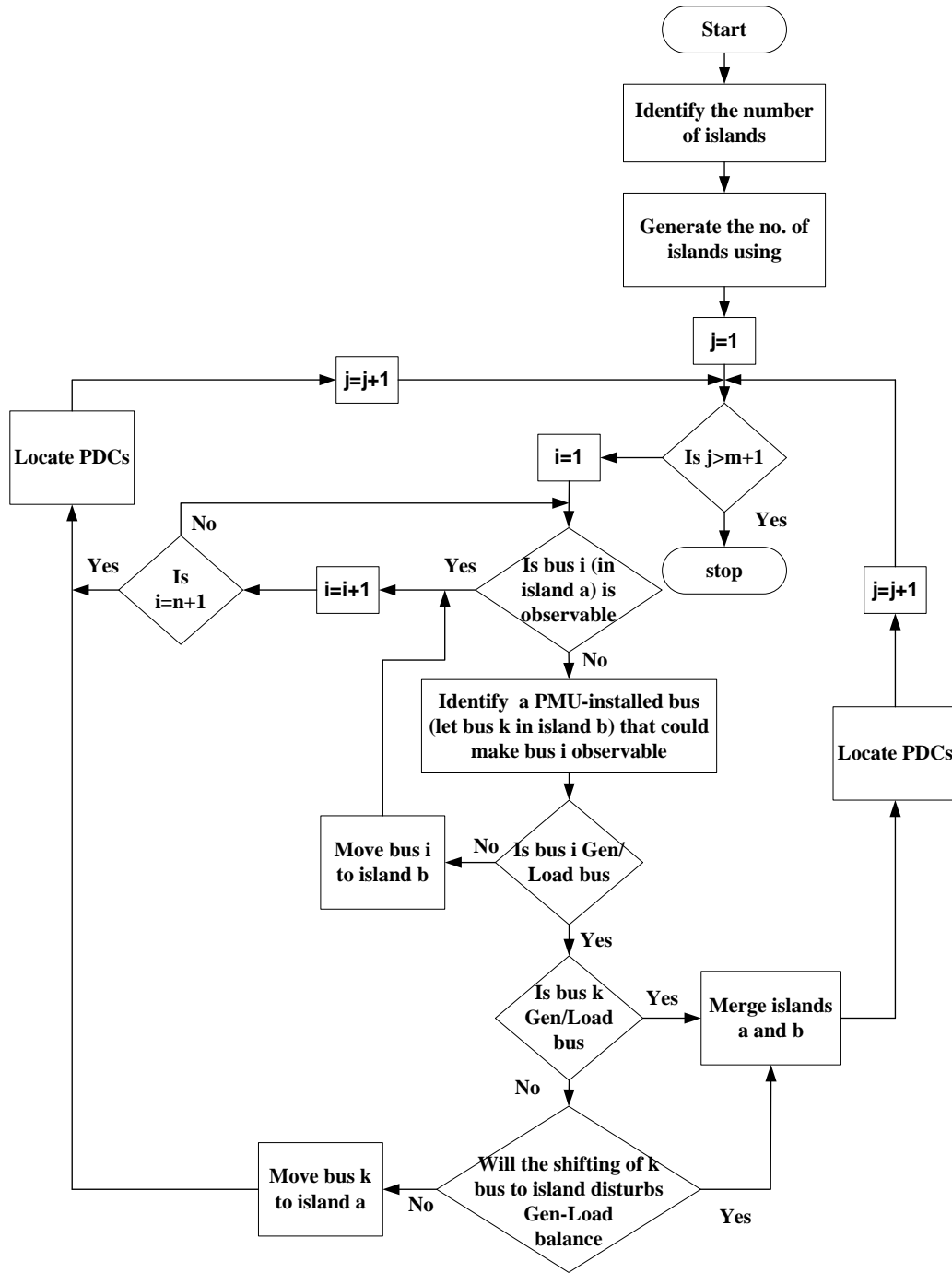
Figure 4.2: Flowchart of the proposed algorithm

After identifying the initial number of islands as 6, the initial regional matrix becomes R_1 as shown in (4.13). And, the second order uncorrected regional matrix will be obtained as

(4.14). On applying the corrections suggested in section 4, the second order regional matrix of IEEE-30 bus system is obtained as (4.15). The final regional matrix is obtained as (4.16).

$$R_1 = \begin{bmatrix}
1 & 0 & 1 & 0 & 0 & 0 & 0 & 0 & 0 & 0 & 0 & 0 & 0 & 0 & 0 & 0 & 0 & 0 & 0 & 0 & 0 & 0 & 0 & 0 & 0 & 0 & 0 & 0 & 0 & 0 \\
0 & 1 & 0 & 1 & 0 & 0 & 0 & 0 & 0 & 0 & 0 & 0 & 0 & 0 & 0 & 0 & 0 & 0 & 0 & 0 & 0 & 0 & 0 & 0 & 0 & 0 & 0 & 0 & 0 & 0 \\
0 & 0 & 0 & 0 & 0 & 0 & 0 & 0 & 0 & 0 & 0 & 1 & 1 & 0 & 0 & 0 & 0 & 0 & 0 & 0 & 0 & 0 & 0 & 0 & 0 & 0 & 0 & 0 & 0 & 0 \\
0 & 0 & 0 & 0 & 0 & 0 & 0 & 0 & 0 & 0 & 0 & 0 & 0 & 0 & 0 & 0 & 0 & 0 & 0 & 0 & 0 & 1 & 1 & 0 & 0 & 0 & 0 & 0 & 0 & 0 \\
0 & 0 & 0 & 0 & 0 & 0 & 0 & 0 & 0 & 0 & 0 & 0 & 0 & 0 & 1 & 0 & 0 & 0 & 0 & 0 & 0 & 0 & 1 & 0 & 0 & 0 & 0 & 0 & 0 & 0 \\
0 & 0 & 0 & 0 & 0 & 0 & 0 & 0 & 0 & 0 & 0 & 0 & 0 & 0 & 0 & 0 & 0 & 0 & 0 & 0 & 0 & 0 & 0 & 0 & 0 & 0 & 1 & 0 & 0 & 1
\end{bmatrix} \quad (4.13)$$

$$R_2' = \begin{bmatrix}
1 & 1 & 1 & 0 & 0 & 0 & 0 & 0 & 0 & 0 & 0 & 0 & 0 & 0 & 0 & 0 & 0 & 0 & 0 & 0 & 0 & 0 & 0 & 0 & 0 & 0 & 0 & 0 & 0 & 0 \\
2 & 1 & 1 & 2 & 1 & 1 & 0 & 0 & 0 & 0 & 0 & 0 & 0 & 0 & 0 & 0 & 0 & 0 & 0 & 0 & 0 & 0 & 0 & 0 & 0 & 0 & 0 & 0 & 0 & 0 \\
0 & 0 & 0 & 1 & 0 & 0 & 0 & 0 & 0 & 0 & 0 & 2 & 2 & 1 & 1 & 1 & 0 & 0 & 0 & 0 & 0 & 0 & 0 & 0 & 0 & 0 & 0 & 0 & 0 & 0 \\
0 & 0 & 0 & 0 & 0 & 0 & 0 & 0 & 0 & 2 & 0 & 0 & 0 & 0 & 0 & 0 & 0 & 0 & 0 & 0 & 2 & 2 & 0 & 1 & 0 & 0 & 0 & 0 & 0 & 0 \\
0 & 0 & 0 & 0 & 0 & 0 & 0 & 0 & 0 & 0 & 1 & 0 & 1 & 2 & 0 & 0 & 1 & 0 & 0 & 0 & 0 & 2 & 1 & 0 & 0 & 0 & 0 & 0 & 0 & 0 \\
0 & 0 & 0 & 0 & 0 & 0 & 0 & 0 & 0 & 0 & 0 & 0 & 0 & 0 & 0 & 0 & 0 & 0 & 0 & 0 & 0 & 0 & 0 & 1 & 0 & 2 & 1 & 2 & 2
\end{bmatrix} \quad (4.14)$$

$$R_2 = \begin{bmatrix}
1 & 1 & 1 & 0 & 0 & 0 & 0 & 0 & 0 & 0 & 0 & 0 & 0 & 0 & 0 & 0 & 0 & 0 & 0 & 0 & 0 & 0 & 0 & 0 & 0 & 0 & 0 & 0 & 0 & 0 \\
0 & 1 & 0 & 1 & 1 & 1 & 0 & 0 & 0 & 0 & 0 & 0 & 0 & 0 & 0 & 0 & 0 & 0 & 0 & 0 & 0 & 0 & 0 & 0 & 0 & 0 & 0 & 0 & 0 & 0 \\
0 & 0 & 0 & 0 & 0 & 0 & 0 & 0 & 0 & 0 & 0 & 1 & 1 & 0 & 0 & 1 & 0 & 0 & 0 & 0 & 0 & 0 & 0 & 0 & 0 & 0 & 0 & 0 & 0 & 0 \\
0 & 0 & 0 & 0 & 0 & 0 & 0 & 0 & 0 & 0 & 1 & 0 & 0 & 0 & 0 & 0 & 0 & 0 & 0 & 0 & 0 & 1 & 1 & 0 & 1 & 0 & 0 & 0 & 0 & 0 \\
0 & 0 & 0 & 0 & 0 & 0 & 0 & 0 & 0 & 0 & 0 & 0 & 0 & 1 & 1 & 0 & 0 & 1 & 0 & 0 & 0 & 1 & 0 & 0 & 0 & 0 & 0 & 0 & 0 & 0 \\
0 & 0 & 0 & 0 & 0 & 0 & 0 & 0 & 0 & 0 & 0 & 0 & 0 & 0 & 0 & 0 & 0 & 0 & 0 & 0 & 0 & 0 & 0 & 0 & 1 & 0 & 1 & 1 & 1 & 1
\end{bmatrix} \quad (4.15)$$

$$R_4 = \begin{bmatrix}
1 & 0 & 1 & 0 & 0 & 0 & 0 & 0 & 0 & 0 & 0 & 0 & 0 & 0 & 0 & 0 & 0 & 0 & 0 & 0 & 0 & 0 & 0 & 0 & 0 & 0 & 0 & 0 & 0 & 0 \\
0 & 1 & 0 & 1 & 1 & 1 & 1 & 0 & 0 & 0 & 0 & 0 & 0 & 0 & 0 & 0 & 0 & 0 & 0 & 0 & 0 & 0 & 0 & 0 & 0 & 0 & 0 & 0 & 0 & 0 \\
0 & 0 & 0 & 0 & 0 & 0 & 0 & 0 & 0 & 0 & 0 & 1 & 1 & 1 & 1 & 1 & 1 & 1 & 1 & 1 & 1 & 0 & 0 & 1 & 0 & 0 & 0 & 0 & 0 & 0 \\
0 & 0 & 0 & 0 & 0 & 0 & 0 & 0 & 1 & 1 & 1 & 0 & 0 & 0 & 0 & 0 & 0 & 0 & 0 & 1 & 1 & 0 & 1 & 0 & 0 & 0 & 0 & 0 & 0 & 0 \\
0 & 0 & 0 & 0 & 0 & 0 & 0 & 0 & 0 & 0 & 0 & 1 & 1 & 1 & 1 & 1 & 1 & 1 & 1 & 1 & 0 & 0 & 1 & 0 & 0 & 0 & 0 & 0 & 0 & 0 \\
0 & 0 & 0 & 0 & 0 & 0 & 0 & 1 & 0 & 0 & 0 & 0 & 0 & 0 & 0 & 0 & 0 & 0 & 0 & 0 & 0 & 0 & 0 & 0 & 1 & 1 & 1 & 1 & 1 & 1
\end{bmatrix} \quad (4.16)$$

From this equation, it is quite clear that the regions r3 and r5 were combined to supply the load at bus 19. So, the system is portioned into five stable regions as shown in Fig. 4.3. The system presented in Fig. 4.3 inherently exhibits generation-load balance as the first constraint is satisfied. Next, the regions that present on either side of transformer need to be joined to satisfy the second restoration constraint. So, regions r2, r3 (or r5) will be joined.

On applying the final portioning step for the system obtained above, since the island (r6) alone cannot afford the loads at buses 24 and 8, the set of regions {r3, r6} and {r2, r6} are combined via boundary lines. Figure 4.4 represents the final network. And, it infers that the island r3 covers larger. This is because of the fact that the generation in this region is accumulated whereas the load is distributed.
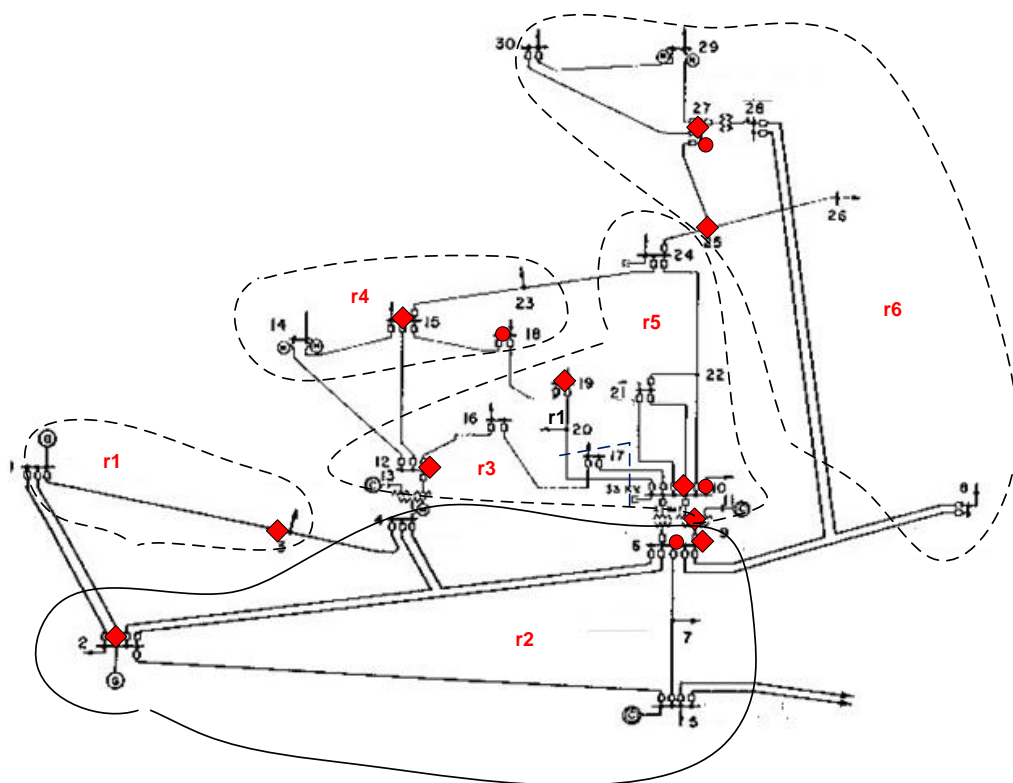
Figure 4.3: Initial Partition of the IEEE-30 bus system
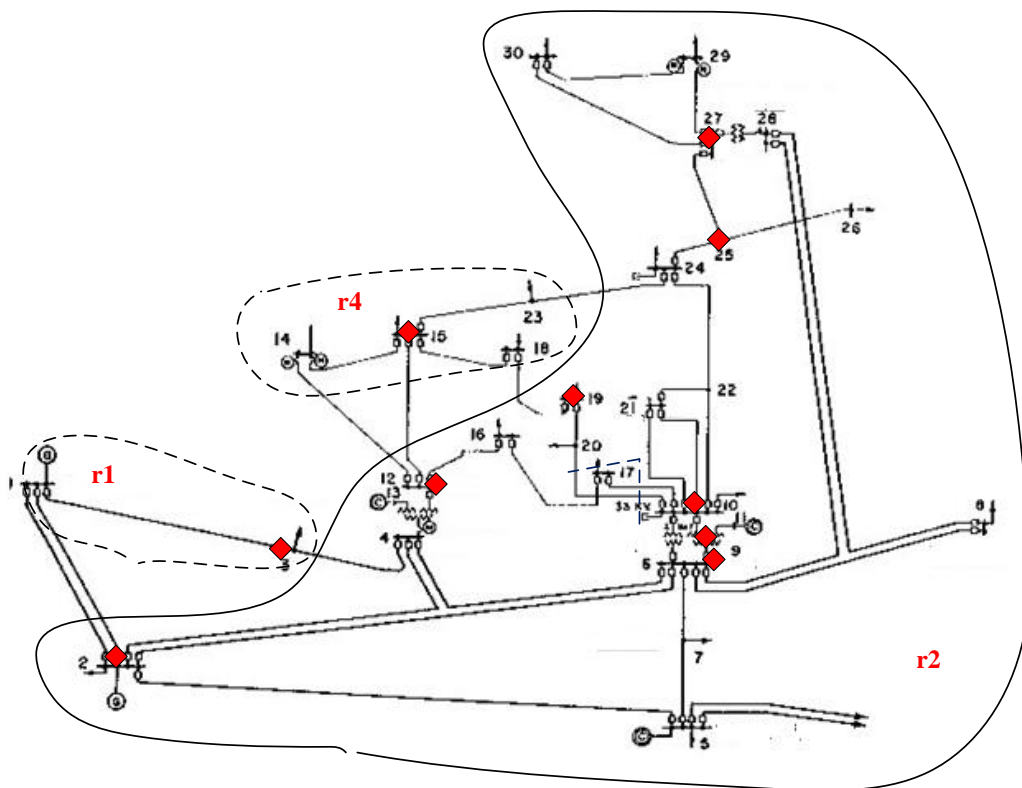
Figure 4.4: Final Partition of the IEEE-30 bus system

The locations of PDCs obtained by applying the PDC placement algorithm are shown in Table 4.2 below.

Table 4.2: Regional information and PDCs locations after final partitioning IEEE-30 bus system

Region	Buses	PMU locations	PDC locations
r1	1, 3	3	3
r4	14, 15, 18, 23	15	15
r2	2,4,5,6,7,8,9,10,11,12,13,16,17,19,20,21,22, 24, 25, 26, 27, 28, 29, 30	2, 6, 9, 10, 12, 19, 25, 27	4, 9, 19, 27

4.6.2. IEEE 39-bus system

On applying the proposed scheme to IEEE-39 system initially, it is clear that the bus 18 is not observable and also it is found that it can be made observable by the PMU on bus 17. Moreover, as the island r2 can afford the load at bus 18, it has been moved to region r2. Figures 4.5, 4.6 show the initial, final partitioning of IEEE-39 test system respectively. Table 4.3 gives the regions, PMU locations, and PDCs locations after final partition.
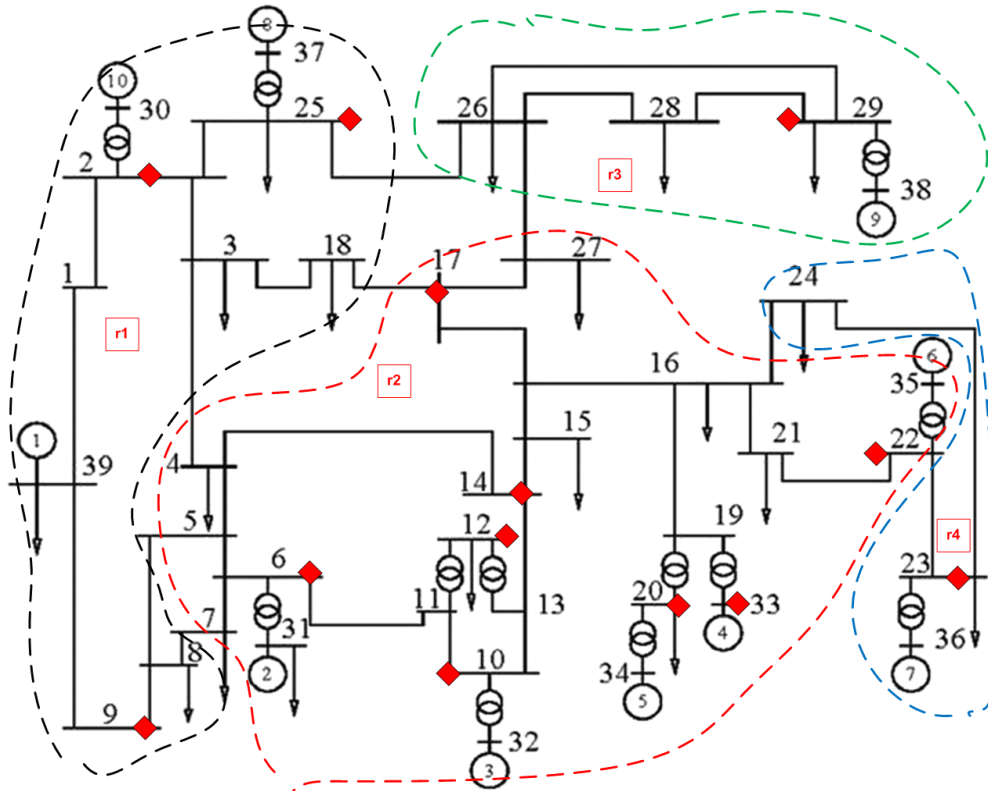
Figure 4.5: Initial Partition of the IEEE-39 bus system

Table 4.3: Regional information and PDCs locations after final partitioning IEEE-39 bus system

Region	Buses	PMU locations	PDC locations
r1	1,2,3,8,9,25,30,37,39	2,9	2, 9
r2	4,5,6,7,10,11,12,13,14,15,16,17,18,19,20,21,22,31,32,33,34,35	6,10,12,14,17,33,20	11, 14, 17, 19, 22
r3	26,27,28,29,38	26,29	29
r4	23,24,36	23	23
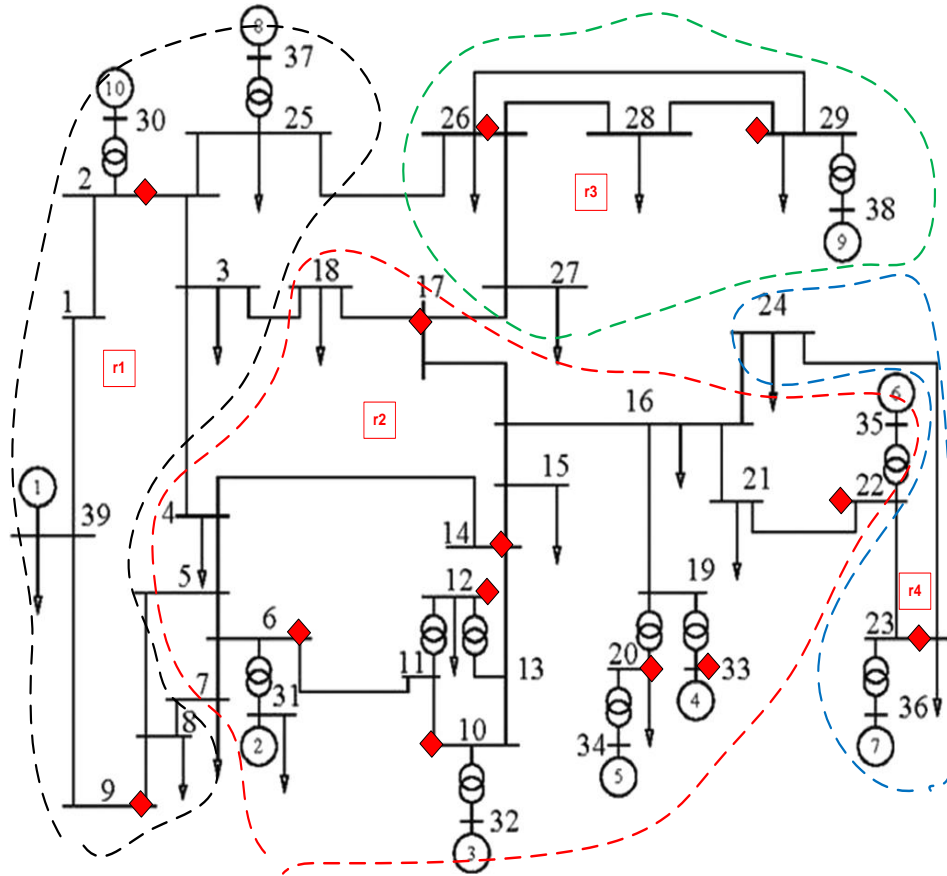
Figure 4.6: Final Partition of the IEEE-39 bus system

4.6.3. IEEE 118-bus system

Similarly, for IEEE-118 system, the buses 24, 15, 35, 55, 59, 65, 67, 106 and 107 are found to be unobserved. The bus 24 is moved to an island containing bus 23 which could observe bus. Similarly, the buses 15 and 35 have been moved to the region 5. Even though the islands 5 and 13 could observe the buses 55, 59, 65 and 67, they cannot supply the required load at the respective buses. So, these two islands are combined. Similarly, the island containing buses 106 and 107 is joined with an island containing bus 105 which could make the buses 106 and 107 observable. The figures 4.7 and 4.8 depict the initial and final partition

of the IEEE-118 test system. Table 4.4 contains the PMUs and PDCs location for different islands.

Table 4.4: Regional information and PDCs locations after final partitioning IEEE-118 bus system

Region	Buses	PMU locations	PDC locations
r1	1,2,3,4,5,6,7,8,9,10,11,12,14,16,17,18,19,20,21, 22,34,36,43,113,117	2,5,9,12,17,21, 34	8,12,21, 34
r2	28,29,31	29	29
r3	23,24,25,26,27,32,114,115	23,26,115	25,27,115
r4	44,45,46	45	45
r5	13,15,33,35,37,38,39,40,41,42,47,48,49,50,51,5 5,56,57,58,59,60,61,62,63,64,65,66,67,68,52	13,37,42,49, 56,62,64	40,66,56, 64
r6	68,69,70,71,72,73,74,75,76,77,78,116,118,82	71,75,77,116	69,71
r7	53,54	53	53
r8	79,80,81,96,97,98,99	80	80
r9	92,93,94,95,100,101,102,103,104, 105,106,107,108	94,101,105	100, 105
r10	83,84,85,88,89,90,91	85,90	89
r11	86,87	86	86
r12	109,110,111,112	110	110

4.6.4. Indian Grid-75 bus system

A practical Indian Grid-75 bus (IG-75) system has been considered here. Its final partition has been shown in the Fig. 4.9. The details of PMUs and PDCs are given in Table 4.5.

Table 4.5: Regional information and PDCs locations after final partitioning Indian -75 bus system

Region	Buses	PMU locations	PDC locations
r1	1,17,19,23,24,29,10,54,67,75,54,63,55,11,40,20,48,12, 41,26,74,22,27,73,51,52,49,64,66,8,34,54,4,28,15,44,4 5,53,30,61,21,14,43,25,56,58,60,65,72,13,42,57,38	4,13,17,20,24,25,2 9,30,34,40,41,43,4 4,49,51,54,70,73	43,24,74, 19,25,40
r2	2,16,46,50	16	16
r3	3,18,47,68,71	18	18
r5	5,31,59	31	31
r6	6,32,62	32	32
r7	7,33,39	33	33
r9	9,35,36,37,69	35,69	36
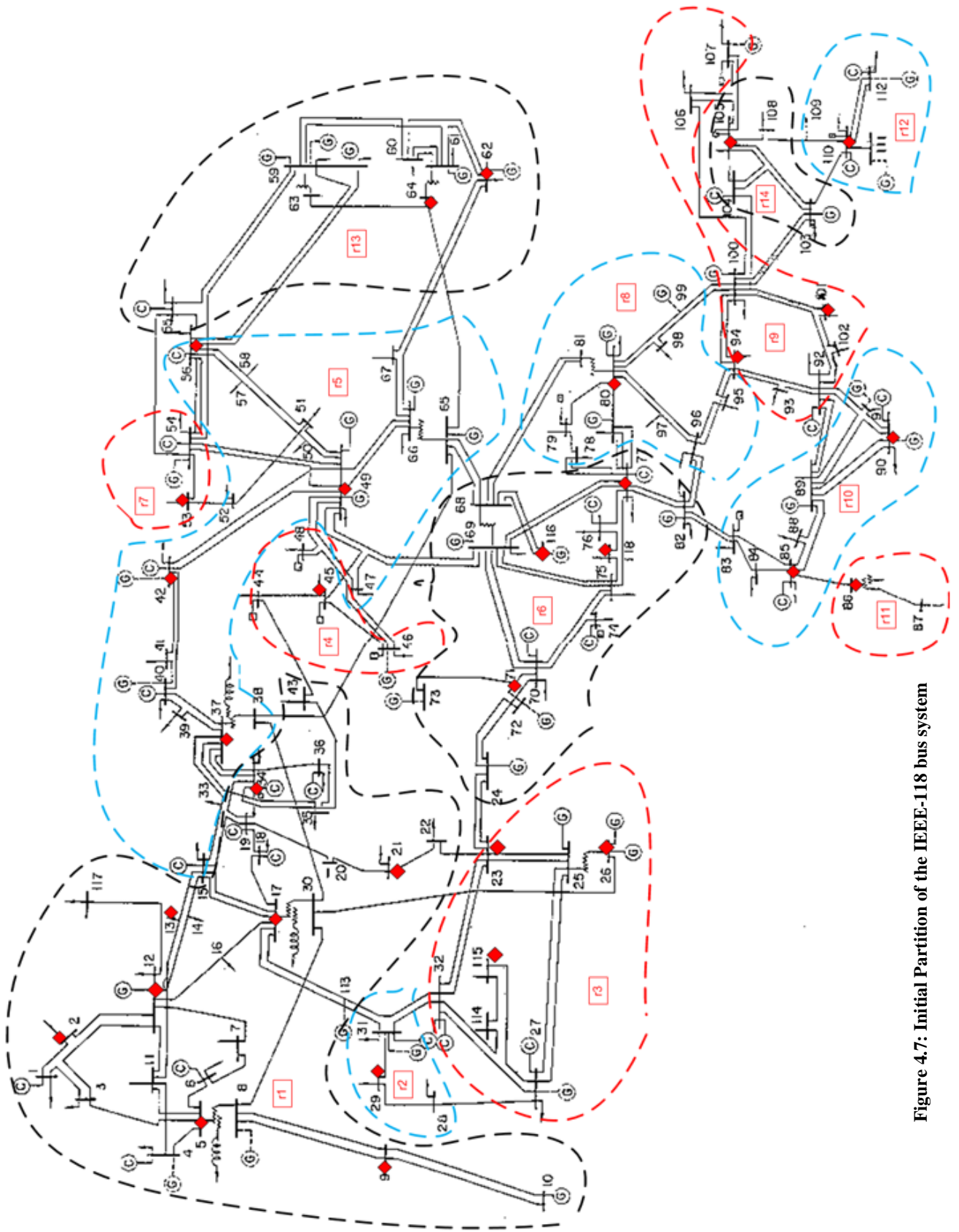
Figure 4.7: Initial Partition of the IEEE-118 bus system

73
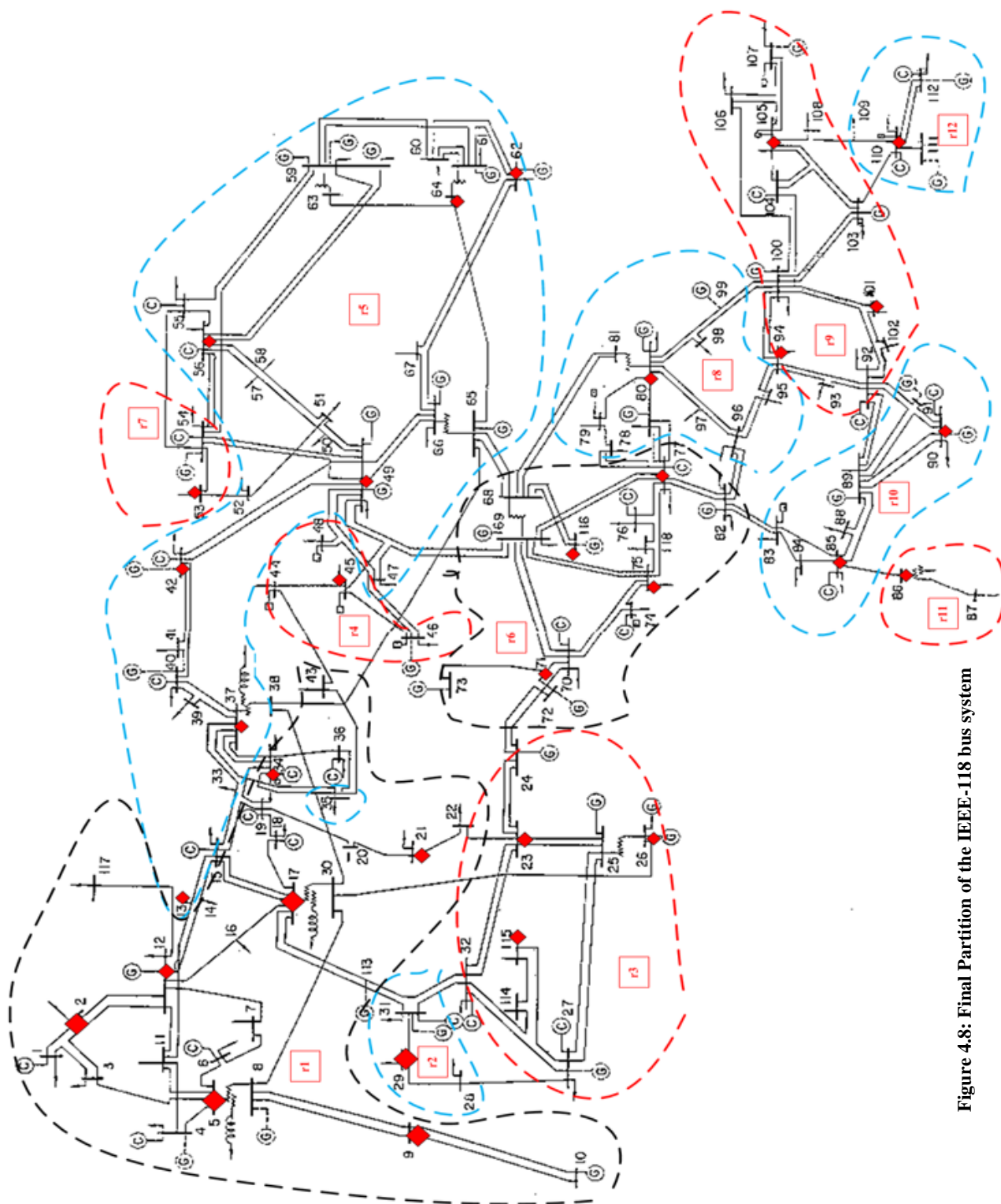
Figure 4.8: Final Partition of the IEEE-118 bus system

74

Figure 4.9: Final Partition of the IG-75 system

Table 4.6: Comparison of the number of restorable WAMS regions

System	Paper [63]	Proposed Work
IEEE-30	-	2
IEEE-39	4	4
IEEE-118	8	12
India-75	-	7

More the number of islands faster the restoration process will be. From the results, it could be clear that this method has successfully produced more stable and observable islands which fasten the restoration process. This will really help the countries which are yet to establish the WAMS. Table 4.6 compares the results obtained from the proposed algorithm with those from the literature. This shows that the effectiveness of the algorithm is proven to be best even for the large test systems.

4.7. Summary

This **chapter of work** assures a faster restoration process by partitioning the network into many regions which are easier to be restored during build-up strategy. Initially, these partitions starts with sectionalizing network subjecting to Generation-Load balance constraint, and next to ensure the remaining two restoration constraints. This approach provides synchronized phase angle data between any two adjacent islands by ensuring complete observability of all regions. This partition algorithm sectionalizes IEEE-39 system into four regions, the IEEE-118 system into 12 islands and Indian-75 bus system into four stable islands.

Chapter-5:

CRITICAL ELEMENTS BASED OPTIMAL PMU PLACEMENT CONSIDERING SUBSTATION COVERAGE

5.1. Introduction

The Phasor Measurement Unit is becoming the most prominent tool for power system applications like power system operation, control, and protection. For a robust and accurate wide-area measuring system, the PMU should observe not only the elements in its own substation but also the critical lines and its incident busses. As the PMU-cost limits their deployment, they must be installed optimally considering the substation installation and the critical lines in power system. This can be done based on the assumption that there must be a PMU in each constructed substation. This will assure the observability of all the elements in substation. The power system will be operated securely and accurately if it is possible to estimate the system state with a variety of measurements. With the integration of the Phasor Measurement Unit into the measurement system, it has become easy to monitor, control and protect the power system. As the PMU costs considerably, the deployment of PMUs and their number are needed to be optimized. In practical substations, buses exist at different voltage levels as shown in Fig. 5.1. The circles in the figure represent substations. One should not forget that one bus being observed inside the substation should not transfer it to other buses inside the same substation. The above methods were developed based on the thumb rule that the PMU installed bus could observe all the buses connected to it including itself. And, as the practical tap ratios are not known, authors have assumed that the buses with different voltages were decoupled in-order to observe them in an individual manner which will increase both search space and bus number. So, it is clear that they have only concentrated on reducing the number of PMUs rather than reducing the substation number.
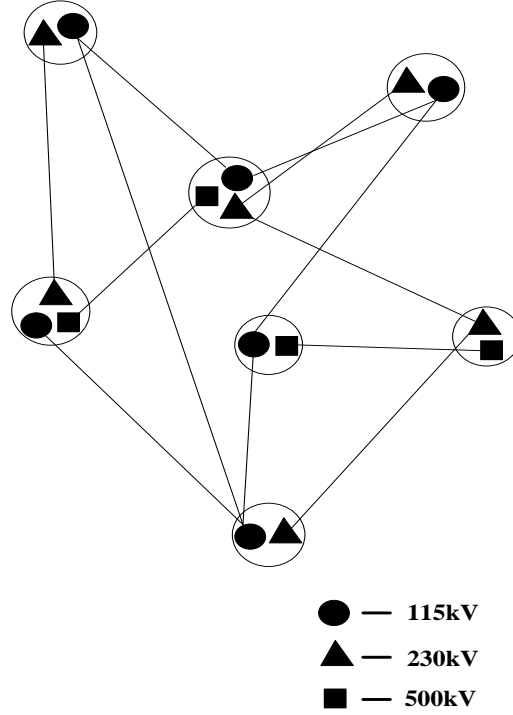
Figure 5.1: A sample transmission system.

Wide-area system planning studies say that the major part of the cost of synchrophasor measurement system deployment is associated with transmission network outages and maintenance costs but not with PMU devices. So, optimization must be towards reducing the substation number. Moreover, the blackout reports suggest that the critical elements which may be zero injection buses must be observed directly to design a robust security system and, so to avoid major blackouts. Therefore, it is essential to implement a policy that considers both the lines and buses based on their role in driving the system to blackout rather than simply considering them based on their connectivity. These considerations have been done in the proposed methodology. It has done the optimal coverage of substation by assuming that one PMU could observe the whole substation provided the tap ratios are known, and then introduces critical lines identification in Blackout situation point of view. Finally, it proposes a new OPP problem considering the critical elements whose outage lead to system blackout and the optimal substation coverage.

5.2. Problem Formulation

Before the network is being considered for OPP problem, it must be undergone one modification given below.

5.2.1. Network reconsideration

This section identifies the optimal substations. In this step, based on the assumption that the tap settings are known, the buses connected through the transformers will be modelled as single equivalent bus called the optimal substation with equivalent generation and load. The identification of optimal substations is purely based on the connectivity of existing network. And, all the remaining buses with no interfacing transformers will be renamed as substations. The estimation of tap settings is explained in section 5.2.1.1. Now, all these substations will be considered virtually as single buses for the placement of PMUs. The optimal substation locations for different test systems are listed in Table 5.1.

Table 5.1: Optimal substations locations of different test systems

System	optimal substations
IEEE-14	(5, 6), (4, 7, 8, 9).
IEEE-30	(4, 12, 13), (6, 9, 10, 11), (27, 28).
IEEE-57	(10, 51), (15, 45), (14, 46), (13, 49), (7, 29), (20, 21), (24, 46), (39, 57), (40, 56), (32, 34), (4, 18), (9, 55), (11, 41, 43).
IEEE-118	(8, 5), (17, 30), (63, 59), (66, 65), (80, 81), (25, 26), (37, 38), (61, 64), (68, 69).
SRIG-75	(1, 2, 16, 17), (12, 41), (23, 24), (5, 31), (7, 33), (13, 42), (6, 32), (3, 18), (26, 27)

5.2.1.1. Estimation of transformer tap settings

The accuracy of a state estimator lies in the modeling of tap setting which could degrade the estimator performance if it is not modeled properly. Sometimes the tap settings may not be communicated to load dispatch center while taking local preventive or controlling actions. So, it is to be estimated accurately in order to take local protection schemes. If the tap ratios are unknown, it is not possible to calculate the parameters on another end of the transformer using the parameters on one end. So, the transformer branches can be ignored from the point of observability, which may consider the transformer as an open circuit. However, the parameters should not be modelled as an open circuit since this modelling may rule out the chances of estimating the tap ratios. An OPP method was introduced in [104] for observability and estimation of transformer tap settings, but the approach they tried in reducing buses is not desired. So, this chapter proposes a new policy for tap settings estimation. As shown in Fig. 5.2, let us consider v_1, i_1, and v_2, i_2 are the voltages and currents on sending end and receiving ends respectively. The observability will be possible if and only if there exists at most one unknown variable among the variables (v_1, i_1, v_2, and i_2). Let E is the e.m.f induced in the primary coil which can be determined as:

$$E = v_1 - i_1(r_1 + j\,x_1) \tag{5.1}$$

$$= k(v_2 + i_2(r_2 + j\,x_2)) \tag{5.2}$$
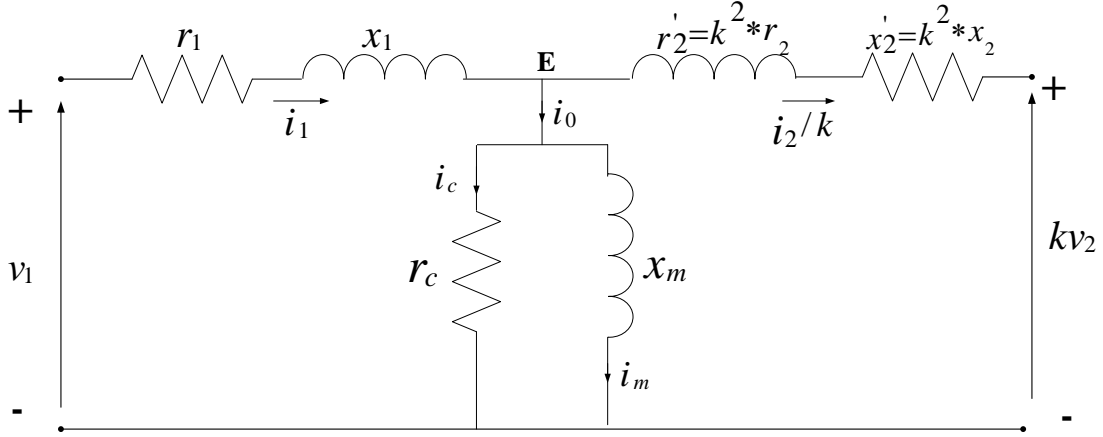
Figure 5.2: Two winding transformer equivalent circuit

Then, the procedure for estimating the unknown variable is given below:

1.   *If i_1 is unknown:* After calculating E from Equation (5.2), it will be used for claculating k from Equation (5.3). After calculating E and k, i_1 can easily be obtained using the equation (5.1).

$$(v_1 - E)/(r_1 + j\,x_1) = (i_2/k) + E \times \left(\frac{1}{r_c} + \frac{1}{jx_m}\right) \tag{5.3}$$

2.   *If v_1 is unknown:* Calculation of E from Equation (5.2) in terms of k and then substituting it in equation (5.4), we can obtain k value as well as v_1 value.

$$i_1 = E \times \left(\frac{1}{r_c} + \frac{1}{jx_m}\right) + (i_2/k) \tag{5.4}$$

3.   *If i_2 is unknown:* From the equations (5.1) and (5.5), the variable k can be obtained. Then, using equation (5.2) and k value obtained, i_2 will be calculated easily.

$$i_1 - E \times \left(\frac{1}{r_c} + \frac{1}{x_m}\right) = (E - kv_2)/(k^2(r_2 + jx_2)) \tag{5.5}$$

4.   *If v_2 is unknown:* On solving equations (5.1) and (5.4), the tap ratio k and unknown v_2 will be known.

5.2.2. Objective function

The PMU installed on one bus observes not only the bus to which it is connected but also the incident buses connected to it. The objective of the proposed OPP problem is to find the least number of PMUs for the complete system observability. The optimization problem is formulated as below.

Minimize,

$$\sum_{q \in N_s} x_q \tag{5.6}$$

Where N_S is the set of substations. The Binary decision variable (x_q) is equal to 0 if q is not a PMU installed substation, and is one otherwise. This objective function will be then subjected to two constraints mentioned below.

5.2.2.1. observability constraint for optimal substation with no critical element

This makes each substation observable by providing atleast one PMU on the same substation or the substations that are being connected to it directly. In this way, it achieves complete observability for the whole network. This constraint can be written as below.

$$s_p(X) \geq 1, \quad \forall p \in N_{snoce} \tag{5..7}$$

Where,

$$s_p = \sum_{q \in N} c_{pq} x_q, \quad \forall p \in N_{snoce} \tag{5.8}$$

From equation (5.8), S_p is the pth substation observability function, and its value should be greater than or equal to 1 for all the substations incident to p^{th} substation to be observable. Here, N_{snoce} represents set of substations with no critical elements, c_{pq} is binary connectivity parameter and is described as,

$$c_{pq} = \begin{cases} 1, \text{if } p = q \\ 1, \text{if substations p, q are connected} \\ 0, \text{otherwise} \end{cases} \tag{5.9}$$

5.2.2.2. Observability of critical elements

In every system, there will be few elements (either buses or lines or maybe both) which are needed to be given high priority. They are most important for the system to be healthy. This may be because of their relevance to the system stability. Let B_i is the critical bus at substation i, and L_{jk} is the critical line connecting j^{th} and k^{th} substations. The critical elements will be made observable directly by using the following constraints.

$$x(j) + x(k) \geq 1, \quad L_{jk} \in critical\,lines \qquad (5.10)$$

$$x(i) = 1, i \in critical\,buses \qquad (5.11)$$

Where, j and k are the sending and receiving end buses of line L. This is because of the fact that for monitoring a line directly, at least one substation on either side of the line must have a PMU. Similarly, the critical bus must have a PMU on it.

5.2.2.3. Identification of critical elements

Till now, the elements with high connectivity or with control devices like FACTS and HVDC links, etc... are said to be critical elements. In this chapter, the concept of Blackout has been introduced to identify the critical elements. So, here, the critical element can be defined as the system element whose outage will drive the complete system into a halted state in terms of power availability. This identification is done using Newton Raphson's method [105]. The workflow for identifying the critical elements is depicted in Fig. 3. The procedure for identification of critical elements is given below.

Step 1: Read the system data.

Step 2: Identify load buses and voltage controlled buses.

Step 3: Calculate ΔP_p^k and ΔQ_p^k using the following equations.

$$\Delta P_p^k = P_p^{actual} - P_p^k \qquad (5.12)$$

$$\Delta Q_p^k = Q_p^{actual} - Q_p^k \qquad (5.13)$$

Step 4: Calculate the elements (J_1, J_2, J_3, J_4) of Jacobian matrix using the following equations:

For J_1,

$$\frac{\partial P_p}{\partial \delta_q} = \sum_{q \neq p} |V_p||V_q||Y_{pq}| \sin(\theta_{pq} - \delta_q + \delta_p), \forall q \neq p \qquad (5.14)$$

$$\frac{\partial P_p}{\partial \delta_p} = -\sum_{\substack{q=1 \\ q \neq p}}^{n} |V_p||V_q||Y_{pq}| \sin(\theta_{pq} - \delta_q + \delta_p) \qquad (5.15)$$

For J_2,

$$\frac{\partial P_p}{\partial |E_q|} = |E_q||Y_{pq}| \cos(\theta_{pq} + \delta_p - \delta_q), \forall q \neq p \qquad (5.16)$$

$$\frac{\partial P_p}{\partial |E_p|} = 2|E_q||Y_{pq}|\cos\theta_{pp} + \sum_{\substack{q=1 \\ q \neq p}}^{n} |E_q||Y_{pq}|\cos(\theta_{pq} + \delta_p - \delta_q) \tag{5.17}$$

For J_3,

$$\frac{\partial Q_p}{\partial \delta_q} = -|E_p||E_q||Y_{pq}|\cos(\theta_{pq} + \delta_p - \delta_q), \forall q \neq p \tag{5..18}$$

$$\frac{\partial Q_p}{\partial \delta_p} = \sum_{\substack{q=1 \\ p \neq q}}^{n} |E_p||E_q||Y_{pq}|\cos(\theta_{pq} + \delta_p - \delta_q) \tag{5.19}$$

For J_4,

$$\frac{\partial Q_p}{\partial |E_q|} = |E_p||Y_{pq}|\sin(\theta_{pq} + \delta_p - \delta_q), \forall q \neq p \tag{5.20}$$

$$\frac{\partial Q_p}{\partial |E_p|} = 2|E_p||Y_{pq}|\sin\theta_{pp} + \sum_{\substack{q=1 \\ q \neq p}}^{n} |E_q||Y_{pq}|\sin(\theta_{pq} + \delta_p - \delta_q) \tag{5.21}$$

With,

$$P_p = \sum_{q=1}^{n} |Y_{pq}||V_q||V_p|\cos(\theta_{pq} - \delta_q + \delta_p) \tag{5.22}$$

$$Q_p = \sum_{q=1}^{n} |Y_{pq}||V_q||V_p|\sin(\theta_{pq} - \delta_q + \delta_p) \tag{5.23}$$

Step 5: Calculate new voltages and phase angles using,

$$\begin{bmatrix} \Delta P \\ \Delta Q \end{bmatrix} = \begin{bmatrix} J_1 & J_2 \\ J_3 & J_4 \end{bmatrix} \begin{bmatrix} \Delta \delta \\ \Delta |V| \end{bmatrix} \tag{5.24}$$

And,

$$\delta_p^{k+1} = \delta_p^k + \Delta \delta_p^k \tag{5.25}$$

$$|V_p^{k+1}| = |V_p^k| + \Delta|V_p^k| \tag{5.26}$$

Step 6: Simulate the contingency

Step 7: Run the load flow i.e. repeat the steps 3 to 5.

Step 8: Identify the number of voltage violations and check whether load flows converge or not.

Step 9: Repeat the steps 6-8 for all the remaining contingencies (i.e. both line and bus contingencies).

Step 10: Define the most critical contingencies which make system blackout as the critical elements.

This identification is carried out exclusively with the help of Power World Simulator 12.0. The details of the critical lines and buses are listed the Table 5.2.
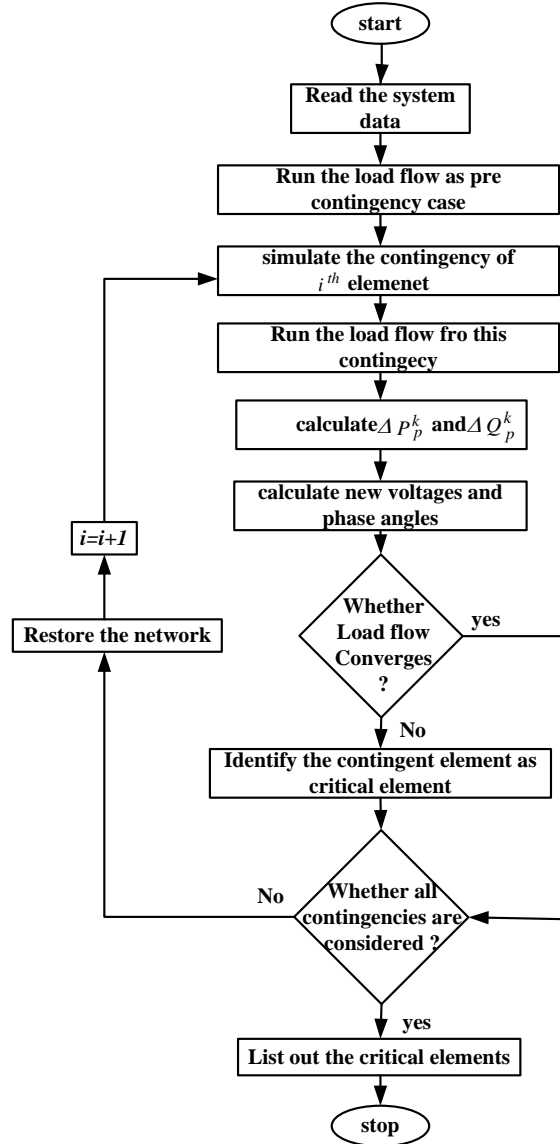
Figure 5.3: Workflow for identifying the critical elements

Table 5.2: Critical elements identified for different test systems

System	Critical lines	Critical buses
IEEE-14	1-2	2
IEEE-30	1-2	2, 6
IEEE-57	1-15, 3-15, 41-43,49-50, 50-51	8, 12
IEEE-118	68-65, 38-65	10, 26, 65, 66
IG-75	41-42, 55-63, 54-63, 74-73	13, 15, 41
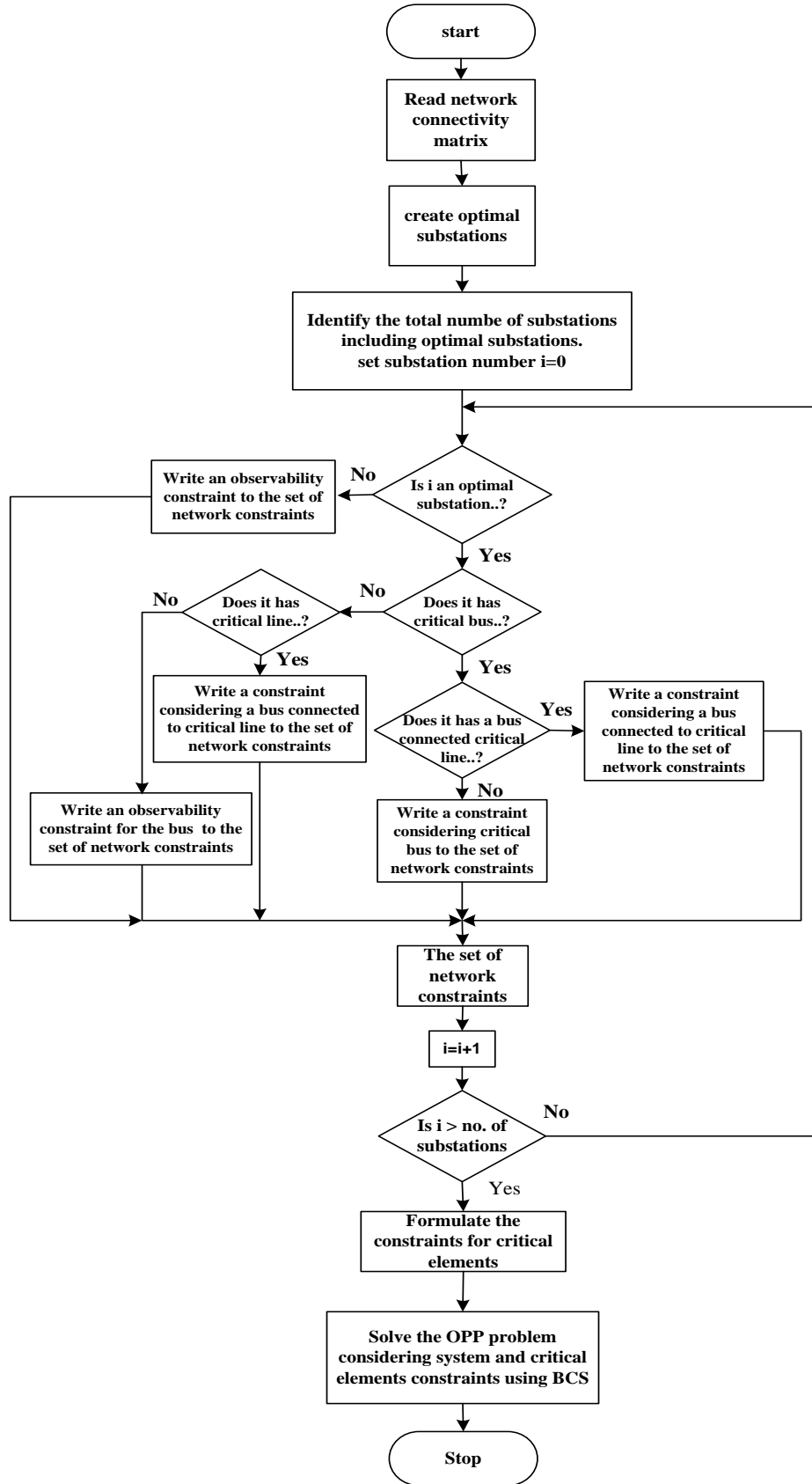
Figure 5.4: The flowchart of the proposed Method

5.3. Results and Discussions

The methodology of the proposed technique can be described using the flowchart given in Fig. 5.4 above. Consider an IEEE-14 bus system with 14 as shown in Fig. 5.5. On applying the network reconsideration, it can be modeled as a 14-bus with two optimal substations and eight substations as shown in Fig. 5.6. Then, the critical elements are found to be L1-2and bus 2, as listed in Table 5.2. Now, on applying the proposed PMU placement algorithm considering all the critical elements, the optimal locations of PMUs are found to be 2, 4 and 5. From Fig. 5.6, it is cleared that the PMUs at substations 4 and 5 not only could observe the system completely but also covers the substations. And, the remaining PMU at substation 2 will observe the line L1-2 and bus 2 directly. Also, the PMU locations considering only substation coverage are given in Table 5.3.
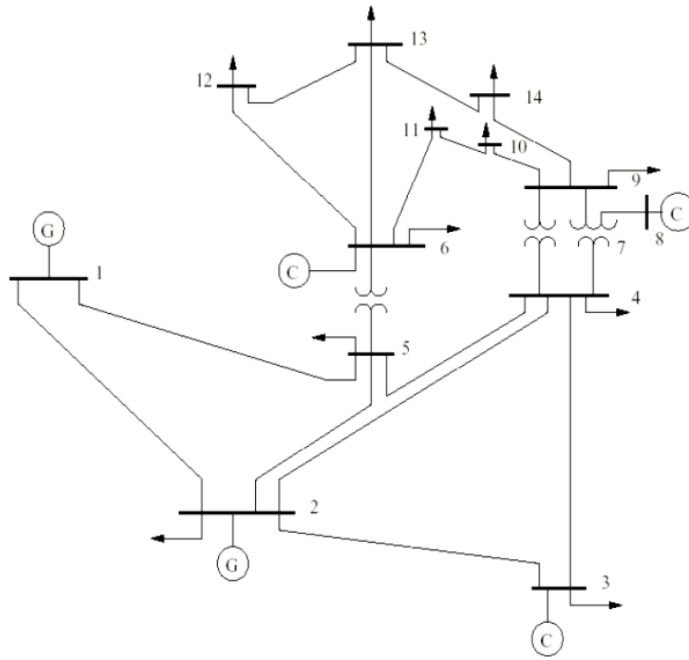
Figure 5.5: The IEEE-14 bus system
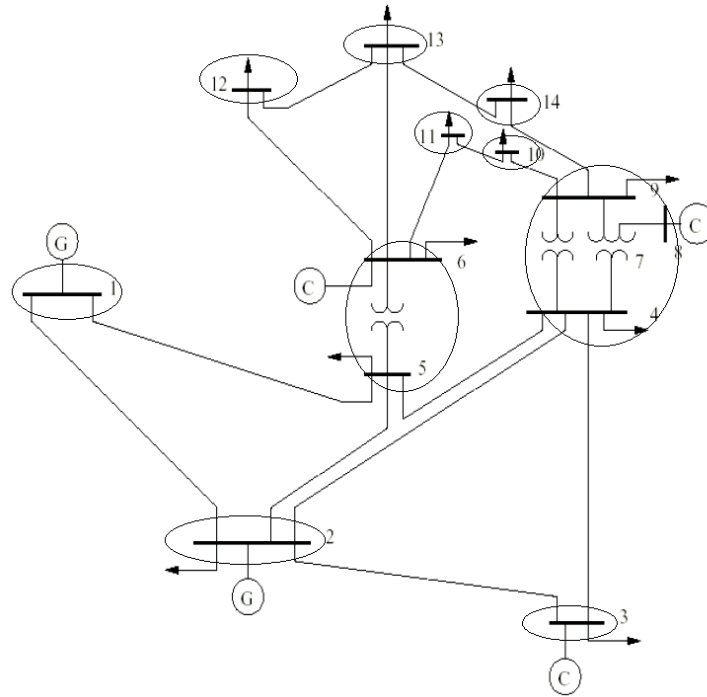
Figure 5.6: Reconsidered IEEE-14 bus system

Table 5.3: PMU locations considering substation coverage

System	No. of substations for PMU placement before network reconsideration	No. of substations for PMU placement after network reconsideration	Buses with PMU locations
IEEE-14	14	10	4,5
IEEE-30	30	24	2,4,6,15,20,25,27
IEEE-57	57	43	1,4,9,10,11,13,14,15,20,24,25,29,32,37,39,53,56
IEEE-118	118	109	2,5,9,12,15,17,21,24,25,29,36,37,40,43,46,50,51,53,59,61,66,69,71,75,77,80,85,87,91,94,101,105,110,114
SRIG-75	75	64	4,8,9,13,15,17,18,20,24,25,27,29,30,31,32,33,37,40,41,43,48,51,63,70,73

Similarly, the optimal locations of PMUs for the different standard test systems with their critical elements are listed in the Table 5.4. In Table 5.5, the resultant PMU number is compared with the PMU number required for only system observability.

Table 5.4: PMU locations for direct measurement of critical elements considering substation coverage

System	PMU locations considering		
	Critical lines	Critical buses	Both
IEEE-14	1,4,5	2,4,5	2,4,5
IEEE-30	2,6,1,2,18,23,25,27	2,6,12,15,19,26,27	2,6,12,15,19,26,27
IEEE-57	1,4,9,10,11,13,14,15,20,24,25,29,32,39,43,50,54,56	3,4,8,9,10,11,12,13,14,15,20,24,25,29,32,39,52,56	3,4,8,9,10,11,12,13,14,15,20,24,29,30,32,39,41,50,54,56
IEEE-118	1,5,10,12,15,17,21,23,25,29,36,37,40,44,46,50,51,53,59,61,6,5,66,69,71,75,77,80,85,87,91,92,96,102,105,110,114	2,5,10,12,13,17,19,22,24,25,26,29,31,36,37,40,43,46,51,52,57,59,61,65,66,69,73,75,77,80,85,86,90,94,102,105,110,115	3,5,10,11,12,17,21,23,23,26,29,34,37,40,45,46,49,53,56,59,61,65,66,69,71,74,78,80,85,86,89,92,96,100,107,108,110,115,118
SRIG-75	4,9,13,17,18,20,24,27,29,30,31,32,33,34,37,40,41,43,44,48,52,60,63,70,74	8,11,13,15,17,18,20,24,27,28,29,30,31,32,33,35,41,43,48,52,55,60,69,70,73	4,13,15,17,18,20,24,27,29,30,31,32,33,34,35,40,41,43,49,52,60,63,69,70,73

Table 5.5: Comparison of the number of PMUs

system	No. of PMUs required for Complete observability	
	Without considering critical elements and substation coverage	Considering critical elements and substation coverage
IEEE-14	4	3
IEEE-30	10	7
IEEE-57	17	20
IEEE-118	32	38
IG-75	25	25

Table 5.6: Comparing the PMU number with literature

system	No. of PMUs required for Complete observability considering			
	Proposed method	high-voltage buses, [65]	High-connectivity buses, [65]	Transient stability of buses, [64]
IEEE-14	3	-	-	-
IEEE-30	7	-	-	-
IEEE-57	20	-	-	20
IEEE-118	38	39	41	37
NRIG-75	25	-	-	-

This shows that, just by installing the additional PMUs worth 15 percent of the total PMU installation cost, one can avoid major power blackouts that incur huge losses which may be many times the total PMU installation cost.

5.5. Summary

As the substation installation costs high, it is required to minimize the number substations than the bus number. So, the traditional PMU placement schemes were failed in reducing the substation installation cost as they aim to reduce only the bus number. However, the proposed method reduces the number of substations and ensures system complete observability. It also provides the direct measurement of critical elements to avoid the most dangerous power interruptions like power system blackouts. Results obtained from the standard test systems witness the effectiveness and economics of the suggested method.

Chapter-6:

SYNCHROPHASOR BASED LINE PROTECTION FOR

SINGLE-PHASE TO GROUND FAULTS

6.1. Introduction

In power systems, single-line-to-ground faults are the most frequent faults. Particularly, if a single line-ground fault occurs with fault resistance, it may mal-operate the relays protecting that particular zone. Sometimes, this causes unnecessary tripping of healthy lines, and it may lead to cascading failure. So, extensive research is required to be done in the area of power system protection. The proposed work aims at identifying the ground faults involving high fault resistance using synchronized voltage phasor data from the relaying point. This scheme calculates the phase difference between relay point voltage and fault point voltage based on the relation between negative sequence of relay point current and fault point current. After, to identify fault existence in the line, the calculated phase difference between relay point voltage and fault point voltage will be compared with the set point voltage phase referred from relay point voltage phase.

6.2. Proposed Phase Comparison Technique

Let us consider the system as shown in Fig. 6.1. E_g is the source voltage estimated by the PMU placed at relay point r. And, z_g is the source impedance, z_{set} is the set-point (or zone) impedance which is for the portion of the line Rs, z_{line} is the total line impedance.
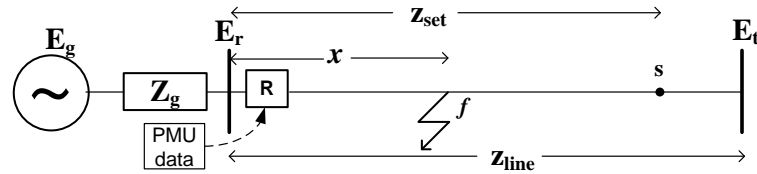
Figure 6.1: Test system.

For a single-phase to ground fault at a point *f,* As shown in Fig. 6.2, the fault sequence currents i_{f1}, i_{f2}, i_{f0} starts flowing through their respective sequence networks with z_{g1}, z_{g2}, z_{g0} as sequence impedances of the source, and z_{line1}, z_{line2}, z_{line0} as sequence impedances of the complete line. Parameter *x* represents the distance to the fault point from the relay end and is expressed as the percentage of the complete line length. Hence, the phase difference (θ_{rf}) between the relay point voltage and fault point voltage can be given as,

$$\theta_{rf} = \arg\left(\frac{\overline{E_r}}{\overline{E_f}}\right) = \arg\left(\frac{\overline{E_r}}{\overline{I_f}}\right) \tag{6.1}$$
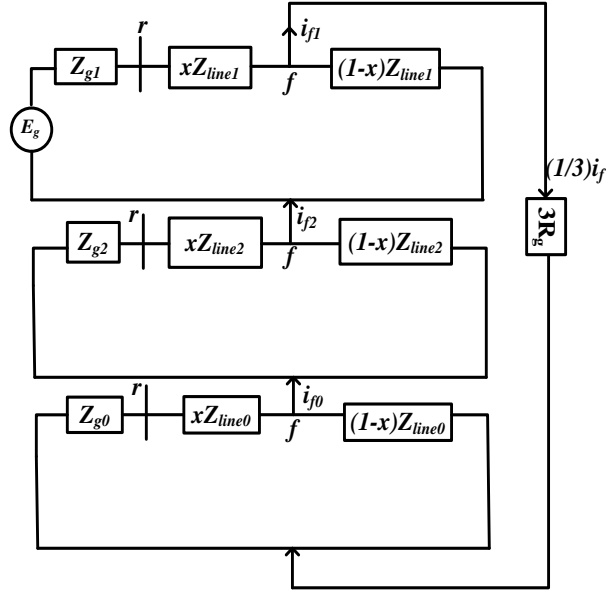
Figure 6.2: Sequence network.

During the fault, the phase of negative sequence current at fault point is same as that of the negative sequence current at relaying point [106]. As the phase of fault current is same as that of fault point sequence current, the phase of fault point current is equivalent to that of sequence current at relaying point. So, the proposed method uses the phase of negative sequence at relaying point instead of the phase of fault point current.

$$= \arg\left(\frac{\overline{E}_r}{\overline{I}_{r2}} \right) \tag{6.2}$$

Here, $\overline{E_r}$ and $\overline{I_r}$ are the synchronized voltage and current phasors measured at relaying point r. Similarly, $\overline{E_f}$ and $\overline{I_f}$ are the fault voltage and fault current at point f. As shown in Fig. 6.3, for different values of R_f at point f, $\overline{E_f}$ moves along the arc. The set-point is the point on line rt which is at 80kms from the point of relay. If $\overline{E_s}$ is the set-point voltage, the phase difference (θ_{rs}) between relay point voltage and set point current can be given as,

$$\theta_{rs} = \arg\left(\frac{\overline{E}_r}{\overline{E}_s} \right) \tag{6.3}$$

Where,
$$\overline{E}_s = \left(\overline{E}_r - \overline{I}_r \cdot z_{set} \right) \tag{6.4}$$

So,
$$\theta_{rs} = \arg\left(\frac{\overline{E}_r}{\left(\overline{E}_r - \overline{I}_r \cdot z_{set}\right)}\right) \tag{6.5}$$
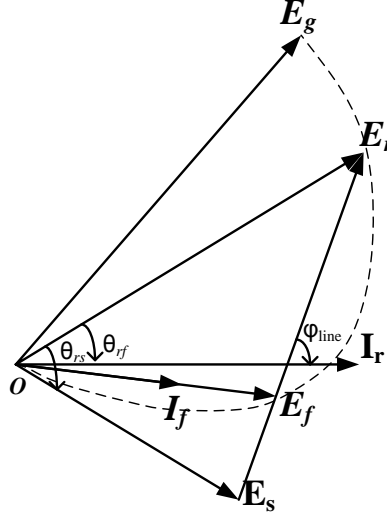
Figure 6.3: Voltage phasor diagram during phase-ground fault.

6.3. The Condition for fault detection

Under the no-load condition, when a single-phase to ground fault occurs in between relay point and set-point, the position of fault current phasor $\overline{I}_f$ will be same as relay point current phasor $\overline{I}_r$. Hence the phasor $\overline{E}_f$ will be in-phase with $\overline{I}_r$. Then the estimated set point voltage $\overline{E}_s$ will lag behind $\overline{I}_r$. But under loaded condition, the phasor $\overline{E}_f$ lags behind $\overline{I}_r$. Whenever a single-phase to ground fault occurs at point f, then the fault voltage lags immediately behind the relay point voltage $\overline{E}_r$. So, the condition for the existence of fault inside set point s is,

$$\theta_{rf} \le \theta_{rs} \tag{6.6}$$

If suppose the fault is beyond the set point then $\overline{E}_f$ lags immediately behind set point voltage $\overline{E}_s$. So the condition becomes,

$$\theta_{rf} > \theta_{rs} \tag{6.7}$$

Finally, the fault protection criterion is as given below:

$\theta_{rf} \le \theta_{rs}$, *if fault is in between relay point and set point*

$\theta_{rf} > \theta_{rs}$, *if the fault is beyond the set point*

```mermaid
flowchart
  Start --> A[Calculate voltage and current phasors at master relaying point using PMU data]
  A --> B[Calculate the change in the current of all three phases]
  B --> C{Check if}
  C -- No --> A
  C -- Yes --> D[Calculate phases of negative-sequence current, relay point voltage, zone-point voltage]
  D --> E[Calculate using equations]
  E --> F{Check the condition}
  F -- No --> G[out-zone fault]
  F -- Yes --> H[In-zone fault]
```

Start

Calculate voltage and current phasors at master relaying point using PMU data

Calculate the change in the current (Δi) of all three phases

Check if $\Delta i \ge 0.1I$ **No**

Yes

Calculate phases of negative-sequence current, relay point voltage, zone-point voltage

Calculate θ_{rf}, θ_{rs} **Using equations (6.2) and (6.3)**

Check the condition (6)   **No** → **out-zone fault**

Yes

In-zone fault

Figure 6.4: Flowchart of the proposed protection scheme

6.4. Results and discussions

The simulation was carried out in EMTDC/PSCAD environment. The proposed scheme, as described in Fig. 6.4, was verified by taking the synchronized phasor data from the relay point at the line end *r*. The fault is simulated at 1sec. The zone is selected as 80kms of the line *rt.*

6.4.1. Under different fault resistances

The increase in fault resistance makes the relay to be under reach. It also affects the directional feature of mho relay. This effect may be less significant if the fault location comes closer to relay point. At a certain value of fault resistance, some of the mho elements become non- directional.

For a single phase-ground fault at different locations in the line *rt*, the simulation results obtained for different fault resistances under different system conditions are presented below. Under no-load, the fault identification results for different fault resistances at different locations considering phase angle variations at end *r* are given in Table 6.1. The simulation results considering RL-load are given in Table 6.2. The correctness of the suggested technique can be seen from Fig. 6.5, Fig. 6.6 and Fig. 6.7.

Table 6.1: Performance of the proposed methodology under no-load conditions

Fault resistance (Ohms)	Fault distance (Kms)	Voltage phase angle (Degrees) (*r*-side)			
		10	15	20	30
50	10	Yes	Yes	Yes	Yes
	30	Yes	Yes	Yes	Yes
	60	Yes	Yes	Yes	Yes
	90	No	No	No	No
100	10	Yes	Yes	Yes	Yes
	30	Yes	Yes	Yes	Yes
	60	Yes	Yes	Yes	Yes
	90	No	No	No	No
200	10	Yes	Yes	Yes	Yes
	30	Yes	Yes	Yes	Yes
	60	Yes	Yes	Yes	Yes
	90	No	No	No	No
500	10	Yes	Yes	Yes	Yes
	30	Yes	Yes	Yes	Yes
	60	Yes	Yes	Yes	Yes
	90	No	No	No	No
1000	10	Yes	Yes	Yes	Yes
	30	Yes	Yes	Yes	Yes
	60	Yes	Yes	Yes	Yes
	90	No	No	No	No

Table 6.2: Performance of the proposed methodology under RL-load conditions

Fault resistance (Ohms)	Fault distance (Kms)	Voltage phase angle (Degrees) (*r*-side)			
		10	15	20	30
50	10	Yes	Yes	Yes	Yes
	30	Yes	Yes	Yes	Yes
	60	Yes	Yes	Yes	Yes
	90	No	No	No	No
100	10	Yes	Yes	Yes	Yes
	30	Yes	Yes	Yes	Yes
	60	Yes	Yes	Yes	Yes
	90	No	No	No	No
200	10	Yes	Yes	Yes	Yes
	30	Yes	Yes	Yes	Yes
	60	Yes	Yes	Yes	Yes
	90	No	No	No	No
500	10	Yes	Yes	Yes	Yes
	30	Yes	Yes	Yes	Yes
	60	Yes	Yes	Yes	Yes
	90	No	No	No	No
1000	10	Yes	Yes	Yes	Yes
	30	Yes	Yes	Yes	Yes
	60	Yes	Yes	Yes	Yes
	90	No	No	No	No

(a)

Figure 6.5: Results for No-load and 100Ω fault resistance at (a) 10kms, (b) 30kms, (c) 60kms, (d) 90kms
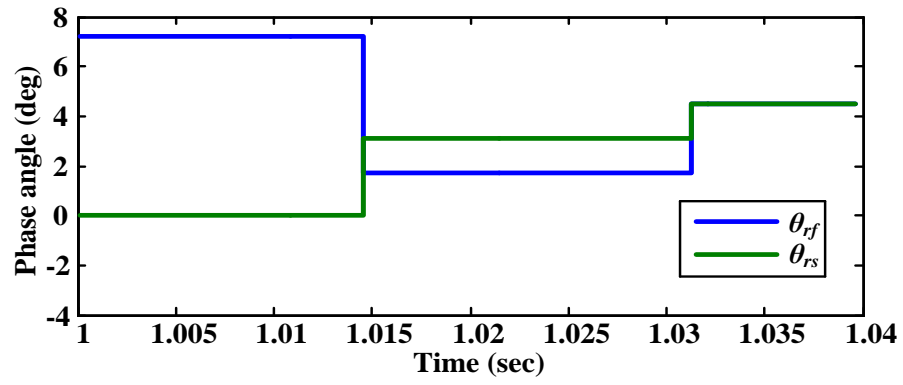
(a)
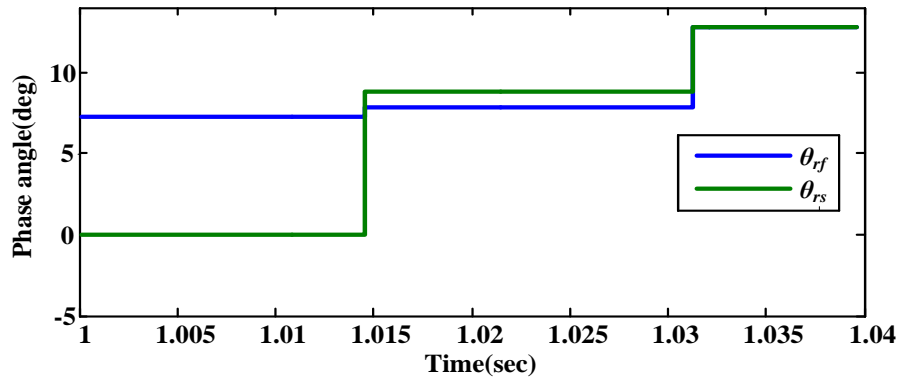
(b)
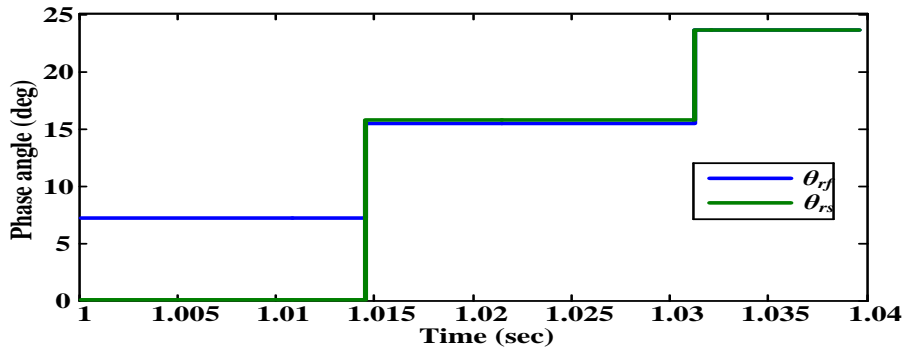
(c)
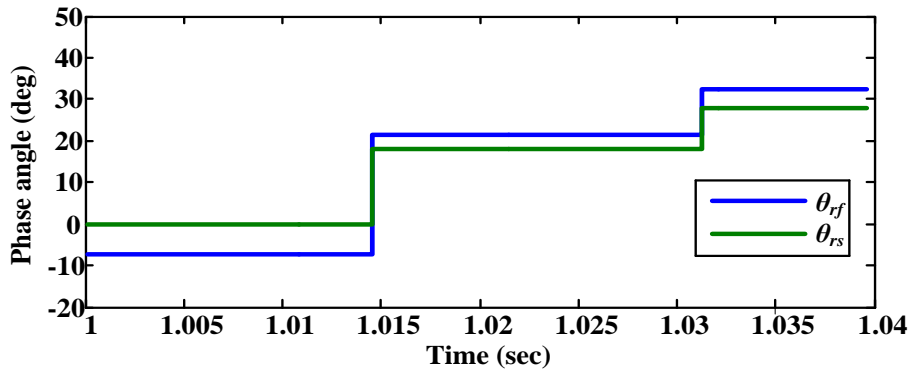
(d)

Figure 6.6 Results for No-load and 1000Ω fault resistance at (a) 10kms, (b) 30kms, (c) 60kms, (d) 90kms
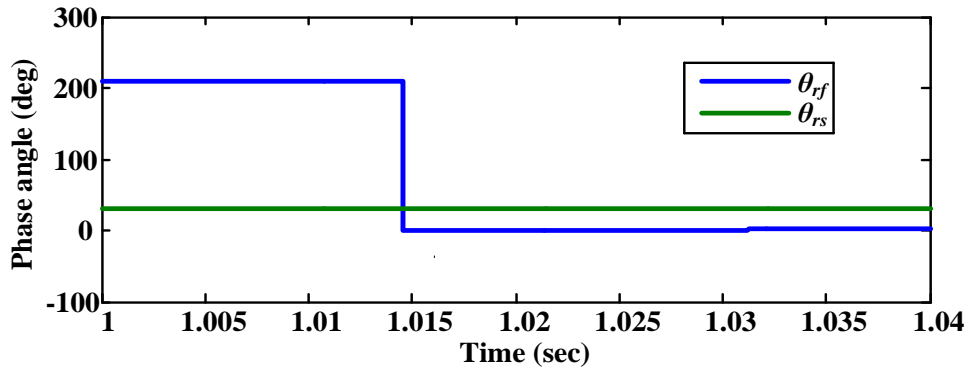
(a)
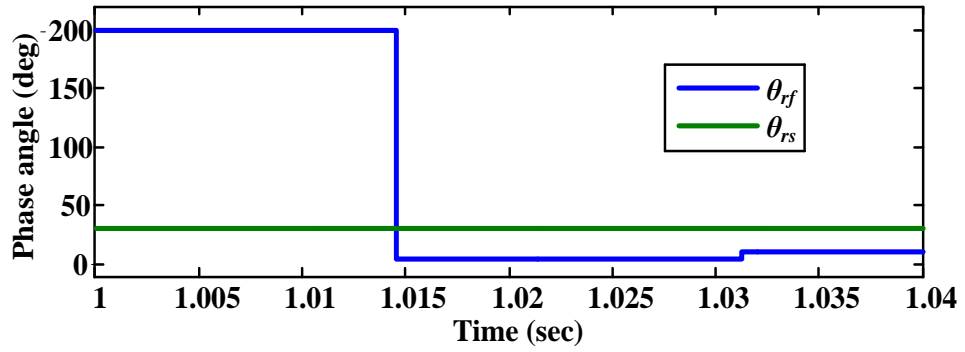
(b)
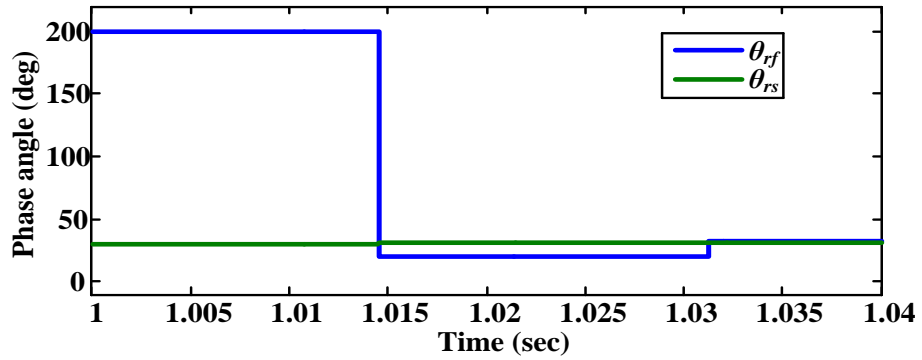
(c)
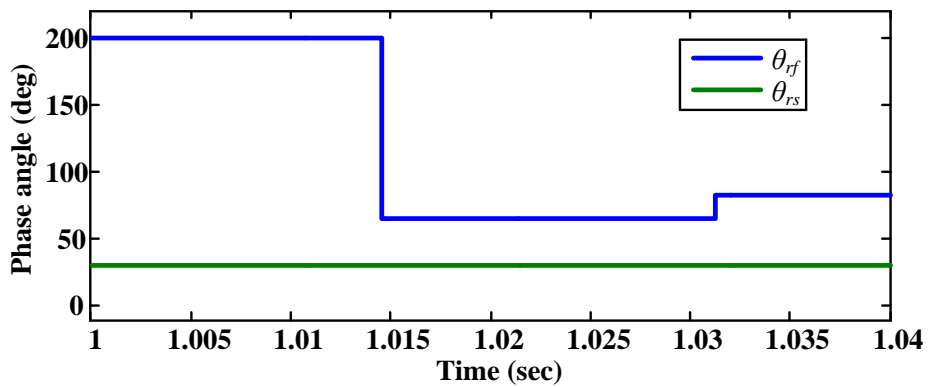
(d)

Figure 6.7 Results for RL-load and 1000Ω fault resistance at (a) 10kms, (b) 30kms, (c) 60kms, (d) 90kms

6.4.2. Under different fault resistances considering a double-sourced system

If the angle $\delta=+10^0$, the line end *r* becomes sending end, and for $\delta=-10^0$ the same end becomes receiving end. Line loading depends on the phasor difference between the two line ends. More is the phasor difference heavily loaded the line is. The performance of proposed methodology for double-sourced system is presented in Fig. 6.8, Fig. 6.9 and Table 6.3.

Table 6.3: Performance of proposed methodology for double-sourced system

Fault resistance (Ohms)	Fault distance (Kms)	Voltage phase angle (Degrees) (*r*-side)					
		10	-10	20	-20	30	-30
50	10	Yes	Yes	Yes	Yes	Yes	Yes
	30	Yes	Yes	Yes	Yes	Yes	Yes
	60	Yes	Yes	Yes	Yes	Yes	Yes
	90	No	No	No	No	No	No
100	10	Yes	Yes	Yes	Yes	Yes	Yes
	30	Yes	Yes	Yes	Yes	Yes	Yes
	60	Yes	Yes	Yes	Yes	Yes	Yes
	90	No	No	No	No	No	No
200	10	Yes	Yes	Yes	Yes	Yes	Yes
	30	Yes	Yes	Yes	Yes	Yes	Yes
	60	Yes	Yes	Yes	Yes	Yes	Yes
	90	No	No	No	No	No	No
500	10	Yes	Yes	Yes	Yes	Yes	Yes
	30	Yes	Yes	Yes	Yes	Yes	Yes
	60	Yes	Yes	Yes	Yes	Yes	Yes
	90	No	No	No	No	No	No
1000	10	Yes	Yes	Yes	Yes	Yes	Yes
	30	Yes	Yes	Yes	Yes	Yes	Yes
	60	Yes	Yes	Yes	Yes	Yes	Yes
	90	No	No	No	No	No	No

(a)

(b)
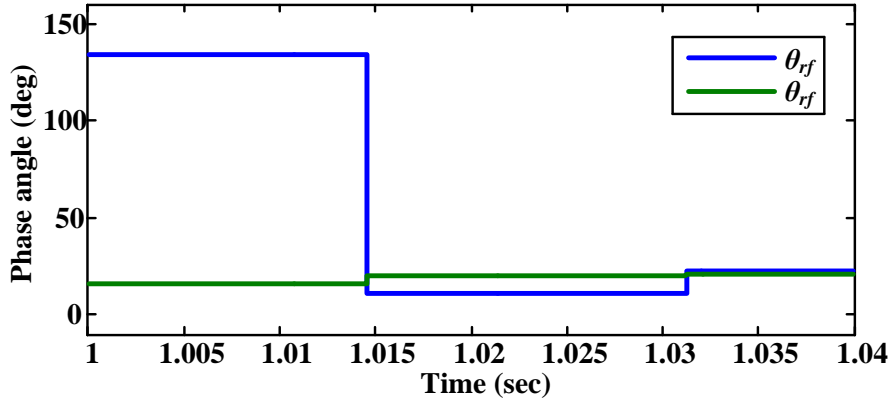
(c)
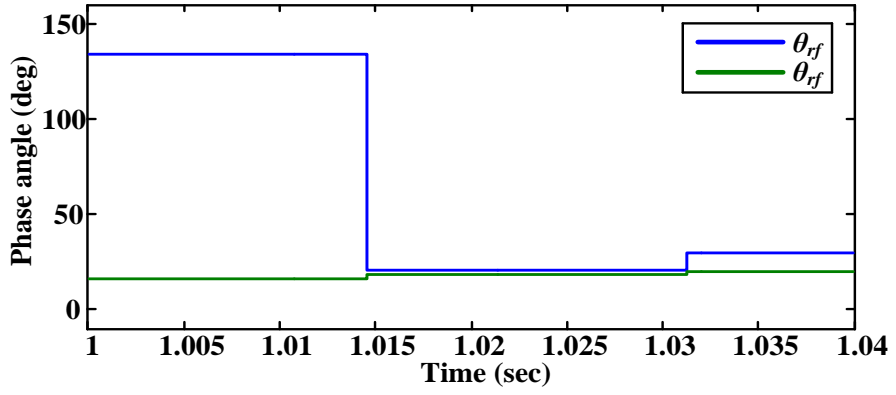
(d)

Figure 6.8: Results for Double-sourced, 100Ω fault resistance and $\delta_1 = 20^0$, $\delta_2 = 0^0$ at (a) 10kms, (b) 30kms, (c) 60kms, (d) 90kms

(a)

(b)

(c)

(d)
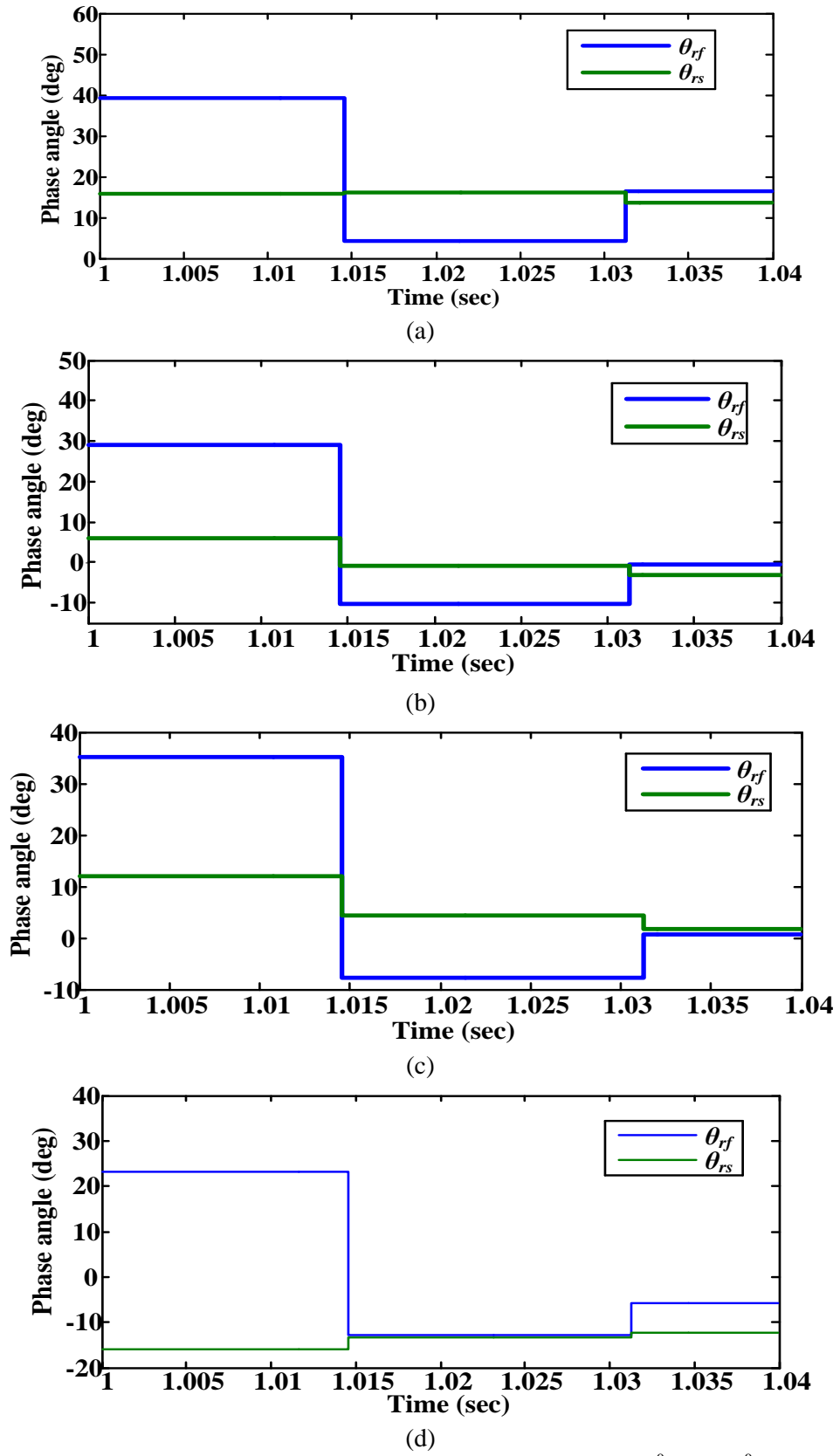
Figure 6.9: Results for Double-sourced, 100Ω fault resistance and $\delta_1 = 0^0$, $\delta_2 = 20^0$ at (a) 10kms, (b) 30kms, (c) 60kms, (d) 90kms

These results show that the algorithm identifies the fault within 14.6ms irrespective of the fault resistance. This means that the proposed scheme has following advantages:

- It is highly immune to fault resistance. It differentiates the in-zone fault from out-zone faults irrespective of fault resistance. So, the problem of relay mal-operation caused by fault resistance is answered.

- The fault identification is unaffected by the system operation and load conditions. It means the algorithm works satisfactorily under any load and/or power flow direction.

- Highly significant in power system protection practices. Finally, the reduction in the time of fault identification significantly improves the transient stability of the system.

6.5. Summary

In this work, a novel scheme of voltage phase comparison based single line-ground fault detection is proposed based on synchronized phasor data. This scheme, after calculating the relation between negative sequence of relay point current and fault point current, it identifies the existence of fault in a line on comparing the calculated phase difference between relay point voltage and fault point voltage with the set point voltage phase referred from relay point voltage phase.

Chapter 7: Conclusions and Scope for Future work

The power system is highly prone to faults which may cause line outages or measurement system failures which will make measurement system unreliable in achieving complete system observability. The thesis work is summarized in section 7.1 as follows.

7.1. Conclusions

Thesis introductory part of the importance Phasor Measurement Units and its applications for power systems protection is discussed in Chapter-1. It also introduces optimal PMU placement. And, from the literature, it presents various strategies applied for optimal PMU placement.

The research work has started with solving the OPP problem using the proposed BCS technique for system complete observability under both normal and abnormal conditions in power system accurately. The proposed method has been tested on few IEEE standard test systems and then applied for four the state level regional grids (SLRG) of Southern Region of Indian power Grid (SRIG) and five Regional Indian power Grids of United Indian power Grid (UIG). From the results and discussions, it is verified that the proposed method has successfully optimized the OPP problem and, also has benefited economically.

The work has been extended for solving the OPP problem for maximizing the observability. It uses Binary Bat Algorithm for solving the optimization problem. It considers both normal and abnormal conditions in power system. The proposed method has been tested on few IEEE standard test systems, and then applied for Southern Region of Indian power Grid (SRIG). From the results and discussions, it is verified that the proposed method has successfully found the optimum solution with maximum observability.

Further, it has considered a faster restoration process by partitioning the network into many regions which are easier to be restored during a build-up strategy. Initially, this partition starts with sectionalizing the network subjecting to the generation-load balance constraint, and next to these sections are reorganized to ensure the remaining two restoration constraints. This approach provides synchronized phase angle data between any two adjacent islands thus ensuring the complete observability of all regions. This partition algorithm was applied to three different systems and sectionalized the IEEE-39 system into four regions, the IEEE-118

system into 12 islands and a Northern Region of the Indian Power Grid into four stable islands.

Later, it suggests a method to reduce the number of substations and ensures system complete observability. It also provides the direct measurement of critical elements to avoid the most dangerous power interruptions like power system blackouts. Results obtained from the standard test systems witness the effectiveness and economics of the suggested method.

Finally, a novel scheme of voltage phase comparison based single line-ground fault detection is proposed based on synchronized phasor data. The proposed scheme is highly immune to fault resistance. It differentiates the in-zone fault from out-zone faults irrespective of fault resistance. This fault identification technique is unaffected by the system operation and load conditions. Finally, the reduction in the time of fault identification significantly improves the transient stability of the system.

7.2. Scope for Future Work

Any research never ends without leaving an open window for further research. Hence the thesis work is inciting with the scope for further research on following issues:

- PMU placement based on the sequences of element outages that could lead the system to blackout.

- Restoration based reliable WAMS partition of the power system.

- Optimal placement of PMUs based on the Real-Time calculation of the criticality of the system elements.

- Zone-3 blocking of distance relays against Load Encroachment using the voltage-phase comparison based technique.

Investigation and identification of vulnerability regions of distance relays, and adopting them by differentiating the fault from vulnerability using phase information of voltages and currents would be an interesting topic of research.

References

[1] Rakesh B. Bobba, Je_ Dagle, Erich Heine, Himanshu Khurana, William H. Sanders, Peter Sauer, and Tim Yardley. "Enhancing Grid Measurements-Wide Area measurement Systems", NASPInet, and Security. IEEE   power & energy magazine, December 2011.

[2] Interim Report of the WECC Disturbance Monitoring Work Group. Technical report, December 2005.

[3] A. G. Phadke, J. S. Thorp, "History And Applications of Phasor Measurements", IEEE Conference, 2006.

[4] Working Group H-7 of the Relaying channels," Synchronized sampling and phasor measurements for relaying and control," IEEE Trans. Power Del., vol.9, no.1, pp 442-452, January 1994.

[5] shiroie,M. ; Daniar,S. ;Akhbari,M. "A New algorithm for fault location on transmission lines ",IEEE power&energy society general meeting, 2009.

[6] J.-A. Jiang, J.-Z. Yang, Y.-H. Lin, C.-W. Liu, and J.-C. Ma, "An adaptive PMU based fault detection/location technique for transmission lines, Part I: Theory and algorithms", IEEE Trans. Power Delivery, vol. 15, pp. 486–493, Apr. 2000.

[7] Seethalekshmi, K. ; singh, S N. ; srivasthav S.C.   "Synchronous Phasor Assisted Adaptive Reach Setting of Distance Relay in Presence of UPFC", IEEE journal & magazines., vol.5, no.3, pp 396-405,January 2011.

[8] M. Khederzadeh and T. S. Sidhu, "Impact of TCSC on the protection of transmission lines," IEEE Trans. Power Del., vol.21, no.1, pp 80-87, January 2006.

[9] Newman,P., Subramanian, S., Wright,J., Mctaggart, C., Taylor,A., "series compensation system modeling, protection challenges and recommendations for the anglo-scottish interconnection", IET international conference , 2014

[10] C.-S.Yu, C.-W.Liu, S.-L.Yu and J.-A.Jiang, "A new PMU based fault algorithm for series compensated lines," IEEE Trans. On Power Del., vol.17, no.1, pp 33 − 46,January 2002.

[11] M.M.Eissa, M.Elshahat Masoud, M.Magdy, "A Novel back up wide area protection technique for power transmission grids using phasor measurement unit", IEEE Transactions on power delivery, vol. 25, no. 1, pp 270-278, 2010.

[12] A. M. Kulkarni, S. A. Soman, Yogesh Bijpuria, and Prashant Navalkar. On Grid Disturbances in India (30/July/2012 and 31/July/2012). Invited lecture at Virginia Tech, October 19, October 2012.

[13] A. G. Phadke, D. Novosel, and S.H. Horowitz. Wide Area Measurement Applications in Functionally Integrated Power Systems. CIGRE B-5 Colloquium, Madrid, Spain, September 2012.

[14] A. N. Sarwade, P.K. Katti, and J.G. Ghodekar. "Adaptive Solutions for Distance Relay Settings", IEEE 9th International Power and Energy Conference, Suntec, pages 493-498,October 2010.

[15] v.centeno, A.G.Phadke, A.E dris, J.Benton, M.Gaudi, G.Michel, "an adaptive out-of-step relay", IEEE transaction on power delivery, Vol. 12, No. 1, January 1997.

[16] Rahman Sk. Rashedur, Hussain Md. Yeakub and Ali Md. SekendarA "New Approach to Coherency Identification in Large Multi-Machine Power System", 2012, 7th International Conference on Electrical and Computer Engineering.

[17] H. B. You, V. Vittal, Z. Yang, "self-healing in power systems: an approach using islanding and rate of change of frequency de-line based load shedding", IEEE transaction on power system, vol. 18, no.1, pp174-181, 2003.

[18] Khalil El-Arroudi, Géza Joós, Kamwa, andDonald T. cGillis "Intelligent-Based Approach to Islanding Detection in Distributed Generation", IEEE transactions on power delivery, vol. 22, no. 2, april 2007.

[19] Tianshu Bi, Jiayin Sui, Hao Yu, Qixun Yang, "Adaptive loss of field protection based on phasor measurements", Power and Energy Society General Meeting, 2011 IEEE.

[20] J. S. Thorp A. G. Phadke S. H. Horowitz, "Some Applications of Phasor Measurements To Adaptive Protection", IEEE Transactions on Power Systems, Vol. 3, No. 2, May 1988.

[21] A. G. Phadke and J. S. Thorp, "synchronized Phasor Measurements and Their Applications", New York: Springer, 2008.

[22] Bretas, A.S. and Phadke, A.G., "Artificial neural networks in power system restoration", IEEE Trans. On Power Delivery, Vol. 18, No. 4, October 2003, pp 1181–1186.

[23] System Disturbance on November 4, 2006, UCTE, February 2007, available at www.ucte.com.

[24] Developments in UCTE and Switzerland, W. Sattinger, WAMC course at ETH Zürich, 30 August–1 September 2005.

[25] Horowitz, S. H. and Phadke, A. G. (2008) Power System Relaying, Third Edition, John Wiley and Sons, Ltd.

[26] Xu, B., Abur, A.: 'Observability analysis and measurement placement for system with PMUs', IEEE Power Systems Conf. Exposition, October 2004, Vol. 2, pp. 943–946.

[27] Gou, B.: 'Optimal placement of PMUs by integer linear programming', IEEE Trans. Power Syst., 2008, 23, (3), pp. 1525–1526.

[28] Gou, B.: 'Generalized integer linear programming formulation for optimal PMU placement', IEEE Trans. Power Syst., 2008, 23, (3), pp. 1099–1104.

[29] J. Chen, A. Abur, "Placement of PMUs to enable bad data detection in state estimation" ,IEEE Trans. Power Systems, vol. 21, no. 4, pp. 1608-1615, Nov. 2006.

[30] D. Dua, S. Dambhare, R. K. Gajbhiye, S. A. Soman, "Optimal multistage scheduling of PMU placement: An ILP approach," IEEE Trans. Power Delivery, vol. 23, no. 4, pp. 1812-1820, Oct. 2008.

[31] Rajesh Kavasseri, Sudarshan K. Srinivasan, "Joint Placement of Phasor and Power Flow Measurements for Observability of Power Systems", IEEE Trans. Power Systems, Vol. 26, No. 4, Nov 2011.

[32]   S. Chakrabarti, E. Kyriakides, M. Albu, "Uncertainty in powersystem state variables obtained through synchronized measurements", *IEEE Trans. Instrumentation and Measurement*, vol. 58, no. 8, pp. 2452-2458, Jan. 2009.

[33]   M. Farsadi, H. Golahmadi, H. Shojaei, "Phasor measurement unit (PMU) allocation in power system with different algorithms", in *2009 Int. Conf. on Electrical and Electronics Engineering*, pp. 396-400.

[34]   G. Venugopal, R. Veilumuthu, P. Avila Theresa, "Optimal PMUplacement and observability of power system using PSAT," in *2010 Int.Joint Journal Conf. on Engineering and Technology*, pp.67-71.

[35]   T.T. Cai, Q. Ai, "Research of PMU optimal placement in power systems," in *2005 World Scientific and Engineering Academy and Society Int. Conf.*, pp. 38-43.

[36]   Y. Yang, H. Shu, L. Yue, "Engineering practical method for PMU placement of 2010 Yunnan power grid in China," in *2009 Int. Conf. on Sustainable Power Generation and Supply*, pp. 1-6.

[37]   T. L. Baldwin, L. Mili, M. B. Boisen, Jr., and R. Adapa, "Power system observability with minimal phasor measurement placement", *IEEE Trans. Power Syst.*, vol. 8, no. 2, pp. 707–715, May 1993.

[38]   K.-S. Cho, J.-R. Shin, S. H. Hyun,"Optimal placement of phasor measurement units with GPS receiver", *Proc. IEEE Power Eng. Soc.Winter Meeting*, pp. 258–262, 2001.

[39]   R. F. Nuqui, A. G. Phadke, "Phasor measurement unit placement techniques for complete and incomplete observability," *IEEE Trans.Power Del.*, vol. 20, no. 4, pp. 2381–2388, Oct. 2005.

[40]   H.-S. Zhao, Y. Li, Z.-Q. Mi, L. Yu, "Sensitivity constrained PMU placement for complete observability of power systems", in *Proc. IEEEPower Eng. Soc. Transm. Distrib. Conf. Exhib.*, 2005.

[41]   Haupt R.L., Haupt S.E. *Practical Genetic Algorithms* (2ed., Wiley, 2004).

[42]   F. Aminifar, C. Lucas, A. Khodaei, M. Fotuhi-Firuzabad, "Optimal placement of phasor measurement units using immunity genetic algorithm," *IEEE Trans. Power Del.*, vol. 24, no. 3, pp. 1014–1020, July 2009.

[43]   Xin-SheYang, Nature-Inspired Optimization Algorithms.

[44]   M. Hajian, A. M. Ranjbar, T. Amraee, B. Mozafari, "Optimal placement of PMUs to maintain network observability using a modified BPSO algorithm," *Int. J. Elect. Power Energy Syst.*, vol. 33, no. 1, pp. 28–34, Jan. 2011.

[45]   A. Ahmadi, Y. Alinejad-Beromi, M. Moradi, "Optimal PMU placement for power system observability using binary particle swarm optimization and considering measurement redundancy," *Expert Syst. Appl.*, vol. 38, pp. 7263–7269, 2011.

[46]   J. Peng, Y. Sun, H. F.Wang, "Optimal PMU placement for full network observability using Tabu search algorithm", *International Journal of Electrical Power Energy Systems*, vol. 28, no. 4, pp. 223–231, May 2006.

[47]   C. Peng, H. Sun, J. Guoa, "Multi-objective optimal PMU placement using a non-dominated sorting differential evolution algorithm", *International Journal of Electrical Power Energy Systems*, vol. 32, no. 8, pp. 886–892, Oct. 2010.

[48]   M. Hurtgen, J.-C. Maun, "Optimal PMU placement using iterated local search", *International Journal of Electrical Power Energy Systems*, vol. 32, no. 8, pp. 857–860, Oct. 2010.

[49]   T. T. Kim, H. V. Poor, "Strategic protection against data injection attacks on power grids," *IEEE Trans. Smart Grid*, vol. 2, no. 2, pp. 326–333, Jun. 2011.

[50]   Aruljeyaraj, Rajasekaran, Nandha Kumar, Chandrasekaran, "A Multi-objective PMU Placement Method Considering Observability and Measurement Redundancy using ABC Algorithm", *Advances in Electrical and Computer Engineering,* Vol. 14, No. 2, 2014.

[51]   Sodhi, R., Srivastava, S.C., Singh, S.N.: 'Optimal PMU placement to ensure system observability under contingencies', Proc. Power and Energy Society General Meeting, July 2009, pp. 1–6.

[52]   B.K. Saha Roy, A.K. Sinha, A.K. Pradhan, "An optimal PMU placement technique for power system observability", *Electrical Power and Energy Systems*, Vol. 42 (2012) 71–77.

[53]   S. Chakrabarti, E. Kyriakides, D. G. Eliades, "Placement of synchronized measurements for power system observability," IEEE Trans. Power Del., vol. 24, no. 1, pp. 12–19, Jan. 2009.

[54]   A. Abur, F. H. Magnago, "Optimal meter placement for maintaining observability during single branch outage," IEEE Trans. Power Syst., vol. 14, no. 4, pp. 1273–1278, Nov. 1999.

[55]   F. H. Magnago, A. Abur, "A unified approach to robust meter placement against loss of measurements and branch outages," IEEE Trans. Power Syst., vol. 15, no. 3, pp. 945–949, Aug. 2000.

[56]   C. Rakpenthai, S. Premrudeepreechacharn, S. Uatrongjit, N. R. Watson, "An optimal PMU placement method against measurement loss and branch outage," IEEE Trans. Power Del., vol. 22, no.1, pp.101–107, Jan. 2007.

[57]   Gopakumar P, Chandra G S, Reddy M J B, Mohanta D K, "Optimal placement of PMUs for the smart grid implementation in Indian power grid — A case study", Frontiers in Energy, 2013, 7(3): 358–372.

[58]   pathirikkat gopakumar, g. surya chandra, m. jaya bharata reddy, dusmata kumar mohanta,"Optimal redundant placement of PMUs in Indian power grid— northern, eastern and north-eastern regions". Frontiers in Energy 2013, 7(4): 413–428.

[59]   M. Adibi, L. H. Fink, "Power system restoration planning," *IEEE Trans. Power Syst.*, vol. 9, no. 1, pp. 22–28, Feb. 1994.

[60]   F. Wu and A. Monticelli, "Analytical tools for power system restoration—Conceptual design," *IEEE Trans. Power Syst.*, vol. 3, no. 1, pp.10–16, Feb. 1988.

[61]   R. J. Kafka, D. R. Penders, S. H. Bouchey, M. M. Adibi, "System restoration plan development for a metropolitan electric system," *IEEE Trans. Power App. Syst.*, vol. PAS-100, pp. 3703–3713, 1981.

[62]   J. A. Huang, F. D. Galiana, G. T.Vuong, "Power system restoration incorporating interactive graphics and optimization," in *Proc. 14th Int. Conf. Power Ind. Appl.*,

Baltimore, 1991, pp. 216.

[63] S. Arash Nezam Sarmadi, Ahmad Salehi Dobakhshari, Sadegh Azizi, Ali Mohammad Ranjbar, "A Sectionalizing Method in Power System Restoration Based on WAMS", IEEE transactions on smart grid, Vol. 2, No. 1, March 2011.

[64] Rokkam, V., & Bhimasingu, R.., An approach for optimal placement of Phasor Measurement Units considering fuzzy logic based critical buses. In *Smart Energy Grid Engineering (SEGE), 2013 IEEE International Conference on* (pp. 1-6)., 2013.

[65] Pal, A., Sanchez-Ayala, G. A., Centeno, V. A., & Thorp, J. S., A PMU placement scheme ensuring real-time monitoring of critical buses of the network. *IEEE Transactions on Power Delivery*, 29(2), pp:510-517, 2014.

[66] Chetan Mishra, Kevin D. Jones, Anamitra Pal, Virgilio A. Centeno**.:** *Binary particle swarm optimization-based optimal substation overage algorithm for phasor measurement unit installations in practical systems*, IET Generation, Transmission & Distribution, doi: 10.1049/iet-gtd.2015.1077.

[67] Working Group H-7 of the Relaying channels," Synchronized sampling and phasor measurements for relaying and control," *IEEE Trans. Power Del.*, vol.9, no.1, pp 442-452, January 1994.

[68] J.-A. Jiang, J.-Z. Yang, Y.-H. Lin, C.-W. Liu, and J.-C. Ma, "An adaptive PMU based fault detection/location technique for transmission lines, Part I: Theory and algorithms," *IEEE Trans. Power Del.*, vol. 15, pp. 486–493, Apr. 2000.

[69] J.-A. Jiang, Y.-H. Lin, J.-Z. Yang, T.-M. Too, and C.-W. Liu, "An adaptive PMU based fault detection/location technique for transmission lines, Part II: PMU implementation and performance evaluation," *IEEE Trans. Power Del.*, vol. 15, pp. 1136–1146, Oct. 2000.

[70] J. A. Jiang, C.-S. Chen, C. –W. Liu," A new protection scheme for fault detection, direction discrimination, classification and location in transmission lines," *IEEE Trans. Power Del.*, vol.18, no.1, pp 34-42, 2003.

[71] W. Bo, Q. Jiang, Y. Cao., "Transmission network fault location using sparse PMU measurements", International Conference on Sustainable Power Generation and Supply (2009), pp. 1–6.

[72] K. Lien, C. Liu, C. Yu, J. Jiang, "Transmission network fault location observability with minimal PMU placement", *IEEE Transactions on Power Delivery*, 21 (3) (2006), pp. 1128–1136.

[73] M. Shiroei, S. Daniar, M. Akhbari, "A new algorithm for fault location on transmission lines", IEEE Power & Energy Society General Meeting (2009), pp. 1–5.

[74] S. Geramian, H. Abyane, K. Mazlumi, Determination of optimal PMU placement for fault location using genetic algorithm, 13th International Conference on Harmonics and Quality of Power (2008), pp. 1–5.

[75] K. Mazlumi, H. Abyane, S. Sadeghi, S. Geramian, Determination of optimal PMU placement for fault-location observability, Third International Conference on Electric Utility Deregulation and Restructuring and Power Technologies (2008), pp. 1938–1942.

[76] C. Chuang, J. Jiang, Y. Wang, C. Chen, Y. Hsiao, An adaptive PMU-based fault location estimation system with a fault-tolerance and load-balancing communication network, IEEE Lausanne PowerTech (2007), pp. 1197–1202.

[77] Y. Lin, C. Liu, C. Chen, A new PMU-based fault detection/location technique for transmission lines with consideration of arcing fault discrimination-Part I: theory and algorithms, IEEE Transactions on Power Delivery, 19 (4) (2004), pp. 1587–1593.

[78] Y. Lin, C. Liu, C. Chen, A new PMU-based fault detection/location technique for transmission lines with consideration of arcing fault discrimination—Part II: performance evaluation, IEEE Transactions on Power Delivery, 19 (4) (2004), pp. 1594–1601.

[79] J.-C. Gu, S.-L. Yu, "Removal of DC offset in current and voltage signals using a novel Fourier filter algorithm", *IEEE Trans. Power Del.*, vol. 15, no. 1, pp. 73-79, Jan. 2000.

[80] Y. Guo, M. Kezunovic, D. Chen, "Simplified algorithms for removal of the effect of exponentially decaying DC-offset on the Fourier algorithm", *IEEE Trans. Power Del.*, vol. 18, no. 3, pp. 711-717, Jul. 2003.

[81] S.-R. Nam, J.-Y. Park, S.-H. Kang, M. Kezunovic, "Phasor estimation in the presence of DC offset and CT saturation", *IEEE Trans. Power Del.*, vol. 24, no. 4, pp. 1842-1849, Oct. 2009.

[82] G. Benmouyal, "Removal of DC-offset in current waveforms using digital mimic filtering", *IEEE Trans. Power Del.*, vol. 10, no. 2, pp. 621-630, Apr. 1995.

[83] S.-H. Kang, D.-G. Lee, S.-R. Nam, P. A. Crossley, Y.-C. Kang, "Fourier transform-based modified phasor estimation method immune to the effect of the DC offsets", *IEEE Trans. Power Del.*, vol. 24, no. 3, pp. 1104-1111, Jul. 2009.

[84] R. K. Mai, L. Fu, Z. Y. Dong, B. Kirby, Z. Q. Bo, "An adaptive dynamic phasor estimator considering DC offset for PMU applications", *IEEE Trans. Power Del.*, vol. 26, no. 3, pp. 1744-1754, Jul. 2011.

[85] M. M. Eissa, "Ground distance relay compensation based on fault resistance calculation," *IEEE Trans. Power Del.*, vol. 21, no. 4, pp. 1830–1835, Oct. 2006.

[86] A. D. Filomena, R. H. Salim, M. Resener, and A. S. Bretas, "Ground distance relaying with fault-resistance compensation for unbalanced systems," *IEEE Trans. Power Del.*, vol. 23, no. 3, pp. 1319–1326, Jul.2008

[87] S. Miao, P. Liu, and X. Lin, "An adaptive operating characteristic toimprove the operation stability of percentage differential protection," *IEEE Trans. Power Del.*, vol. 25, no. 3, pp. 1410–1417, Jul. 2010.

[88] J. Xianguo, W. Zengping, and Z. Zhichao *et al.*, "Single-phase high resistance fault protection based on active power of fault resistance,"*Proc. CSEE*, vol. 33, no. 13, pp. 187–193, 2013.

[89] G. B. Song, X. Chu, and S. P. Gao *et al.*, "Novel line protection based on distributed parameter model for long-distance transmission lines,"*IEEE Trans. Power Del.*, vol. 28, no. 4, pp. 2116–2123, Oct. 2013.

[90] H. Seyedi, S. Teimourzadeh, and P. S. Nezhad, "Adaptive zero sequence compensation

algorithm for double-circuit transmission lineprotection," *IET Gen., Transm. Distrib.*, vol. 8, no. 6, pp. 1107–1116,Jun. 2014.

[91] Jing Ma*,* Xin Yan, Bo Fan, Chang Liu, and James S. Thorp*, "*A Novel Line Protection Scheme for a Single Phase-to-Ground Fault Based on Voltage Phase Comparison", *IEEE transactions on power delivery,* vol. 31, no. 5, October 2016.

[92] Technical report, Ministry of Power, Govt. of India, New Delhi, India, August 2012

[93] Bakshi, A. S., Velayutham, A., Srivastava, S. C., Agrawal, K. K., Nayak, R. N., Soonee, S. K., & Singh, B. (2012). Report of the enquiry committee on grid disturbance in northern region on 30th July 2012 and in northern, eastern & north-eastern region on 31st July 2012. *New Delhi, India.*

[94] Yang, X-S. & Deb, S. (2010) 'Engineering optimisation by cuckoo search', *Int. J. Mathematical Modelling andNumerical Optimisation*, Vol. 1, No. 4, pp.330–34.

[95] Aziz Ouaarab, Belaıd Ahiod, Xin-She Yang," Discrete cuckoo search algorithm for the travelling salesman problem ", Neural Comput & Applic (2014) 24:1659–1669.

[96] http://www.ece.ubc.ca/~hameda/download_files

[97] Power Grid Corporation of India, www.powergridindia.com

[98] Yang X S., "A new metaheuristic bat-inspired algorithm", nature inspired cooperative strategies for optimization (NICSO 2010), vol. 284, Springer, Berlin, pp: 65–74 (2010).

[99] Kennedy J, Eberhart.,"A discrete binary version of the particle swarm algorithm", IEEE international conference on computational cybernetics and simulation, Orlando, USA, pp: 4104–4108 (1997).

[100] Mirjalili S., Mohd Hashim., BMOA: binary magnetic optimization algorithm, 3rd international conference on machine learning and computing, Singapore, pp: 201−206 (2011).

[101] Rashedi E., Nezamabadi pour H., Saryazdi S., BGSA: binary gravitational search algorithm, Natural Computing, vol. 9, no. 3, pp: 727−745 (2010).

[102] Mirjalili, S., Mirjalili, S. M., & Yang, X. S., "Binary bat algorithm", Neural Computing and Applications, 25(3-4), 663-681, 2014.

[103] S. Tamronglak, S. E Horowitz, A. G. Phadke, J. S. Thorp, **"** anatomy of power system blackouts: preventive relaying strategies," *IEEE Transactions on Power Delivery*, Vol. 11, No. 2, April 1996.

[104] M. Shiroie and S. H. Hosseini, "Observability and estimation of transformer tap setting with minimal PMU placement," in Power and Energy Society General Meeting - Conversion and Delivery of Electrical Energy in the 21st Century, 2008 IEEE, 2008, pp. 1-4.

[105] Glenn. W. Stagg, Ahmed. H. El-Abiad, Computer methods in power system analysis, international student edition.

[106] S. S. Zhu, *The Theory and Technology of Power System Relay Protection*, 3rd ed. Beijing, China: China Power Press, 2005.

Appendix-A
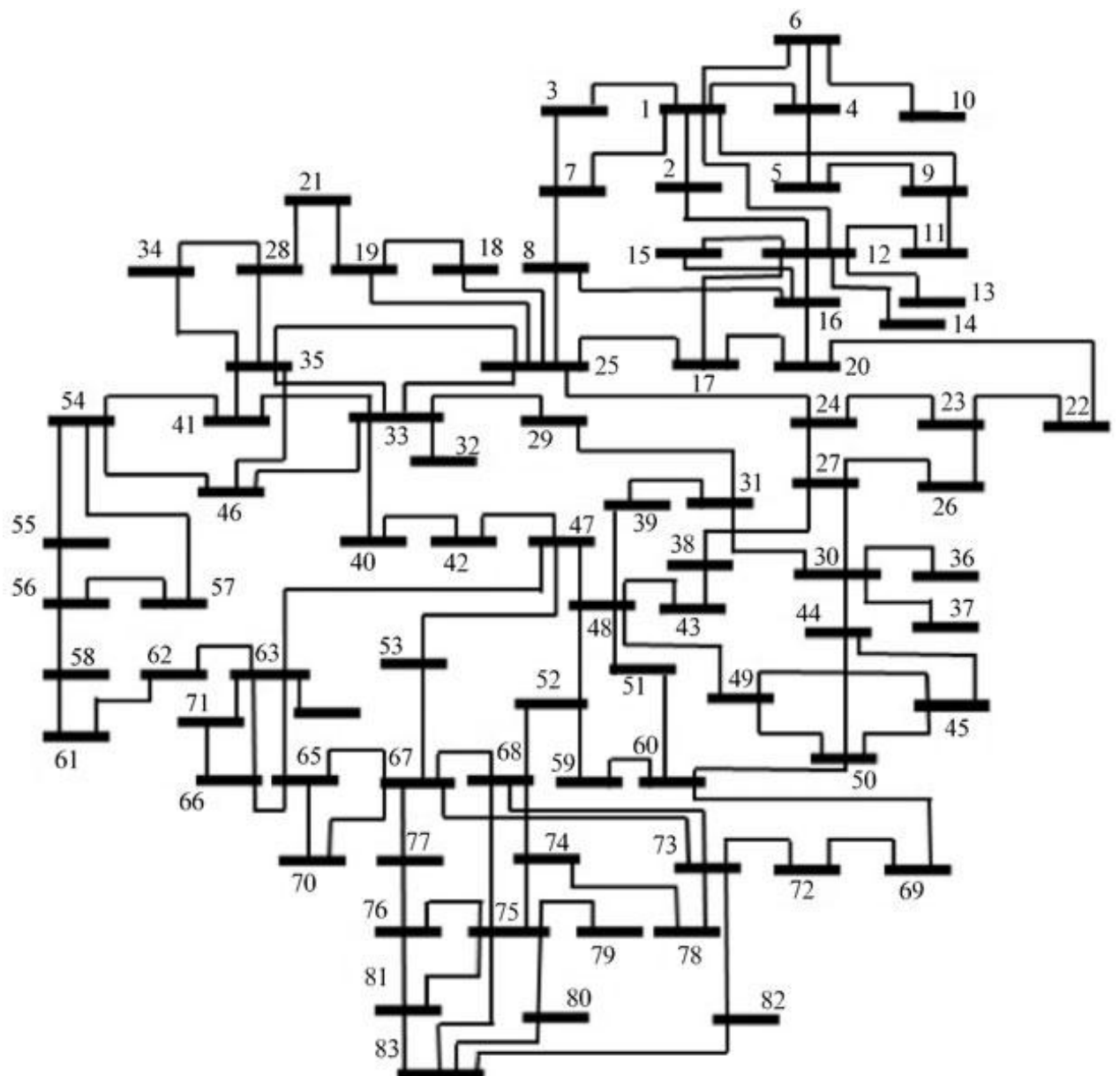
Figure A.1: Single line diagram of Tamil Nadu state regional grid

Table A.1: Bus details for Tamil Nadu state regional grid

No.	Bus name	No.	Bus name	No.	Bus name	No.	Bus name
1	Chennai	22	Acharapakkam	43	Samaypuram	64	Ponnapuram
2	G.Poondi	23	Villupuram	44	Kdalangudu	65	Sembatti
3	Almathy	24	TV Malai	45	Nallur	66	Myvadi
4	Ennore	25	Singarapettai	46	Ingur	67	Madurai
5	Monali	26	Cuddalore	47	Pugalur	68	Pasumalai
6	Tondiarpet	27	Neyveli TS1	48	Trichy	69	Paramkudi
7	Mosur	28	Mettur	49	Thanjavur	70	Theni
8	Thiruvalam	29	D.Kurchi	50	Thiruvarur	71	Kadamparai
9	Korattur	30	NeyveliTS2	51	Pudukottai	72	Sipcot
10	Mylapore	31	STCMS	52	Alagarkoil	73	Tuticorin
11	Koyambedu	32	SAIL	53	RGPuram	74	Sathur
12	Budur	33	Salem	54	Arasur	75	Kayathur
13	Kadperi	34	M.Tunnel	55	Pykara	76	Viranam
14	Hyundai	35	Mettur TPS	56	Kundah3	77	Kodikurchi
15	Tharamani	36	Bahoor	57	Kundah2	78	Sterlite
16	SP Koil	37	Villianur	58	Kundah1	79	Auto
17	Arni	38	Eachengadu	59	Valthur	80	Udayathur
18	V.Mangalam	39	Peranbalur	60	Karaikudi	81	Thirunelveli
19	Hosur	40	Unjanai	61	Thudiyalur	82	S.R.Pudur
20	Kalpakkam	41	Gobi	62	O.K.Mandabam	83	Sankaneri
21	Karimangalam	42	P.Chandai	63	Udumalpet		

Figure A.2: Single line diagram of United Andhra Pradesh state regional grid

Table A.2: Bus details for United Andhra Pradesh state regional grid

No.	Bus name	No.	Bus name	No.	Bus name	No.	Bus name
106	Nirmal	124	Simhadri 3	143	Ongole	162	Almati
107	Ramagundam	125	Kakinada CC	144	S.Palli	163	BB. Vadi
108	Dichpally	126	Vemagiri	145	Muddannur	164	Shahabad
109	Minpur	127	Vijayawada	146	Anantapur	165	Sedam
110	Hyderabad	128	Bommur	147	Hindupur	166	Humnabad
111	Karimnagar	129	Nidadavolu	148	AP3	167	Gulbarga
112	Siddipet	130	Bhimadole	149	AP1	168	Y.Mailaram
113	Bhongir	131	S.Lbph	150	Cuddapah	169	Barsur
114	Khammam	132	Kurnool	151	AP4	170	Balimela
115	Kothagudem	133	N'Sagar	152	Chittoor	171	AP5
116	Manuguru	134	Not used	153	Ranigunta	174	Tiruvalam
117	L.Sileru	135	Mehboob Ngr	154	Sulurpet	175	Nellore
118	U.Sileru	136	Raichur	155	Munirabad	176	Haveri
119	Gazuwaka	137	Gooty	156	L'Sugur	177	Davangere
120	Pendurthi	139	Krishnapatanam	157	Hubli	178	Kalinadi
121	Garividi	140	Warangal	158	Awadi	179	Alamanthi
122	Vizag	141	Siddipet	159	Narendra	180	TN 130
123	Simhadri 2	142	Sri Sailam	161	Ml.Pur	181	Kolar
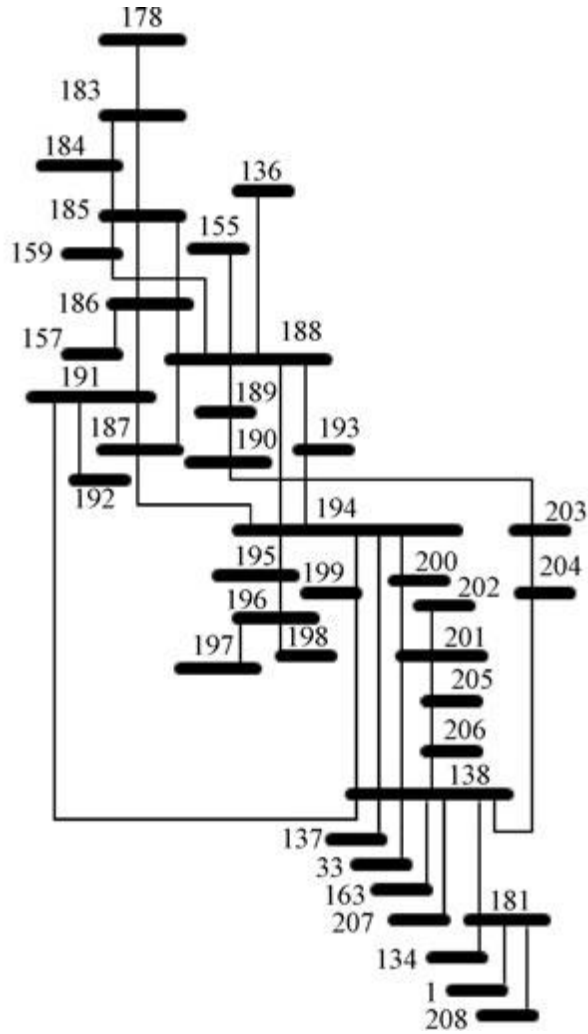
Figure A.3: Single line diagram of Karnataka state regional grid

Table A.3: Bus details for Karnataka state regional grid

No.	Bus name	No.	Bus name	No.	Bus name	No.	Bus name
182	Not used	189	C.Durga	196	Kemar	203	KA2
183	Kadra	190	KA1	197	Mangalore	204	KA3
184	Karwar	191	Talaguppa	198	Kudre Mukh	205	TK Halli
185	Kaiga	192	Tail Race	199	Tiptur	206	H Halli
186	Sirsi	193	Honali	200	Hassan	207	TN7
187	Sharavathi	194	Shimoga	201	Mysore	208	TN4
188	Davangere 2	195	Varahi	138	Bangalore		
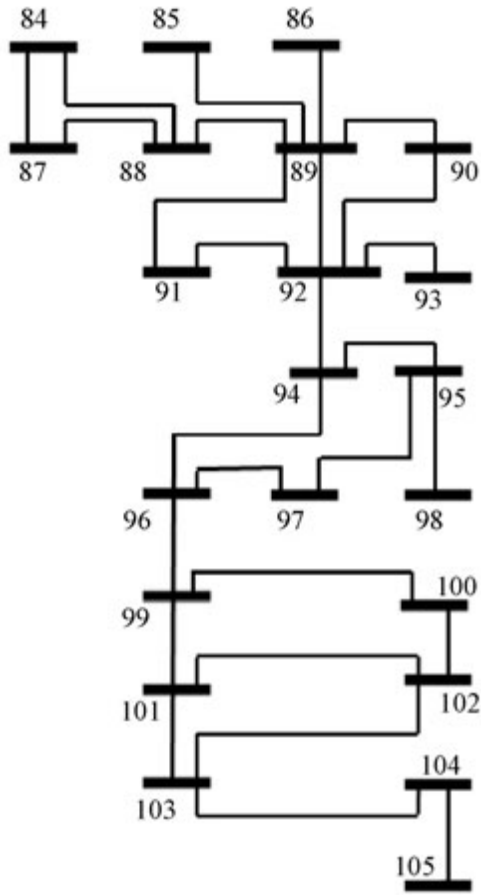
Figure A.4: Single line diagram of Kerala state regional grid

Table A.4: Bus details for Kerala state regional grid

No.	Bus name	No.	Bus name	No.	Bus name
84	Kasarkode	92	Trichur	100	Sabarigiri
85	Nallalm	93	Palakkad	101	Kayamkulam
86	Kaniampet	94	Periyar	102	Edamom
87	Taliparambu	95	Idukki	103	Kundara
88	Kanjikode	96	Bramhapuram	104	Pothencode
89	Areakode	97	Kalamassery	105	Trivandrum
90	Shornur	98	Pallom		
91	Malapparamba	99	New Pallom		
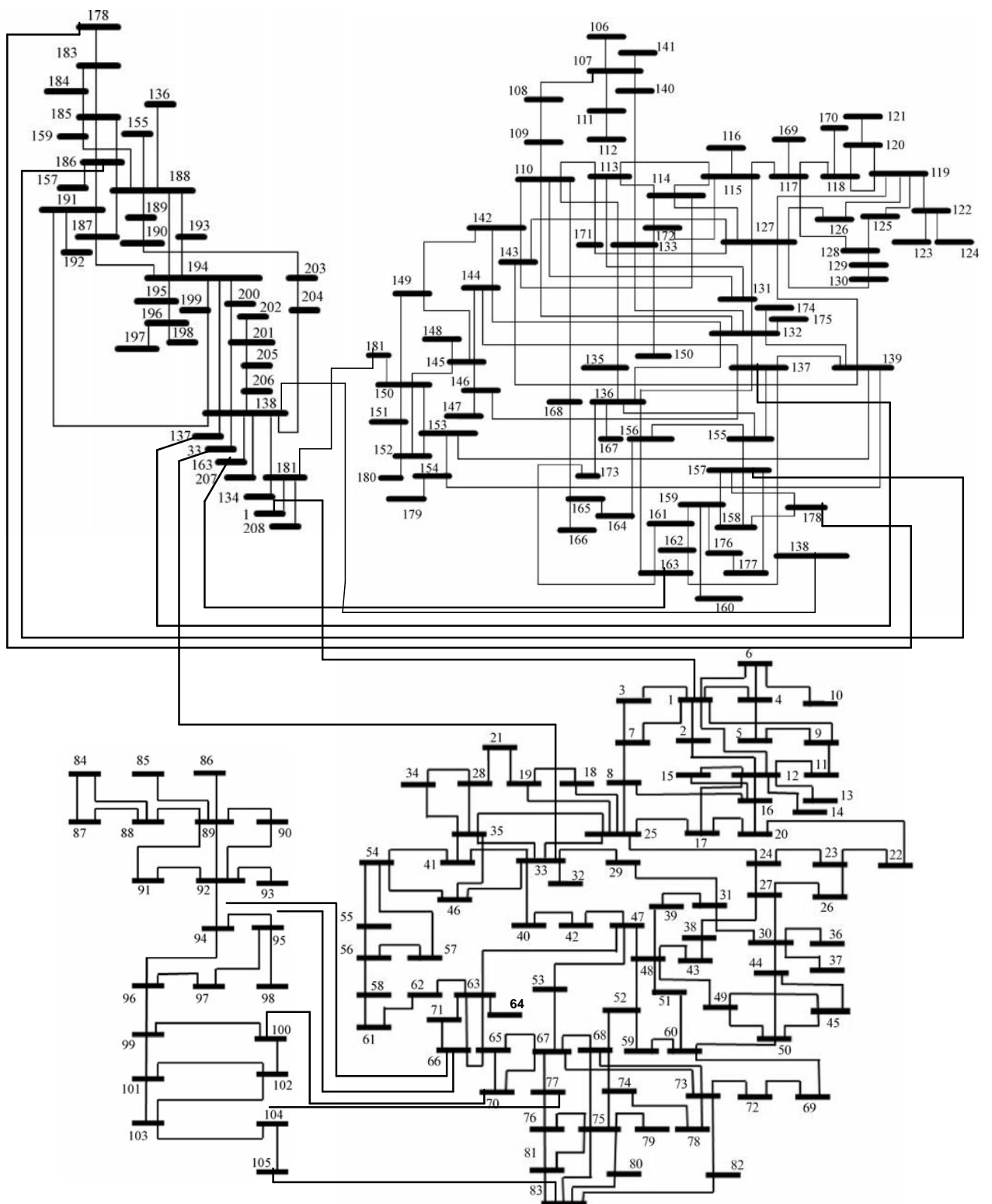
Figure A.5: Single line diagram of Southern Region of Indian Power Grid
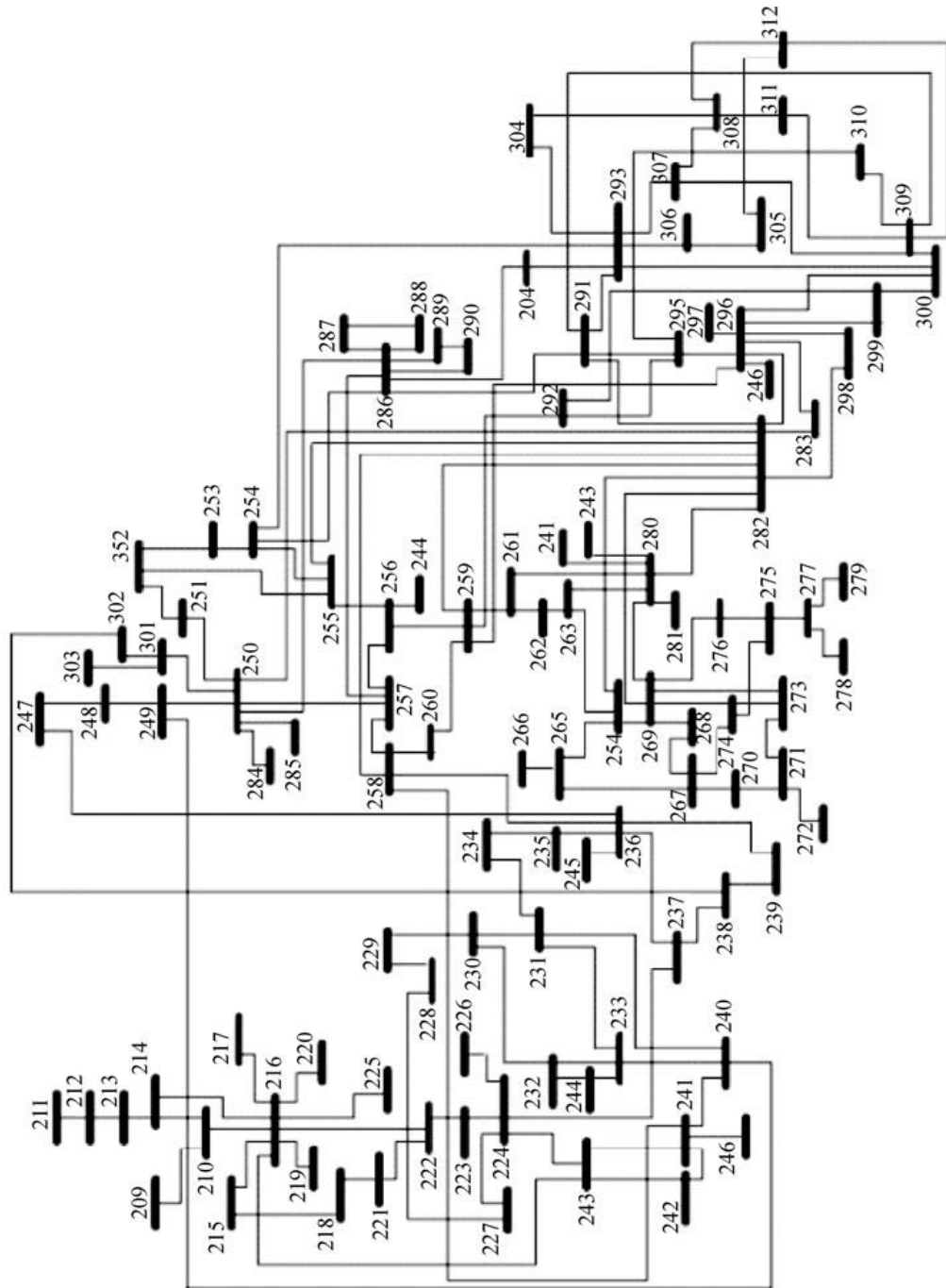
Figure A.6: Single line diagram of Northern Region of Indian Power Grid

Table A.5: Bus details for Northern Region of Indian Power Grid

No.	Bus name	No.	Bus name	No.	Bus name
209	Uri	244	Malerk'L	279	Udaipur
210	Wagoora	245	K.Wangtoo	280	Bhiwadi
211	Amargarh	246	Bhiwani	281	Kotputli
212	Kishenganga	247	Dehradun	282	Agra
213	Alistong	248	Saharanpur	283	Auraiya
214	Wampoh	249	Baghpat	284	Tehri
215	Salal	250	Merrut	285	Koteshwar
216	Kishenpur	251	Muzaffar Ngr	286	Bareilly
217	Dulhasti	252	Rishikesh	287	Pithorgarh
218	Jammu	253	Kashipur	288	Bhauliganga
219	Samba	254	Muradabad	289	Tanakpur
220	Udhampur	255	Murad Nagar	290	Kitchcha
221	Hiranagar	256	Dadri	291	Unnao
222	Sarna	257	Jhatikra	292	Mainpuri
223	Dasuya	258	Bawana	293	Lucknow
224	Jalandhar	259	Ballabgarh	294	Shahjahanpur
225	Chamera	260	Bamnauli	295	Panki
226	Hamirpur	261	Gurgaon	296	Kanpur
227	Amritsar	262	Manesar	297	Unchahap
228	Pooling Point	263	Neemrana	298	Fatehpur
229	Parbati	264	Sikar	299	Allahabad
230	Koldam	265	Ratangarh	300	Rihand
231	Nallagarh	266	Suratgarh	301	Bulandshahr
232	Ludhiana	267	Merta	302	Hapur
233	Patiala	268	Jaipur RSEB	303	Orai
234	N.Jhakri	269	Jaipur	304	Gorakhpur
235	Panchkulan	270	Jodhpur	305	Balia
236	Abdullapur	271	Kankroli	306	Sohawal

237	Kurukshethra	272	Bhinmal	307	Sultanpur
238	New Hissar	273	RAPP-C	308	Azamgarh
239	Sonepat	274	Kota	309	Anpara
240	Kaithal	275	Anta	310	Obra
241	Hissar	276	Dausa	311	Varanasi
242	Fatehbad	277	RAPP-B	312	Mau
243	Moga	278	Chittorg'h		
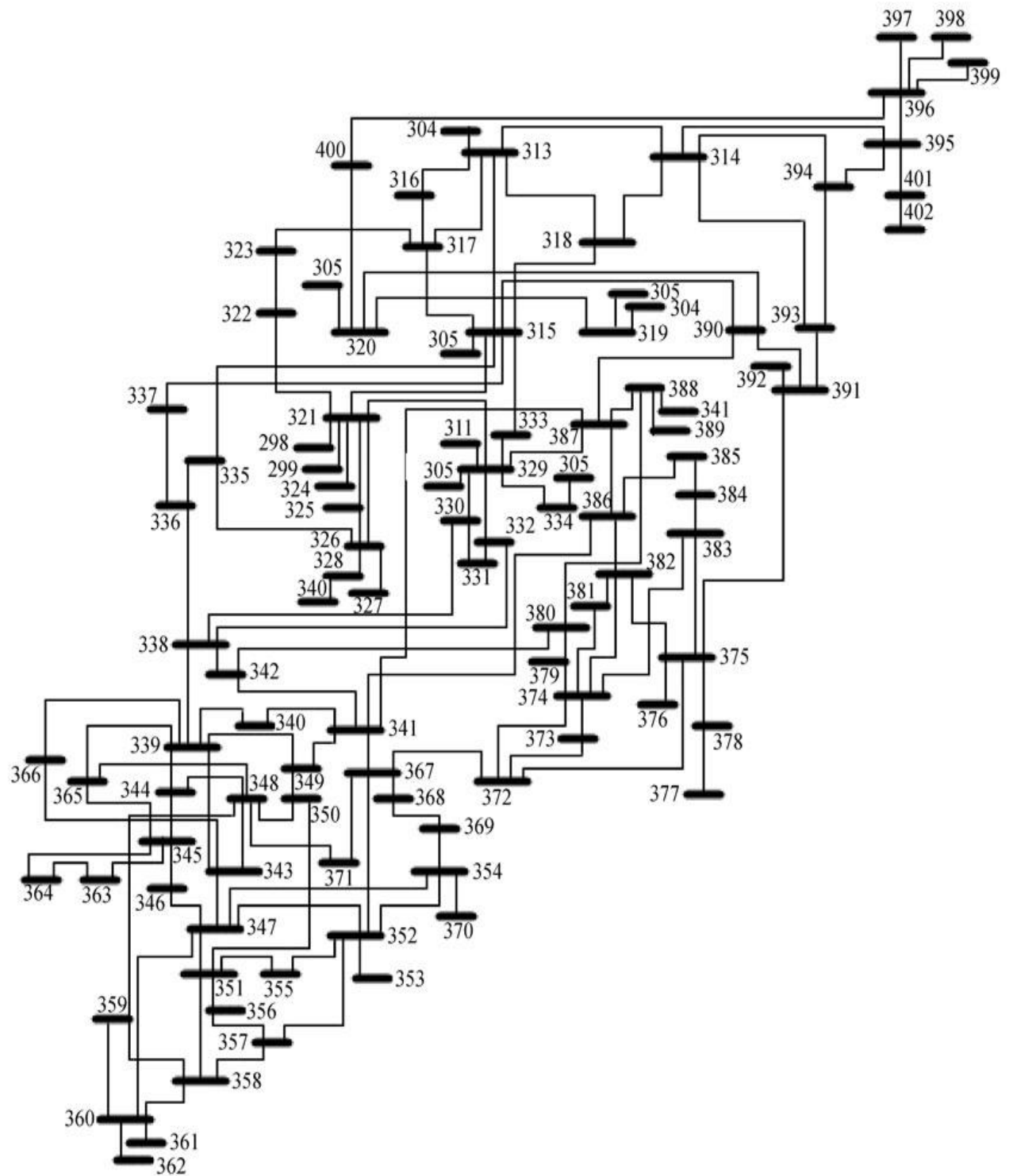
Figure A.7: Single line diagram of Eastern Region of Indian Power Grid

Table A.6: Bus details for Eastern Region of Indian Power Grid

No.	Bus name	No.	Bus name	No.	Bus name
313	Muzaffarpur	343	Talcher TPS	373	Howrah
314	Purnea	344	Tarkeera	374	Arambag
315	BHRSHRF	345	Brajrajnagr	375	Jeerat
316	Hazipur	346	IB Valley	376	Subhasgram
317	Fatwa	347	Mera Mundli	377	LKPUR
318	Begusarai	348	Rengali	378	KASBA
319	Barh	349	Joda	379	Bisnupur
320	Patna	350	Talcher TPS	380	Santaldih
321	Sasaram	351	BHNJNGR	381	Purulia
322	Arrah	352	Chandaka	382	Bidhannagar
323	Khagaul	353	Bhubaneswar	383	Bakreswar
324	DLTNGNJ	354	Duburi	384	Gokarna
325	Karamnasa	355	Nayagarh	385	Sagardighi
326	Dehri	356	Aska	386	Durgapur
327	Nabi NGR	357	Chhatrapur	387	Maithon
328	Garwa	358	Theruvelli	388	Bokaro
329	Gaya	359	Indravati	389	Majia
330	Jharkhand PL	360	Jeypore	390	Kahalgaon
331	Ranchi	361	U.Kolab	391	Farraka
332	NKSTPP	362	Balimela	392	Lalmatia
333	Koderma	363	Hirakud	393	Malda
334	Tilaiyya	364	Bolangir	394	Dalkhola
335	Bogaya	365	Tarkera	395	Siliguri
336	Patratu	366	SNDRGRH	396	Melli
337	Tenughat	367	Baripada	397	Rangit
338	Ranchi	368	Balasore	398	Gangtok
339	Rourkela	369	Bhadrak	399	Rangpo
340	Chaibasa	370	Paradeep	400	Kishanganj

| 341 | Jamshedpur | 371 | Keonjhar | 401 | Birpara |
| 342 | Chandil | 372 | Kolaghat | 402 | Alipurduar |
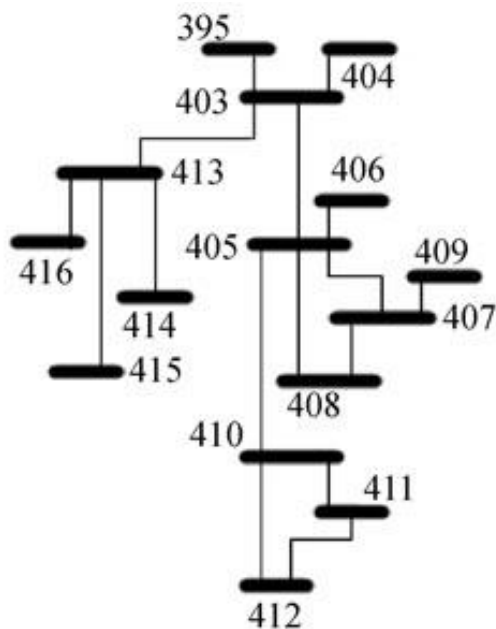
Figure A.8: Single line diagram of North-Eastern Region of Indian Power Grid

Table A.7: Bus details for North-Eastern Region of Indian Power Grid

No.	Bus name	No.	Bus name	No.	Bus name
403	Bongaigaon	408	Ranganadi	413	Silchar
404	BTPS	409	Subansiri	414	Imphal
405	Balipara	410	Misa	415	Melriat
406	Khupi	411	Kathalguri	416	Pallatana
407	B.Chariali	412	Mariani		
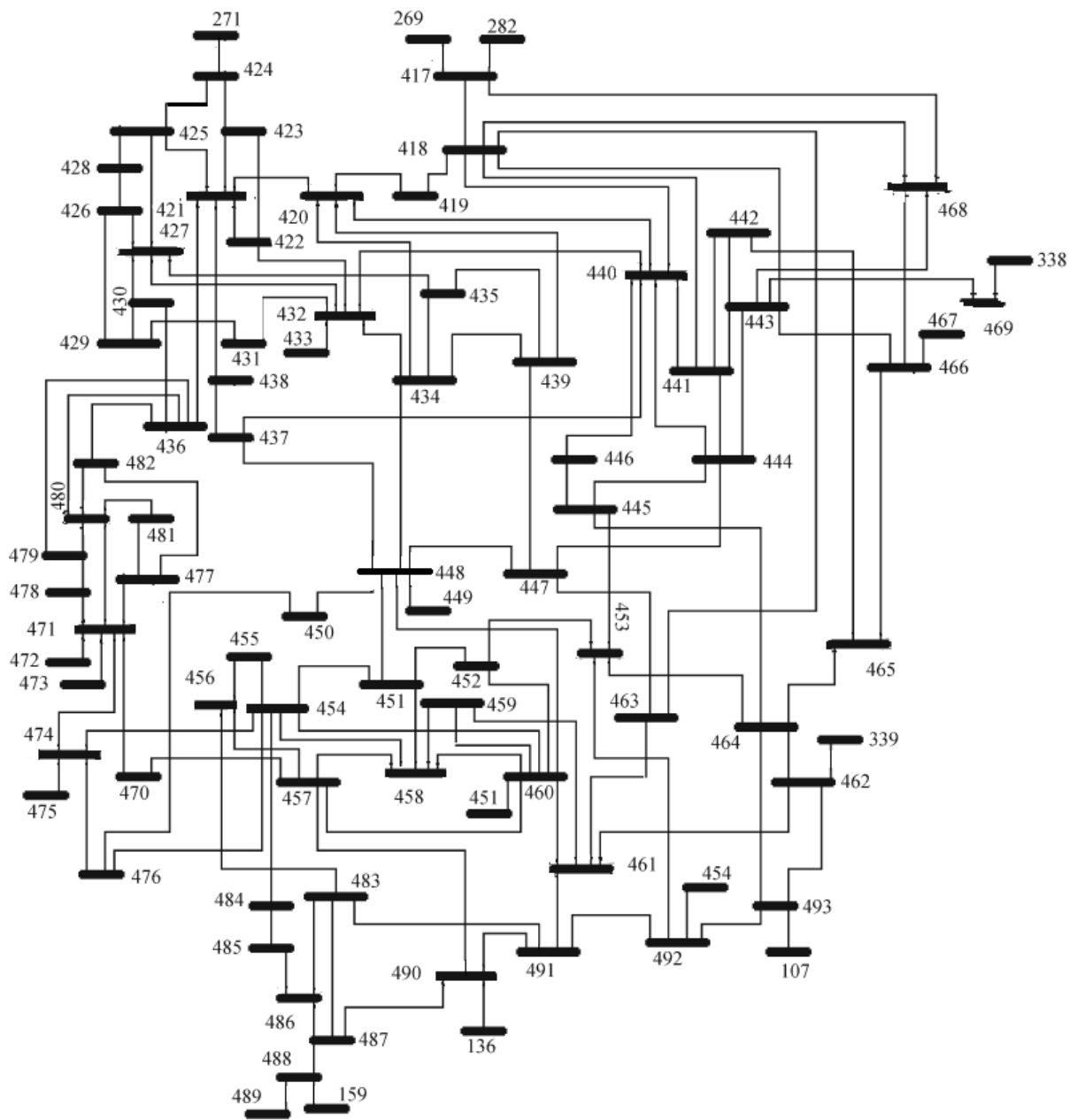
Figure A.9: Single line diagram of Western Region of Indian Power Grid

Table A.8: Bus details for Western Region of Indian Power Grid

No.	Bus name	No.	Bus name	No.	Bus name
417	Gwalior	443	Jabalpur	469	D'jayagarh
418	Bina	444	Itarsi	470	N'Mumbai
419	Shujalpur	445	Satpura	471	Vapi
420	Nagda	446	Narmada Sgr	472	Kharadpada
421	Dehgam	447	Khandwa	473	Khadoli
422	Manakbori	448	Dhule	474	Boisar
423	Nardipur	449	M'Gaon	475	Mumbai
424	Zerda	450	Nasik	476	Tarapur Ex
425	Ranchodpura	451	Bableshwar	477	Kakrapar
426	Mundra	452	Bhusawal	478	Magarwada
427	Limbdi	453	Koradi	479	Navsari
428	Bachchau	454	Padghe	480	Kawas
429	Jetpur	455	Kalwa	481	Valthan
430	Rajkot	456	Kharghar	482	Bharuch
431	Amreli	457	Pune	483	Lonikhand
432	Asoj	458	Aurangabad	484	Nagothane
433	Ukai	459	Akola	485	Dhabo
434	S.Sarovar	460	Aurangabad	486	Koyna
435	Karamsad	461	Wardha	487	Karad
436	Gandhar	462	Raipur	488	Kolhapur
437	Vadodara	463	Seoni	489	Mapusa
438	Pirana	464	Bhilai	490	Solapur
439	Rajgarh	465	Korba	491	Parli
440	Indore	466	Vindhyachal	492	Chandrapur
441	Bhopal	467	Sasan	493	Bhadravati
442	Damoh	468	Satna		

Appendix-B

Table B.1: Bus data for IEEE14 bus system

Bus	Pd (MW)	Qd (MVAR)	Vm(p.u)	Va(deg)	Vmax(p.u)	Vmin(p.u)
1	0	0	1.06	0	1.06	0.94
2	21.7	12.7	1.045	-4.98	1.06	0.94
3	94.2	19	1.01	-12.72	1.06	0.94
4	47.8	-3.9	1.019	-10.33	1.06	0.94
5	7.6	1.6	1.02	-8.78	1.06	0.94
6	11.2	7.5	1.07	-14.22	1.06	0.94
7	0	0	1.062	-13.37	1.06	0.94
8	0	0	1.09	-13.36	1.06	0.94
9	29.5	16.6	1.056	-14.94	1.06	0.94
10	9	5.8	1.051	-15.1	1.06	0.94
11	3.5	1.8	1.057	-14.79	1.06	0.94
12	6.1	1.6	1.055	-15.07	1.06	0.94
13	13.5	5.8	1.05	-15.16	1.06	0.94
14	14.9	5	1.036	-16.04	1.06	0.94

Table B.2: Generator data for IEEE14 bus system

Bus	Pg(MW)	Qg(MVAR)	Qmax(MVAR)	Qmin(MVAR)	Pmax(MW)
1	232.4	-16.9	10	0	332.4
2	40	42.4	50	-40	140

Table B.3: Line data for IEEE14 bus system

From	To	R(p.u)	X(p.u)	B/2(p.u)	Rate(MVA)	ratio
1	2	0.01938	0.05917	0.0528	120	0
1	5	0.05403	0.22304	0.0492	65	0
2	3	0.04699	0.19797	0.0438	36	0
2	4	0.05811	0.17632	0.034	65	0
2	5	0.05695	0.17388	0.0346	50	0
3	4	0.06701	0.17103	0.0128	65	0
4	5	0.01335	0.04211	0	45	0
4	7	0	0.20912	0	55	0.978
4	9	0	0.55618	0	32	0.969
5	6	0	0.25202	0	45	0.932
6	11	0.09498	0.1989	0	18	0
6	12	0.12291	0.25581	0	32	0
6	13	0.06615	0.13027	0	32	0
7	8	0	0.17615	0	32	0

7	9	0	0.11001	0	32	0
9	10	0.03181	0.0845	0	32	0
9	14	0.12711	0.27038	0	32	0
10	11	0.08205	0.19207	0	12	0
12	13	0.22092	0.19988	0	12	0
13	14	0.17093	0.34802	0	12	0

Table B.4: Bus data for IEEE30 bus system

Bus	Pd (MW)	Qd (MVAR)	Vm(p.u)	Va(deg)	Vmax(p.u)	Vmin(p.u)
1	0	0	1	0	1.05	0.95
2	21.7	12.7	1	0	1.1	0.95
3	2.4	1.2	1	0	1.05	0.95
4	7.6	1.6	1	0	1.05	0.95
5	0	0	1	0	1.05	0.95
6	0	0	1	0	1.05	0.95
7	22.8	10.9	1	0	1.05	0.95
8	30	30	1	0	1.05	0.95
9	0	0	1	0	1.05	0.95
10	5.8	2	1	0	1.05	0.95
11	0	0	1	0	1.05	0.95
12	11.2	7.5	1	0	1.05	0.95
13	0	0	1	0	1.1	0.95
14	6.2	1.6	1	0	1.05	0.95
15	8.2	2.5	1	0	1.05	0.95
16	3.5	1.8	1	0	1.05	0.95
17	9	5.8	1	0	1.05	0.95
18	3.2	0.9	1	0	1.05	0.95
19	9.5	3.4	1	0	1.05	0.95
20	2.2	0.7	1	0	1.05	0.95
21	17.5	11.2	1	0	1.05	0.95
22	0	0	1	0	1.1	0.95
23	3.2	1.6	1	0	1.1	0.95
24	8.7	6.7	1	0	1.05	0.95
25	0	0	1	0	1.05	0.95
26	3.5	2.3	1	0	1.05	0.95
27	0	0	1	0	1.1	0.95
28	0	0	1	0	1.05	0.95
29	2.4	0.9	1	0	1.05	0.95
30	10.6	1.9	1	0	1.05	0.95

Table B.5: Generator data for IEEE30 bus system

Bus	Pg(MW)	Qg(MVAR)	Qmax(MVAR)	Qmin(MVAR)	Pmax(MW)
1	23.54	0	150	-20	80
2	60.97	0	60	-20	80
22	21.59	0	62.5	-15	50
27	26.91	0	48.7	-15	55
23	19.2	0	40	-10	30
13	37	0	44.7	-15	40

Table B.6: Line data for IEEE30 bus system

From	To	R(p.u)	X(p.u)	B/2(p.u)	Rate(MVA)	Tap Ratio
1	2	0.02	0.06	0.0528	130	0
1	3	0.05	0.19	0.0408	130	0
2	4	0.06	0.17	0.0368	65	0
3	4	0.01	0.04	0.0084	130	0
2	5	0.05	0.2	0.0418	130	0
2	6	0.06	0.18	0.0374	65	0
4	6	0.01	0.04	0.009	90	0
5	7	0.05	0.12	0.0204	70	0
6	7	0.03	0.08	0.017	130	0
6	8	0.01	0.04	0.009	32	0
6	9	0	0.21	0	65	0.978
6	10	0	0.56	0	32	0.969
6	28	0.02	0.06	0.013	32	0
8	28	0.06	0.2	0.0428	32	0
9	11	0	0.21	0	65	0
9	10	0	0.11	0	65	0
4	12	0	0.26	0	65	0.932
12	13	0	0.14	0	65	0
12	14	0.12	0.26	0	32	0
12	15	0.07	0.13	0	32	0
12	16	0.09	0.2	0	32	0
14	15	0.22	0.2	0	16	0
16	17	0.08	0.19	0	16	0
15	18	0.11	0.22	0	16	0
18	19	0.06	0.13	0	16	0
19	20	0.03	0.07	0	32	0
10	20	0.09	0.21	0	32	0
10	17	0.03	0.08	0	32	0
10	21	0.03	0.07	0	32	0

10	22	0.07	0.15	0	32	0
21	22	0.01	0.02	0	32	0
15	23	0.1	0.2	0	16	0
22	24	0.12	0.18	0	16	0
23	24	0.13	0.27	0	16	0
24	25	0.19	0.33	0	16	0
25	26	0.25	0.38	0	16	0
25	27	0.11	0.21	0	16	0
28	27	0	0.4	0	65	0.968
27	29	0.22	0.42	0	16	0
27	30	0.32	0.6	0	16	0
29	30	0.24	0.45	0	16	0

Table B.7: Bus data for IEEE39 bus system

Bus	Pd (MW)	Qd (MVAR)	Vm(p.u)	Va(deg)	Vmax(p.u)	Vmin(p.u)
1	97.6	44.2	1.03938	-13.537	1.06	0.94
2	0	0	1.04849	-9.7853	1.06	0.94
3	322	2.4	1.03071	-12.276	1.06	0.94
4	500	184	1.00446	-12.627	1.06	0.94
5	0	0	1.00601	-11.192	1.06	0.94
6	0	0	1.00823	-10.408	1.06	0.94
7	233.8	84	0.9984	-12.756	1.06	0.94
8	522	176.6	0.99787	-13.336	1.06	0.94
9	6.5	-66.6	1.03833	-14.178	1.06	0.94
10	0	0	1.01784	-8.1709	1.06	0.94
11	0	0	1.01339	-8.937	1.06	0.94
12	8.53	88	1.00082	-8.9988	1.06	0.94
13	0	0	1.01492	-8.9299	1.06	0.94
14	0	0	1.01232	-10.715	1.06	0.94
15	320	153	1.01619	-11.345	1.06	0.94
16	329	32.3	1.03252	-10.033	1.06	0.94
17	0	0	1.03424	-11.116	1.06	0.94
18	158	30	1.03157	-11.986	1.06	0.94
19	0	0	1.05011	-5.4101	1.06	0.94
20	680	103	0.99101	-6.8212	1.06	0.94
21	274	115	1.03232	-7.6287	1.06	0.94
22	0	0	1.05014	-3.1831	1.06	0.94
23	247.5	84.6	1.04515	-3.3813	1.06	0.94
24	308.6	-92.2	1.038	-9.9138	1.06	0.94
25	224	47.2	1.05768	-8.3692	1.06	0.94

26	139	17	1.05256	-9.4388	1.06	0.94
27	281	75.5	1.03834	-11.362	1.06	0.94
28	206	27.6	1.05037	-5.9284	1.06	0.94
29	283.5	26.9	1.05011	-3.1699	1.06	0.94
30	0	0	1.0499	-7.3705	1.06	0.94
31	9.2	4.6	0.982	0	1.06	0.94
32	0	0	0.9841	-0.1884	1.06	0.94
33	0	0	0.9972	-0.1932	1.06	0.94
34	0	0	1.0123	-1.6311	1.06	0.94
35	0	0	1.0494	1.77651	1.06	0.94
36	0	0	1.0636	4.46844	1.06	0.94
37	0	0	1.0275	-1.5829	1.06	0.94
38	0	0	1.0265	3.89282	1.06	0.94
39	1104	250	1.03	-14.535	1.06	0.94

Table B.8: Generator data for IEEE39 bus system

Bus	Pg(MW)	Qg(MVAR)	Qmax(MVAR)	Qmin(MVAR)	Pmax(MW)
30	250	161.762	400	140	1040
31	677.871	221.574	300	-100	646
32	650	206.965	300	150	725
33	632	108.293	250	0	652
34	508	166.688	167	0	508
35	650	210.661	300	-100	687
36	560	100.165	240	0	580
37	540	-1.3695	250	0	564
38	830	21.7327	300	-150	865
39	1000	78.4674	300	-100	1100

Table B.9: Line data for IEEE39 bus system

From	To	R(p.u)	X(p.u)	B/2(p.u)	Rate(MVA)	Tap Ratio
1	2	0.0035	0.0411	0.6987	600	0
1	39	0.001	0.025	0.75	1000	0
2	3	0.0013	0.0151	0.2572	500	0
2	25	0.007	0.0086	0.146	500	0
2	30	0	0.0181	0	900	1.025
3	4	0.0013	0.0213	0.2214	500	0
3	18	0.0011	0.0133	0.2138	500	0
4	5	0.0008	0.0128	0.1342	600	0
4	14	0.0008	0.0129	0.1382	500	0
5	6	0.0002	0.0026	0.0434	1200	0

5	8	0.0008	0.0112	0.1476	900	0
6	7	0.0006	0.0092	0.113	900	0
6	11	0.0007	0.0082	0.1389	480	0
6	31	0	0.025	0	1800	1.07
7	8	0.0004	0.0046	0.078	900	0
8	9	0.0023	0.0363	0.3804	900	0
9	39	0.001	0.025	1.2	900	0
10	11	0.0004	0.0043	0.0729	600	0
10	13	0.0004	0.0043	0.0729	600	0
10	32	0	0.02	0	900	1.07
12	11	0.0016	0.0435	0	500	1.006
12	13	0.0016	0.0435	0	500	1.006
13	14	0.0009	0.0101	0.1723	600	0
14	15	0.0018	0.0217	0.366	600	0
15	16	0.0009	0.0094	0.171	600	0
16	17	0.0007	0.0089	0.1342	600	0
16	19	0.0016	0.0195	0.304	600	0
16	21	0.0008	0.0135	0.2548	600	0
16	24	0.0003	0.0059	0.068	600	0
17	18	0.0007	0.0082	0.1319	600	0
17	27	0.0013	0.0173	0.3216	600	0
19	20	0.0007	0.0138	0	900	1.06
19	33	0.0007	0.0142	0	900	1.07
20	34	0.0009	0.018	0	900	1.009
21	22	0.0008	0.014	0.2565	900	0
22	23	0.0006	0.0096	0.1846	600	0
22	35	0	0.0143	0	900	1.025
23	24	0.0022	0.035	0.361	600	0
23	36	0.0005	0.0272	0	900	1
25	26	0.0032	0.0323	0.531	600	0
25	37	0.0006	0.0232	0	900	1.025
26	27	0.0014	0.0147	0.2396	600	0
26	28	0.0043	0.0474	0.7802	600	0
26	29	0.0057	0.0625	1.029	600	0
28	29	0.0014	0.0151	0.249	600	0
29	38	0.0008	0.0156	0	1200	1.025

Table B.10: Bus data for IEEE57 bus system

Bus	Pd (MW)	Qd (MVAR)	Vm(p.u)	Va(deg)	Vmax(p.u)	Vmin(p.u)
1	55	17	1.04	0	1.06	0.94
2	3	88	1.01	-1.18	1.06	0.94
3	41	21	0.985	-5.97	1.06	0.94
4	0	0	0.981	-7.32	1.06	0.94
5	13	4	0.976	-8.52	1.06	0.94
6	75	2	0.98	-8.65	1.06	0.94
7	0	0	0.984	-7.58	1.06	0.94
8	150	22	1.005	-4.45	1.06	0.94
9	121	26	0.98	-9.56	1.06	0.94
10	5	2	0.986	-11.43	1.06	0.94
11	0	0	0.974	-10.17	1.06	0.94
12	377	24	1.015	-10.46	1.06	0.94
13	18	2.3	0.979	-9.79	1.06	0.94
14	10.5	5.3	0.97	-9.33	1.06	0.94
15	22	5	0.988	-7.18	1.06	0.94
16	43	3	1.013	-8.85	1.06	0.94
17	42	8	1.017	-5.39	1.06	0.94
18	27.2	9.8	1.001	-11.71	1.06	0.94
19	3.3	0.6	0.97	-13.2	1.06	0.94
20	2.3	1	0.964	-13.41	1.06	0.94
21	0	0	1.008	-12.89	1.06	0.94
22	0	0	1.01	-12.84	1.06	0.94
23	6.3	2.1	1.008	-12.91	1.06	0.94
24	0	0	0.999	-13.25	1.06	0.94
25	6.3	3.2	0.982	-18.13	1.06	0.94
26	0	0	0.959	-12.95	1.06	0.94
27	9.3	0.5	0.982	-11.48	1.06	0.94
28	4.6	2.3	0.997	-10.45	1.06	0.94
29	17	2.6	1.01	-9.75	1.06	0.94
30	3.6	1.8	0.962	-18.68	1.06	0.94
31	5.8	2.9	0.936	-19.34	1.06	0.94
32	1.6	0.8	0.949	-18.46	1.06	0.94
33	3.8	1.9	0.947	-18.5	1.06	0.94
34	0	0	0.959	-14.1	1.06	0.94
35	6	3	0.966	-13.86	1.06	0.94
36	0	0	0.976	-13.59	1.06	0.94
37	0	0	0.985	-13.41	1.06	0.94

38	14	7	1.013	-12.71	1.06	0.94
39	0	0	0.983	-13.46	1.06	0.94
40	0	0	0.973	-13.62	1.06	0.94
41	6.3	3	0.996	-14.05	1.06	0.94
42	7.1	4.4	0.966	-15.5	1.06	0.94
43	2	1	1.01	-11.33	1.06	0.94
44	12	1.8	1.017	-11.86	1.06	0.94
45	0	0	1.036	-9.25	1.06	0.94
46	0	0	1.05	-11.89	1.06	0.94
47	29.7	11.6	1.033	-12.49	1.06	0.94
48	0	0	1.027	-12.59	1.06	0.94
49	18	8.5	1.036	-12.92	1.06	0.94
50	21	10.5	1.023	-13.39	1.06	0.94
51	18	5.3	1.052	-12.52	1.06	0.94
52	4.9	2.2	0.98	-11.47	1.06	0.94
53	20	10	0.971	-12.23	1.06	0.94
54	4.1	1.4	0.996	-11.69	1.06	0.94
55	6.8	3.4	1.031	-10.78	1.06	0.94
56	7.6	2.2	0.968	-16.04	1.06	0.94
57	6.7	2	0.965	-16.56	1.06	0.94

Table B.11: Generator data for IEEE57 bus system

Bus	Pg(MW)	Qg(MVAR)	Qmax(MVAR)	Qmin(MVAR)	Pmax(MW)
1	128.9	-16.1	200	-140	575.88
3	40	-1	60	-10	140
8	450	62.1	200	-140	550
12	310	128.5	155	-150	410

Table B.12: Line data for IEEE57 bus system

From	To	R(p.u)	X(p.u)	B/2(p.u)	Rate(MVA)	Tap Ratio
1	2	0.0083	0.028	0.129	9900	0
2	3	0.0298	0.085	0.0818	9900	0
3	4	0.0112	0.0366	0.038	9900	0
4	5	0.0625	0.132	0.0258	9900	0
4	6	0.043	0.148	0.0348	9900	0
6	7	0.02	0.102	0.0276	9900	0
6	8	0.0339	0.173	0.047	9900	0
8	9	0.0099	0.0505	0.0548	9900	0
9	10	0.0369	0.1679	0.044	9900	0
9	11	0.0258	0.0848	0.0218	9900	0

9	12	0.0648	0.295	0.0772	9900	0
9	13	0.0481	0.158	0.0406	9900	0
13	14	0.0132	0.0434	0.011	9900	0
13	15	0.0269	0.0869	0.023	9900	0
1	15	0.0178	0.091	0.0988	9900	0
1	16	0.0454	0.206	0.0546	9900	0
1	17	0.0238	0.108	0.0286	9900	0
3	15	0.0162	0.053	0.0544	9900	0
4	18	0	0.555	0	9900	0.97
4	18	0	0.43	0	9900	0.978
5	6	0.0302	0.0641	0.0124	9900	0
7	8	0.0139	0.0712	0.0194	9900	0
10	12	0.0277	0.1262	0.0328	9900	0
11	13	0.0223	0.0732	0.0188	9900	0
12	13	0.0178	0.058	0.0604	9900	0
12	16	0.018	0.0813	0.0216	9900	0
12	17	0.0397	0.179	0.0476	9900	0
14	15	0.0171	0.0547	0.0148	9900	0
18	19	0.461	0.685	0	9900	0
19	20	0.283	0.434	0	9900	0
21	20	0	0.7767	0	9900	1.043
21	22	0.0736	0.117	0	9900	0
22	23	0.0099	0.0152	0	9900	0
23	24	0.166	0.256	0.0084	9900	0
24	25	0	1.182	0	9900	1
24	25	0	1.23	0	9900	1
24	26	0	0.0473	0	9900	1.043
26	27	0.165	0.254	0	9900	0
27	28	0.0618	0.0954	0	9900	0
28	29	0.0418	0.0587	0	9900	0
7	29	0	0.0648	0	9900	0.967
25	30	0.135	0.202	0	9900	0
30	31	0.326	0.497	0	9900	0
31	32	0.507	0.755	0	9900	0
32	33	0.0392	0.036	0	9900	0
34	32	0	0.953	0	9900	0.975
34	35	0.052	0.078	0.0032	9900	0
35	36	0.043	0.0537	0.0016	9900	0
36	37	0.029	0.0366	0	9900	0
37	38	0.0651	0.1009	0.002	9900	0

37	39	0.0239	0.0379	0	9900	0
36	40	0.03	0.0466	0	9900	0
22	38	0.0192	0.0295	0	9900	0
11	41	0	0.749	0	9900	0.955
41	42	0.207	0.352	0	9900	0
41	43	0	0.412	0	9900	0
38	44	0.0289	0.0585	0.002	9900	0
15	45	0	0.1042	0	9900	0.955
14	46	0	0.0735	0	9900	0.9
46	47	0.023	0.068	0.0032	9900	0
47	48	0.0182	0.0233	0	9900	0
48	49	0.0834	0.129	0.0048	9900	0
49	50	0.0801	0.128	0	9900	0
50	51	0.1386	0.22	0	9900	0
10	51	0	0.0712	0	9900	0.93
13	49	0	0.191	0	9900	0.895
29	52	0.1442	0.187	0	9900	0
52	53	0.0762	0.0984	0	9900	0
53	54	0.1878	0.232	0	9900	0
54	55	0.1732	0.2265	0	9900	0
11	43	0	0.153	0	9900	0.958
44	45	0.0624	0.1242	0.004	9900	0
40	56	0	1.195	0	9900	0.958
56	41	0.553	0.549	0	9900	0
56	42	0.2125	0.354	0	9900	0
39	57	0	1.355	0	9900	0.98
57	56	0.174	0.26	0	9900	0
38	49	0.115	0.177	0.003	9900	0
38	48	0.0312	0.0482	0	9900	0
9	55	0	0.1205	0	9900	0.94

Table B.13: Bus data for IEEE118 bus system

Bus	Pd (MW)	Qd (MVAR)	Vm(p.u)	Va(deg)	Vmax(p.u)	Vmin(p.u)
1	51	27	0.955	10.67	1.06	0.94
2	20	9	0.971	11.22	1.06	0.94
3	39	10	0.968	11.56	1.06	0.94
4	39	12	0.998	15.28	1.06	0.94
5	0	0	1.002	15.73	1.06	0.94
6	52	22	0.99	13	1.06	0.94
7	19	2	0.989	12.56	1.06	0.94

8	28	0	1.015	20.77	1.06	0.94
9	0	0	1.043	28.02	1.06	0.94
10	0	0	1.05	35.61	1.06	0.94
11	70	23	0.985	12.72	1.06	0.94
12	47	10	0.99	12.2	1.06	0.94
13	34	16	0.968	11.35	1.06	0.94
14	14	1	0.984	11.5	1.06	0.94
15	90	30	0.97	11.23	1.06	0.94
16	25	10	0.984	11.91	1.06	0.94
17	11	3	0.995	13.74	1.06	0.94
18	60	34	0.973	11.53	1.06	0.94
19	45	25	0.963	11.05	1.06	0.94
20	18	3	0.958	11.93	1.06	0.94
21	14	8	0.959	13.52	1.06	0.94
22	10	5	0.97	16.08	1.06	0.94
23	7	3	1	21	1.06	0.94
24	13	0	0.992	20.89	1.06	0.94
25	0	0	1.05	27.93	1.06	0.94
26	0	0	1.015	29.71	1.06	0.94
27	71	13	0.968	15.35	1.06	0.94
28	17	7	0.962	13.62	1.06	0.94
29	24	4	0.963	12.63	1.06	0.94
30	0	0	0.968	18.79	1.06	0.94
31	43	27	0.967	12.75	1.06	0.94
32	59	23	0.964	14.8	1.06	0.94
33	23	9	0.972	10.63	1.06	0.94
34	59	26	0.986	11.3	1.06	0.94
35	33	9	0.981	10.87	1.06	0.94
36	31	17	0.98	10.87	1.06	0.94
37	0	0	0.992	11.77	1.06	0.94
38	0	0	0.962	16.91	1.06	0.94
39	27	11	0.97	8.41	1.06	0.94
40	66	23	0.97	7.35	1.06	0.94
41	37	10	0.967	6.92	1.06	0.94
42	96	23	0.985	8.53	1.06	0.94
43	18	7	0.978	11.28	1.06	0.94
44	16	8	0.985	13.82	1.06	0.94
45	53	22	0.987	15.67	1.06	0.94
46	28	10	1.005	18.49	1.06	0.94
47	34	0	1.017	20.73	1.06	0.94

48	20	11	1.021	19.93	1.06	0.94
49	87	30	1.025	20.94	1.06	0.94
50	17	4	1.001	18.9	1.06	0.94
51	17	8	0.967	16.28	1.06	0.94
52	18	5	0.957	15.32	1.06	0.94
53	23	11	0.946	14.35	1.06	0.94
54	113	32	0.955	15.26	1.06	0.94
55	63	22	0.952	14.97	1.06	0.94
56	84	18	0.954	15.16	1.06	0.94
57	12	3	0.971	16.36	1.06	0.94
58	12	3	0.959	15.51	1.06	0.94
59	277	113	0.985	19.37	1.06	0.94
60	78	3	0.993	23.15	1.06	0.94
61	0	0	0.995	24.04	1.06	0.94
62	77	14	0.998	23.43	1.06	0.94
63	0	0	0.969	22.75	1.06	0.94
64	0	0	0.984	24.52	1.06	0.94
65	0	0	1.005	27.65	1.06	0.94
66	39	18	1.05	27.48	1.06	0.94
67	28	7	1.02	24.84	1.06	0.94
68	0	0	1.003	27.55	1.06	0.94
69	0	0	1.035	30	1.06	0.94
70	66	20	0.984	22.58	1.06	0.94
71	0	0	0.987	22.15	1.06	0.94
72	12	0	0.98	20.98	1.06	0.94
73	6	0	0.991	21.94	1.06	0.94
74	68	27	0.958	21.64	1.06	0.94
75	47	11	0.967	22.91	1.06	0.94
76	68	36	0.943	21.77	1.06	0.94
77	61	28	1.006	26.72	1.06	0.94
78	71	26	1.003	26.42	1.06	0.94
79	39	32	1.009	26.72	1.06	0.94
80	130	26	1.04	28.96	1.06	0.94
81	0	0	0.997	28.1	1.06	0.94
82	54	27	0.989	27.24	1.06	0.94
83	20	10	0.985	28.42	1.06	0.94
84	11	7	0.98	30.95	1.06	0.94
85	24	15	0.985	32.51	1.06	0.94
86	21	10	0.987	31.14	1.06	0.94
87	0	0	1.015	31.4	1.06	0.94

88	48	10	0.987	35.64	1.06	0.94
89	0	0	1.005	39.69	1.06	0.94
90	163	42	0.985	33.29	1.06	0.94
91	10	0	0.98	33.31	1.06	0.94
92	65	10	0.993	33.8	1.06	0.94
93	12	7	0.987	30.79	1.06	0.94
94	30	16	0.991	28.64	1.06	0.94
95	42	31	0.981	27.67	1.06	0.94
96	38	15	0.993	27.51	1.06	0.94
97	15	9	1.011	27.88	1.06	0.94
98	34	8	1.024	27.4	1.06	0.94
99	42	0	1.01	27.04	1.06	0.94
100	37	18	1.017	28.03	1.06	0.94
101	22	15	0.993	29.61	1.06	0.94
102	5	3	0.991	32.3	1.06	0.94
103	23	16	1.001	24.44	1.06	0.94
104	38	25	0.971	21.69	1.06	0.94
105	31	26	0.965	20.57	1.06	0.94
106	43	16	0.962	20.32	1.06	0.94
107	50	12	0.952	17.53	1.06	0.94
108	2	1	0.967	19.38	1.06	0.94
109	8	3	0.967	18.93	1.06	0.94
110	39	30	0.973	18.09	1.06	0.94
111	0	0	0.98	19.74	1.06	0.94
112	68	13	0.975	14.99	1.06	0.94
113	6	0	0.993	13.74	1.06	0.94
114	8	3	0.96	14.46	1.06	0.94
115	22	7	0.96	14.46	1.06	0.94
116	184	0	1.005	27.12	1.06	0.94
117	20	8	0.974	10.67	1.06	0.94
118	33	15	0.949	21.92	1.06	0.94

Table B.14: Generator data for IEEE118 bus system

Bus	Pg(MW)	Qg(MVAR)	Qmax(MVAR)	Qmin(MVAR)	Pmax(MW)
10	450	0	200	-147	550
12	85	0	120	-35	185
25	220	0	140	-47	320
26	314	0	1000	-1000	414
31	7	0	300	-300	107
46	19	0	100	-100	119

49	204	0	210	-85	304
54	48	0	300	-300	148
59	155	0	180	-60	255
61	160	0	300	-100	260
65	391	0	200	-67	491
66	392	0	200	-67	492
69	516.4	0	300	-300	805.2
80	477	0	280	-165	577
87	4	0	1000	-100	104
89	607	0	300	-210	707
100	252	0	155	-50	352
103	40	0	40	-15	140
111	36	0	1000	-100	136

Table B.15: Line data for IEEE118 bus system

From	To	R(p.u)	X(p.u)	B/2(p.u)	Rate(MVA)	Tap Ratio
1	2	0.0303	0.0999	0.0254	9900	0
1	3	0.0129	0.0424	0.01082	9900	0
4	5	0.00176	0.00798	0.0021	9900	0
3	5	0.0241	0.108	0.0284	9900	0
5	6	0.0119	0.054	0.01426	9900	0
6	7	0.00459	0.0208	0.0055	9900	0
8	9	0.00244	0.0305	1.162	9900	0
8	5	0	0.0267	0	9900	0.985
9	10	0.00258	0.0322	1.23	9900	0
4	11	0.0209	0.0688	0.01748	9900	0
5	11	0.0203	0.0682	0.01738	9900	0
11	12	0.00595	0.0196	0.00502	9900	0
2	12	0.0187	0.0616	0.01572	9900	0
3	12	0.0484	0.16	0.0406	9900	0
7	12	0.00862	0.034	0.00874	9900	0
11	13	0.02225	0.0731	0.01876	9900	0
12	14	0.0215	0.0707	0.01816	9900	0
13	15	0.0744	0.2444	0.06268	9900	0
14	15	0.0595	0.195	0.0502	9900	0
12	16	0.0212	0.0834	0.0214	9900	0
15	17	0.0132	0.0437	0.0444	9900	0
16	17	0.0454	0.1801	0.0466	9900	0
17	18	0.0123	0.0505	0.01298	9900	0
18	19	0.01119	0.0493	0.01142	9900	0

19	20	0.0252	0.117	0.0298	9900	0
15	19	0.012	0.0394	0.0101	9900	0
20	21	0.0183	0.0849	0.0216	9900	0
21	22	0.0209	0.097	0.0246	9900	0
22	23	0.0342	0.159	0.0404	9900	0
23	24	0.0135	0.0492	0.0498	9900	0
23	25	0.0156	0.08	0.0864	9900	0
26	25	0	0.0382	0	9900	0.96
25	27	0.0318	0.163	0.1764	9900	0
27	28	0.01913	0.0855	0.0216	9900	0
28	29	0.0237	0.0943	0.0238	9900	0
30	17	0	0.0388	0	9900	0.96
8	30	0.00431	0.0504	0.514	9900	0
26	30	0.00799	0.086	0.908	9900	0
17	31	0.0474	0.1563	0.0399	9900	0
29	31	0.0108	0.0331	0.0083	9900	0
23	32	0.0317	0.1153	0.1173	9900	0
31	32	0.0298	0.0985	0.0251	9900	0
27	32	0.0229	0.0755	0.01926	9900	0
15	33	0.038	0.1244	0.03194	9900	0
19	34	0.0752	0.247	0.0632	9900	0
35	36	0.00224	0.0102	0.00268	9900	0
35	37	0.011	0.0497	0.01318	9900	0
33	37	0.0415	0.142	0.0366	9900	0
34	36	0.00871	0.0268	0.00568	9900	0
34	37	0.00256	0.0094	0.00984	9900	0
38	37	0	0.0375	0	9900	0.935
37	39	0.0321	0.106	0.027	9900	0
37	40	0.0593	0.168	0.042	9900	0
30	38	0.00464	0.054	0.422	9900	0
39	40	0.0184	0.0605	0.01552	9900	0
40	41	0.0145	0.0487	0.01222	9900	0
40	42	0.0555	0.183	0.0466	9900	0
41	42	0.041	0.135	0.0344	9900	0
43	44	0.0608	0.2454	0.06068	9900	0
34	43	0.0413	0.1681	0.04226	9900	0
44	45	0.0224	0.0901	0.0224	9900	0
45	46	0.04	0.1356	0.0332	9900	0
46	47	0.038	0.127	0.0316	9900	0
46	48	0.0601	0.189	0.0472	9900	0

47	49	0.0191	0.0625	0.01604	9900	0
42	49	0.0715	0.323	0.086	9900	0
42	49	0.0715	0.323	0.086	9900	0
45	49	0.0684	0.186	0.0444	9900	0
48	49	0.0179	0.0505	0.01258	9900	0
49	50	0.0267	0.0752	0.01874	9900	0
49	51	0.0486	0.137	0.0342	9900	0
51	52	0.0203	0.0588	0.01396	9900	0
52	53	0.0405	0.1635	0.04058	9900	0
53	54	0.0263	0.122	0.031	9900	0
49	54	0.073	0.289	0.0738	9900	0
49	54	0.0869	0.291	0.073	9900	0
54	55	0.0169	0.0707	0.0202	9900	0
54	56	0.00275	0.00955	0.00732	9900	0
55	56	0.00488	0.0151	0.00374	9900	0
56	57	0.0343	0.0966	0.0242	9900	0
50	57	0.0474	0.134	0.0332	9900	0
56	58	0.0343	0.0966	0.0242	9900	0
51	58	0.0255	0.0719	0.01788	9900	0
54	59	0.0503	0.2293	0.0598	9900	0
56	59	0.0825	0.251	0.0569	9900	0
56	59	0.0803	0.239	0.0536	9900	0
55	59	0.04739	0.2158	0.05646	9900	0
59	60	0.0317	0.145	0.0376	9900	0
59	61	0.0328	0.15	0.0388	9900	0
60	61	0.00264	0.0135	0.01456	9900	0
60	62	0.0123	0.0561	0.01468	9900	0
61	62	0.00824	0.0376	0.0098	9900	0
63	59	0	0.0386	0	9900	0.96
63	64	0.00172	0.02	0.216	9900	0
64	61	0	0.0268	0	9900	0.985
38	65	0.00901	0.0986	1.046	9900	0
64	65	0.00269	0.0302	0.38	9900	0
49	66	0.018	0.0919	0.0248	9900	0
49	66	0.018	0.0919	0.0248	9900	0
62	66	0.0482	0.218	0.0578	9900	0
62	67	0.0258	0.117	0.031	9900	0
65	66	0	0.037	0	9900	0.935
66	67	0.0224	0.1015	0.02682	9900	0
65	68	0.00138	0.016	0.638	9900	0

47	69	0.0844	0.2778	0.07092	9900	0
49	69	0.0985	0.324	0.0828	9900	0
68	69	0	0.037	0	9900	0.935
69	70	0.03	0.127	0.122	9900	0
24	70	0.00221	0.4115	0.10198	9900	0
70	71	0.00882	0.0355	0.00878	9900	0
24	72	0.0488	0.196	0.0488	9900	0
71	72	0.0446	0.18	0.04444	9900	0
71	73	0.00866	0.0454	0.01178	9900	0
70	74	0.0401	0.1323	0.03368	9900	0
70	75	0.0428	0.141	0.036	9900	0
69	75	0.0405	0.122	0.124	9900	0
74	75	0.0123	0.0406	0.01034	9900	0
76	77	0.0444	0.148	0.0368	9900	0
69	77	0.0309	0.101	0.1038	9900	0
75	77	0.0601	0.1999	0.04978	9900	0
77	78	0.00376	0.0124	0.01264	9900	0
78	79	0.00546	0.0244	0.00648	9900	0
77	80	0.017	0.0485	0.0472	9900	0
77	80	0.0294	0.105	0.0228	9900	0
79	80	0.0156	0.0704	0.0187	9900	0
68	81	0.00175	0.0202	0.808	9900	0
81	80	0	0.037	0	9900	0.935
77	82	0.0298	0.0853	0.08174	9900	0
82	83	0.0112	0.03665	0.03796	9900	0
83	84	0.0625	0.132	0.0258	9900	0
83	85	0.043	0.148	0.0348	9900	0
84	85	0.0302	0.0641	0.01234	9900	0
85	86	0.035	0.123	0.0276	9900	0
86	87	0.02828	0.2074	0.0445	9900	0
85	88	0.02	0.102	0.0276	9900	0
85	89	0.0239	0.173	0.047	9900	0
88	89	0.0139	0.0712	0.01934	9900	0
89	90	0.0518	0.188	0.0528	9900	0
89	90	0.0238	0.0997	0.106	9900	0
90	91	0.0254	0.0836	0.0214	9900	0
89	92	0.0099	0.0505	0.0548	9900	0
89	92	0.0393	0.1581	0.0414	9900	0
91	92	0.0387	0.1272	0.03268	9900	0
92	93	0.0258	0.0848	0.0218	9900	0

92	94	0.0481	0.158	0.0406	9900	0
93	94	0.0223	0.0732	0.01876	9900	0
94	95	0.0132	0.0434	0.0111	9900	0
80	96	0.0356	0.182	0.0494	9900	0
82	96	0.0162	0.053	0.0544	9900	0
94	96	0.0269	0.0869	0.023	9900	0
80	97	0.0183	0.0934	0.0254	9900	0
80	98	0.0238	0.108	0.0286	9900	0
80	99	0.0454	0.206	0.0546	9900	0
92	100	0.0648	0.295	0.0472	9900	0
94	100	0.0178	0.058	0.0604	9900	0
95	96	0.0171	0.0547	0.01474	9900	0
96	97	0.0173	0.0885	0.024	9900	0
98	100	0.0397	0.179	0.0476	9900	0
99	100	0.018	0.0813	0.0216	9900	0
100	101	0.0277	0.1262	0.0328	9900	0
92	102	0.0123	0.0559	0.01464	9900	0
101	102	0.0246	0.112	0.0294	9900	0
100	103	0.016	0.0525	0.0536	9900	0
100	104	0.0451	0.204	0.0541	9900	0
103	104	0.0466	0.1584	0.0407	9900	0
103	105	0.0535	0.1625	0.0408	9900	0
100	106	0.0605	0.229	0.062	9900	0
104	105	0.00994	0.0378	0.00986	9900	0
105	106	0.014	0.0547	0.01434	9900	0
105	107	0.053	0.183	0.0472	9900	0
105	108	0.0261	0.0703	0.01844	9900	0
106	107	0.053	0.183	0.0472	9900	0
108	109	0.0105	0.0288	0.0076	9900	0
103	110	0.03906	0.1813	0.0461	9900	0
109	110	0.0278	0.0762	0.0202	9900	0
110	111	0.022	0.0755	0.02	9900	0
110	112	0.0247	0.064	0.062	9900	0
17	113	0.00913	0.0301	0.00768	9900	0
32	113	0.0615	0.203	0.0518	9900	0
32	114	0.0135	0.0612	0.01628	9900	0
27	115	0.0164	0.0741	0.01972	9900	0
114	115	0.0023	0.0104	0.00276	9900	0
68	116	0.00034	0.00405	0.164	9900	0
12	117	0.0329	0.14	0.0358	9900	0

75	118	0.0145	0.0481	0.01198	9900	0
76	118	0.0164	0.0544	0.01356	9900	0

Figure B.1: Single line diagram of IG-75 bus system

Table B.16: Bus details for IG-75 bus system

Bus	Volt.(p.u)	Angle (Deg)	Pd (Mw)	Qd (MVAr)	Pg (Mw)	Qg (MVAr)	Qmin (MVAr)	Qmax (MVAr)
1	1.03	0	0	0	749.00	0.00	-150	400
2	1.05	0	0	0	260.00	0.00	-25	96
3	1.01	0	0	0	180.00	0.00	-50	83
4	1.04	0	0	0	100.00	0.00	-20	60
5	1.04	0	0	0	180.00	0.00	-50	80
6	1.05	0	0	0	120.00	0.00	-25	50
7	1.05	0	0	0	60.00	0.00	-10	25
8	1.02	0	0	0	80.00	0.00	-10	68
9	1.05	0	0	0	550.00	0.00	100	250
10	1.01	0	0	0	80.00	0.00	-10	56
11	1.02	0	0	0	109.00	0.00	-20	50
12	1.04	0	0	0	0.00	0.00	0	344
13	1.05	0	0	0	900.00	0.00	150	280
14	1.03	0	0	0	150.00	0.00	100	84
15	1.01	0	0	0	454.00	0.00	-80	150
16	1	0	-58.69	27.56	0.00	27.56	0	0
17	1	0	0	0	0.00	0.00	0	0
18	1	0	0	0	0.00	0.00	0	0
19	1	0	0	0	0.00	0.00	0	0
20	1	0	156.37	33.93	0.00	33.93	0	0
21	1	0	0	0	0.00	0.00	0	0
22	1	0	0	0	0.00	0.00	0	0
23	1	0	0	0	0.00	0.00	0	0
24	1	0	227.95	40.53	0.00	40.53	0	0
25	1	0	210.48	43.43	0.00	43.43	0	0
26	1	0	0	0	0.00	0.00	0	0
27	1	0	306	40.7	0.00	40.70	0	0
28	1	0	127.75	28.35	0.00	28.35	0	0
29	1	0	0	0	0.00	0.00	0	0
30	1	0	226.46	44.24	0.00	44.24	0	0
31	1	0	0	0	0.00	0.00	0	0
32	1	0	78.11	11.59	0.00	11.59	0	0
33	1	0	0	0	0.00	0.00	0	0
34	1	0	81.7	83.84	0.00	83.84	0	0
35	1	0	0	0	0.00	0.00	0	0
36	1	0	0	0	0.00	0.00	0	0
37	1	0	144.28	40.93	0.00	40.93	0	0

38	1	0	0	0	0.00	0.00	0	0
39	1	0	85.12	29.46	0.00	29.46	0	0
40	1	0	0	0	0.00	0.00	0	0
41	1	0	0	0	0.00	0.00	0	0
42	1	0	1000	0	0.00	0.00	0	0
43	1	0	0	0	0.00	0.00	0	0
44	1	0	0	0	0.00	0.00	0	0
45	1	0	0	0	0.00	0.00	0	0
46	1	0	156.32	83.36	0.00	83.36	0	0
47	1	0	74.55	8.77	0.00	8.77	0	0
48	1	0	50.83	13.97	0.00	13.97	0	0
49	1	0	85.72	51.58	0.00	51.58	0	0
50	1	0	202.1	74.94	0.00	74.94	0	0
51	1	0	57.76	0.62	0.00	0.62	0	0
52	1	0	98.27	18.15	0.00	18.15	0	0
53	1	0	82.63	-0.33	0.00	-0.33	0	0
54	1	0	161.95	29	0.00	29.00	0	0
55	1	0	274.23	31.08	0.00	31.08	0	0
56	1	0	140.28	34.32	0.00	34.32	0	0
57	1	0	152.78	18.53	0.00	18.53	0	0
58	1	0	94.19	11.29	0.00	11.29	0	0
59	1	0	121.89	11.01	0.00	11.01	0	0
60	1	0	74.2	7.42	0.00	7.42	0	0
61	1	0	106.5	6.58	0.00	6.58	0	0
62	1	0	100.18	18.13	0.00	18.13	0	0
63	1	0	58.01	5.31	0.00	5.31	0	0
64	1	0	56.79	13.33	0.00	13.33	0	0
65	1	0	147.84	12.81	0.00	12.81	0	0
66	1	0	31.74	15.18	0.00	15.18	0	0
67	1	0	96.43	10.55	0.00	10.55	0	0
68	1	0	42.87	33.6	0.00	33.60	0	0
69	1	0	55.94	32.53	0.00	32.53	0	0
70	1	0	23.34	2.3	0.00	2.30	0	0
71	1	0	91.73	21.36	0.00	21.36	0	0
72	1	0	52.52	11.76	0.00	11.76	0	0
73	1	0	447.00	0	0.00	0.00	0	0
74	1	0	288.00	0	0.00	0.00	0	0
75	1	0	-444.00	0	0.00	0.00	0	0

Bus code: 1- slack bus; 2 – Generator bus; 0 – Load bus

Table B.17: Line details for IG-75 bus system

From	To	R (p.u.)	X (p.u.)	B/2 (p.u.)	Line limits
19	20	0.0006	0.026	0	480
16	2	0.0012	0.0247	0	472
18	3	0	0.0292	0	480
17	16	0.0006	0.026	0	480
17	1	0.0007	0.0146	0	990
22	25	0.0006	0.026	0	480
23	24	0.0006	0.026	0	510
26	27	0.0006	0.026	0	480
28	4	0.0031	0.0614	0	185
29	30	0.0004	0.0174	0	720
31	5	0.0024	0.0471	0	276
32	6	0.0051	0.1029	0	250
33	7	0.0055	0.1098	0	200
34	8	0	0.0486	0	250
35	9	0.0005	0.0194	0	720
36	37	0.0006	0.026	0	480
38	39	0.0013	0.0521	0	240
24	10	0.0024	0.0486	0	250
40	11	0.0077	0.0272	0	375
12	41	0.0002	0.0059	0	2050
42	13	0.0003	0.012	0	1176
43	14	0	0.0284	0	528
44	15	0	0.0227	0	660
45	44	0.0006	0.0222	0	630
16	46	0.0081	0.0388	0.2806	300
16	50	0.0099	0.0475	0.7729	420
17	19	0.0047	0.0477	1.259	500
17	23	0.0078	0.0799	2.0948	500
23	29	0.0081	0.0817	2.1362	500
20	64	0.0183	0.0927	0.1478	250
19	26	0.0029	0.03	0.7841	550
47	50	0.0109	0.0522	0.3778	300
35	41	0.0003	0.0031	0.0811	600
47	67	0.0066	0.0316	0.229	300
24	27	0.005	0.0242	0.1746	300
24	54	0.0129	0.0617	0.4465	500
27	51	0.016	0.081	0.1288	300
51	52	0.0155	0.0794	0.126	250

25	60	0.0166	0.0843	0.1344	250
25	43	0.0127	0.0641	0.1044	250
34	54	0.0177	0.0851	0.6052	300
54	28	0.0106	0.0506	0.3664	300
28	43	0.0058	0.029	0.0474	180
28	56	0.0037	0.0178	0.0644	300
56	30	0.0049	0.0237	0.1718	300
30	57	0.0075	0.0384	0.0622	280
53	30	0.0068	0.0341	0.0556	280
53	61	0.0067	0.0339	0.0534	250
30	61	0.0144	0.0731	0.117	250
57	58	0.0067	0.0339	0.0534	280
57	59	0.0058	0.0296	0.0469	280
59	31	0.0141	0.0718	0.114	225
39	31	0.0144	0.0725	0.118	250
39	33	0.007	0.0359	0.228	300
54	63	0.0099	0.0509	0.0802	250
55	63	0.0078	0.0398	0.0628	280
61	62	0.0116	0.0583	0.095	250
62	32	0.0069	0.035	0.2252	300
31	32	0.0005	0.0025	0.0161	360
35	36	0.0048	0.0488	1.2723	500
46	37	0.0173	0.0878	0.1396	250
19	36	0.0025	0.0258	0.676	500
17	35	0.0005	0.0052	0.1352	600
20	40	0.0058	0.0294	0.1884	300
40	48	0.0083	0.0424	0.0668	250
74	41	0.0043	0.0446	0.192	720
74	73	0.0056	0.0569	1.4871	500
26	22	0.0065	0.0662	1.7304	500
29	22	0.0026	0.0265	0.6922	550
26	41	0.0082	0.0838	0.1911	400
48	49	0.0093	0.0475	0.0748	250
49	40	0.0133	0.0668	0.1084	250
38	29	0.0037	0.0376	0.9774	550
38	22	0.0032	0.0331	0.8653	550
18	47	0.0044	0.0255	0.188	360
30	65	0.0025	0.0119	0.0859	360
41	42	0.0003	0.0031	0.0811	600
42	74	0.0092	0.0931	2.4336	500

20	66	0.0133	0.0667	0.1083	250
23	74	0.0001	0.0015	0.0541	1200
24	67	0.0012	0.0059	0.0429	360
18	68	0.0034	0.0196	0.0372	280
18	71	0.0134	0.0785	0.1446	270
27	68	0.0134	0.0785	0.1446	270
27	71	0.0034	0.0196	0.0362	280
25	72	0.016	0.0811	0.1287	250
43	58	0.0132	0.067	0.1156	250
39	32	0.0144	0.0725	0.118	250
43	56	0.005	0.024	0.1705	300
55	44	0.01	0.0479	0.3409	500
73	45	0.0012	0.0111	1.4563	1000
29	75	0.0005	0.0052	0.1352	600
37	69	0.0121	0.061	0.0991	300
70	72	0.0088	0.0443	0.0716	280
21	65	0.0008	0.004	0.0286	350
21	30	0.0069	0.035	0.0569	250

Table B.18: Genenrator details for IG-75 bus system

Bus number	Active power limits	
	P_g^{max} (MW)	P_g^{min} (MW)
1	849.0	25.0
2	360.0	25.0
3	280.0	25.0
4	200.0	25.0
5	280.0	25.0
6	220.0	25.0
7	160.0	25.0
8	180.0	25.0
9	650.0	25.0
10	180.0	25.0
11	209.0	25.0
12	1900.0	25.0
13	1000.0	25.0
14	250.0	25.0
15	554.0	25.0

Appendix-C: BCS approach for proposed OPP problem
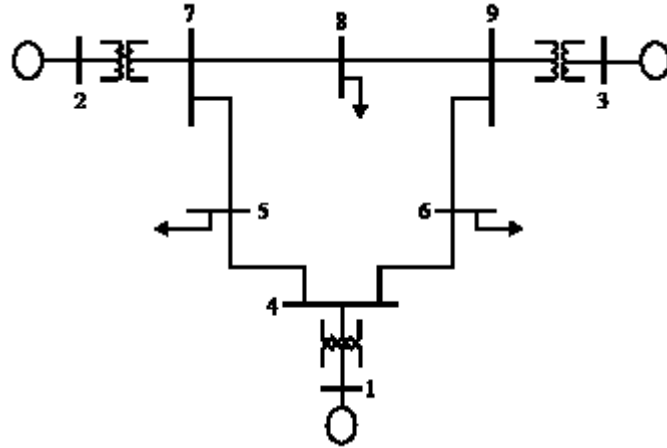
Fig: IEEE-9 bus system

(considering above Fig.)

No. of nests =9, (no. of buses)
no.of bits in nest=9, (no. of buses)
pa=0.11; abandon factor
No. of iterations=100
nest =

1	1	0	0	0	1	0	0	1
1	0	0	1	1	1	1	1	0
1	1	1	0	1	0	1	0	0
0	0	1	0	1	0	0	1	1
1	1	1	0	1	0	0	1	1
1	0	0	0	0	0	0	0	1
1	**1**	**0**	**0**	**1**	**1**	**0**	**0**	**1=5, best sol in nest**
1	1	0	0	1	1	1	0	1
0	1	0	1	0	1	1	1	0

Fitness=

2000004
2000006
2000005
4000004
6
6000002
5=best fitness
6

2000005

Evaluate this set of solutions considering new_nest

new_nest 1=

0	1	0	0	0	1	0	0	1
0	0	0	1	1	1	1	1	0
0	1	1	0	1	0	1	0	0
0	0	1	0	1	0	0	1	1
0	1	1	0	1	0	0	1	1
0	0	0	0	0	0	0	0	0
0	1	0	0	1	1	0	0	1
0	0	0	0	1	1	1	0	0
0	1	0	1	0	1	1	0	0

since no solution is satisfying the constraint and minimizing the PMU number,
best nest=nest

bes sol=1 1 0 0 1 1 0 0 1

iteration2

new_nest 2=

0	0	0	1	0	0	0	1	0	
0	0	0	0	0	1	0	1	0	
0	1	1	0	1	1	0	0	0	
1	**0**	**0**	**0**	**0**	**1**	**1**	**0**	**1=4, (best sol in new-nest2)**
1	1	1	0	1	0	0	1	0	
0	0	0	1	0	0	1	1	1	
0	1	0	0	1	0	0	0	0	
0	1	0	1	0	1	1	0	1	
0	1	1	0	1	0	1	1	1	

Since 4<5

best nest=new_nest2

best sol=1 0 0 0 0 1 1 0 1

.
.
.
.
.
.
.
.
.
On continuing it till iterations count reaches 20:

iteration20

new-nest20=

0	0	0	1	0	0	0	1	0	
0	**0**	**0**	**1**	**0**	**0**	**1**	**0**	**1=3, (best sol in new-nest20)**
0	1	1	0	1	1	0	0	0	
1	0	0	0	0	1	1	0	1	
1	1	1	0	0	0	0	1	0	
0	0	0	1	0	0	1	1	1	
0	1	0	0	1	0	0	0	0	
0	1	0	1	0	1	1	0	1	
0	1	1	0	0	0	1	1	1	

Since 3<4

best nest=new_nest20

best sol=0   0   0   1   0   0   1   0   1

On continuing it till iterations count reaches 100:

best sol=0   0   0   1   0   0   1   0   1

So, if PMUs are placed at 4, 7 and 9, the IEEE-9 system shown above will be observed completely

Appendix-D: Verification of observability

The observability of buses can be computed effectively using the equation given below.

$$[O]_{N\times 1} = [A]_{N\times N}[P]_{N\times 1}$$

Here, N represents the set of network buses. Where, *P* represents a PMU matrix. It is a column matrix whose entries are 1 for a PMU_bus and 0 otherwise. A is a incidence matrix whose entries (A_{pq}) can be calculated as below:

$$A_{pq} = \begin{cases} 1, \text{if } p = q \\ 1, \text{if buses } p, q \text{ are connected} \\ 0, \text{otherwise} \end{cases}$$

For the bus to be observable, it must be connected to at least one PMU-installed bus. For the system to be observable completely, none of the element of the matrix O should be zero.

For example, if we consider IEEE-9 bus system given in Appendix-C, the incidence matrix *A* becomes,

```
A=[ 1   0   0   1   0   0   0   0   0
    0   1   0   0   0   0   1   0   0
    0   0   1   0   0   0   0   0   1
    1   0   0   1   1   1   0   0   0
    0   0   0   1   1   0   1   0   0
    0   0   0   1   0   1   0   0   1
    0   1   0   0   1   0   1   1   0
    0   0   0   0   0   0   1   1   1
    0   0   1   0   0   1   0   1   1];
```

If we take any one solution from new_nest1,
P=[0 1 0 0 0 1 0 0 1]$^{\text{T}}$
Now, if we calculate O:
O= [0 1 1 1 0 1 1 1 1]$^{\text{T}}$
 It says that for the given set of PMUs, the buses 1 and 5 are unobserved. And if we consider,
P=[0 0 0 1 0 0 1 0 1]$^{\text{T}}$
All the buses become observable. For the system to be observable under Line/PMU outage, all the elements of *P* should be at least 2.

Publications:

Journals Published:

1. N V Phanendra Babu, Dr. P Suresh Babu, "A Robust Wide-Area Measurement System for Southern Region of Indian power Grid Using Binary Cuckoo Search (BCS): A Case Study", Journal of electrical systems (JES), 12-1(2016), 45-67. (ESCI)
2. N V Phanendra Babu, Dr. P Suresh Babu, Prof. D V S S Siva Sarma," A New Technique for Restoration based WAMS Partition", Engineering Technology and Applied Science Research (ETASR), Vol. 7, No. 4, 2017. (ESCI)
3. N. V. Phanendra Babu, Dr. P Suresh Babu, Prof. D V S S Siva Sarma,"A Novel Placement of Phasor Measurement Units Using Binary Bat Algorithm", Journal of Electrical Engineering (JEE), Vol. 17(4), N0. 30. (SCOPUS)
4. N V Phanendra Babu, Dr. P Suresh Babu, Prof. D V S S Siva Sarma, "A Robust Optimal PMU Placement Scheme for United Indian Grid - A Case Study ", International Journal of Engineering, Science and Technology, Vol. 10, No. 2, 10-24, ISSN: 2141-2839, 2018.

Journal under Revision:

1. N. V. Phanendra Babu, Dr. P Suresh Babu, Prof. D V S S Siva Sarma," Critical Elements Based Optimal PMU Placement Considering Substation Coverage", International Journal on Electrical Engineering and Informatics, (SCOPUS).

Conferences Published:

1. N V Phanendra Babu, Dr. P Suresh Babu, Prof. D V S S SivaSarma, "A Wide-Area Prospective On Power System Protection: A State-of-Art", IEEE International Conference on Energy, Power and Environment (ICEPE-2015), NIT Meghalaya.
2. N V Phanendra Babu, Dr. P Suresh Babu, Prof. D V S S SivaSarma, "Importance of Phasor Measurements in Wide Area Protection of Power System: A Review", National Conference on Power System Protection, Central Power Research Institute, Bangalore, 27-28 Feb, 2015

N.VENKATA PHANENDRA BABU

S/o N.V.Seshachalasasthri,
Gunupadu(vi)(po),
Chittamoor (md),
Nellore (Dt.)-524402,
A.P, India.

Mobile No: +91-7702578106

Email:phanendra229@gmail.com

Professional Objectives:

Seeking a responsible post of Assistant Professor for giving the practical knowledge which make the student's career progressive. Dedicated Engineer with a strong record in both teaching and Research. Good at teaching complex engineering theories and practices in a clear and accessible manner to a variety of professional and non-professional audiences. Committed to offer my full attention and expertise to all interested students for their academic and professional goals.

Experience:
Research:
National Institute of Technology Warangal
(4 Years 6Months)
Areas of Interest: Wide-Area Power Systems, Power Systems Protection, Optimization Techniques.

Dec 2013-Now

Teaching: (Assistant Professor)
Gurunanak Institute of Technology, Hyd (6 Months)
Subjects Handled: Electrical Circuits, Control Systems

June 2013-Nov 2013

Keshav Memorial Institute of Technology, Hyd (2 Years)
Subjects Handled: Fundamental of Electrical Engineering, Basic Electrical Engineering, Control Systems
Labs Handled: BEE Lab, Transducers & Instrumentation Lab, ET Lab

June 2011-May 2013

Education:
Master of Technology, 8.65 CGPA
Power systems Engineering
SRM University, Kattankulathur

2011

Bachelor Of Technology, 71.82%
Electrical and Electronics Engineering
Narayana Engineering College, Gudur

2008

Intermediate, 81.9%
Mathematics-Physics-Chemistry
Sri Vema Junior College

2004

Secondary School Certificate, 83.33%
Regular, ZPP High School

2002

Dissertations:

M.Tech: Fuzzy Logic Controller of SVC for Power Oscillations Damping.

B.Tech: Protection Schemes Employed for the Protection of Generator and Generating Transformer.

Tool/Software Expertise:
Matlab/Simulink
EMTDC/PSCAD
Power World Simulator
Basics of ETAP